CORNET
Final Report / Schlussbericht

ThermNat

Building components with insulation from sustainable raw materials: focus (hygro-) thermal conditions
Bauteile mit Dämmmaterial aus nachwachsenden Rohstoffen: Fokus (Hygro-)Thermik

Funded by / Gefördert durch CORNET

IGF-Project 271 EN supported by Forschungsvereinigung Trägerverein Institut für Holztechnologie Dresden e.V., AiF und BMWK on the basis of a decision by the German Bundestag
Project 877670 funded by Österreichische Forschungsförderungsgesellschaft mbH (FFG)

RTO / Forschungseinrichtungen

Fraunhofer Institut für Bauphysik, Standort Holzkirchen, Valley, Germany (Fraunhofer-IBP)
Holzforschung Austria, Wien, Austria (HFA)

Applicant / AiF-Forschungsvereinigung

Holztechnologie / Trägerverein Institut für Holztechnologie Dresden e.V., Dresden, Germany (TIHD)

Authors / Autoren/Autorinnen:

Dr. Daniel Zirkelbach, Johannes Tieben, Eri Tanaka, Notburga Pfabigan, Nis Andresen, Dr. Julia Bachinger, Dr. Bernd Nusser

with contributions by / unter Mitwirkung von:

B. Brunnhuber, L. Orlowski, Dr. R. Schwerd, M. Senoner BSc.

kindly supported by / unterstützt durch:

best wood SCHNEIDER GmbH, Daniel Kehl - büro für holzbauphysik, EGS-plan GmbH, Energie- und Umweltzentrum am Deister GmbH, GUTEX Holzfaserplattenwerk GmbH & CO. KG, Hanffaser Uckermark eG, Holzbau Deutschland Institut e.V., ISOCELL GmbH & Co KG, Isolena Naturfaservliese GmbH, LOPAS GmbH, Martin Epple - Bau.Tragwerk Ingenieurbüro, SonnenKlee GmbH, Soprema GmbH, STEICO SE, Sto GmbH, Tobias Tumfart GmbH, Verband Dämmstoffe aus nachwachsenden Rohstoffen e.V.

Holzkirchen/Wien/Dresden, 30.06.2023

TABLE OF CONTENTS

1 Introduction

1.1 Overview

In the context of climate change and limiting CO_2 emissions, the building sector plays a significant role in terms of energy requirements for heating and cooling as well as so-called grey energy. There is a growing awareness of the problem in society and an increasing willingness to make the necessary contributions within one's own sphere of influence. Building materials made from renewable raw materials offer the considerable advantage that they have a significantly better CO_2 balance than most conventional building materials. Currently, two aspects still stand in the way of an even broader use of these materials:

1. Building materials made from renewable raw materials are generally sensitive to moisture and can be damaged or destroyed if not used appropriately.
2. Insulation materials made from renewable resources (IMRR) often need to declare increased thermal conductivities compared to conventional competitors - possibly also due to unjustifiably high surcharges for the moisture content of the materials.

Initial findings from research projects of Holzforschung Austria (HFA) and Fraunhofer-Institut für Bauphysik (IBP) [1, 2] indicated that the assessment of the thermal conductivity of IMRR might be too high. The determination of the thermal conductivity according to the current standards seems to disadvantage IMRR accordingly. In the present research project, therefore, the actual insulation potential of IMRR should be evaluated and, above all, the influencing factors of moisture content and moisture changes should be investigated in detail. The aim is to develop a validated method for measuring the thermal conductivity of IMRR.

The hygrothermal behaviour of IMRR can already be predicted by appropriate simulation programs. At the moment, however, there is still a lack of suitable evaluation models that allow a simulation-based prediction of the durability of these insulation materials (resistance to wood-decay fungi) based on the simulated temperature and moisture conditions.

In Austria, the new ÖNORM B 8110-2 [3] requires hygrothermal simulations for a large part of building component structures. Without a sufficient basis for the evaluation of IMRR, these are often classified as unsuitable.

For solid wood, rot resistance studies have already been performed and an isopleth model for rot prediction has been developed ([4] based on [5, 6]). Based on this model, an assessment model for hygrothermal simulation results was developed [7].

At the Fraunhofer-Institut für Bauphysik (IBP), as part of the recently completed "In2EuroBuild" project [8], comparative rot resistance tests were carried out with solid wood and IMRR samples of interior insulation materials. Similar or even higher resistance of the investigated IMRR was shown compared to the solid wood samples.

In the current research project, additional investigations were carried out on the rot resistance and durability of IMRR for different areas of application to enable a suitable evaluation of IMRR with different durability.

1.2 Background

1.2.1 Thermal conductivity of IMRR

It is commonly known that moisture in insulation materials increases their thermal conductivity. In the case of vapor-retarding insulating materials such as EPS, a significant water content of about 10 vol.-% is required to increase the thermal conductivity by 0.01 W/(mK) or, for an initial thermal conductivity of 0.04 W/(mK), by 25%. For fibre-based materials, a much smaller amount of water can temporarily even double the heat flux through the insulation layer compared to the dry state, when it comes to strong vapor flux in the temperature gradient. This phenomenon is known as latent heat effect and occurs because moisture evaporates on the warm side and is transported by vapor diffusion to the cold side, where it can condense again. In this process, heat is withdrawn on the warm side by evaporative cooling and supplied again on the cold side as condensation heat, which increases the heat flow through the insulation material accordingly. Unlike mineral wool or EPS, for example, natural fibre insulation can store moisture on the inner surfaces of its pore structures. This means that natural fibre insulations are normally never dry but have a so-called equilibrium moisture content depending on the ambient RH. Therefore, these materials normally receive higher moisture-related surcharges on the dry thermal conductivity to account for both increased humid thermal conductivity and latent heat transfer [9, 10]. However, unlike the measurement of normally dry mineral wool or EPS, a certain moisture content is already automatically included when measuring the thermal conductivity of natural fibre materials (equilibrium moisture in ambient climate). However, latent heat transport in insulated building components results not only from sorption moisture in the insulating material itself, but also from redistribution of moisture from the adjacent materials. This also evaporates on the warm side and migrates through the vapor-permeable insulation layer to the cold side, where it condenses again [2]. This effect is theoretically particularly pronounced in non-hygroscopic insulating materials such as mineral wool, since the water vapor migrates from the warm to the cold side in a short time without being de- and absorbed by the fibres along the way. The hygroscopicity of natural fibres causes this process to be slowed down, since they absorb part of the penetrating vapor [11]. This may reduce the latent heat transfer compared to a mineral wool insulation layer. This effect is only partially observed in the laboratory (moisture in the insulation material itself), since the insulation materials are tested as individual layers without adjacent material layers. Accordingly, it can be assumed that the normal test conditions disadvantage natural fibre insulation to a certain extent.

Therefore, within the current research project, a laboratory method for hygroscopic insulation materials is developed which enables both better differentiation between thermal conductivity

(= sensible heat) and latent heat parts in the measured heat flow and also realistically represents the energy behaviour of the materials. On this basis, the moisture surcharge applied up to now according to ÖNORM B 6015-2 [9] and DIN 4108-4 [10] may need to be re-evaluated and reduced.

1.2.2 Durability of IMRR

Wood and natural fibre insulation are biological materials and thus subject to natural degradation under "favourable" temperature and humidity conditions. Therefore, it is important to expose such materials only to hygrothermal conditions that prevent germination and growth of decay fungi. A general but rather careful and conservative limit for moisture content in solid wood is the limit of 20% by mass [12]. However, this limit value contains a high safety buffer, since decay only occurs at moisture contents above fibre saturation of about 27 to 30% by mass. In addition, biological processes such as degradation only proceed at a relevant rate if temperatures are also at a level favourable for fungal growth. The WTA guideline 6-8 [7] on the evaluation of wood structures has therefore established a new criterion for solid wood that does not depend on the water content in % by mass, but on the relative humidity in the pores of the building material (Figure 1). The relative pore humidity in the wood is a suitable measure of how "easily" the moisture is available for the fungi in the material. This limit curve increases as a function of temperature from 86 RH at 30 °C to 95% RH at 0 °C, and is based mainly on the studies of Viitanen [5, 6] and Kehl [4].

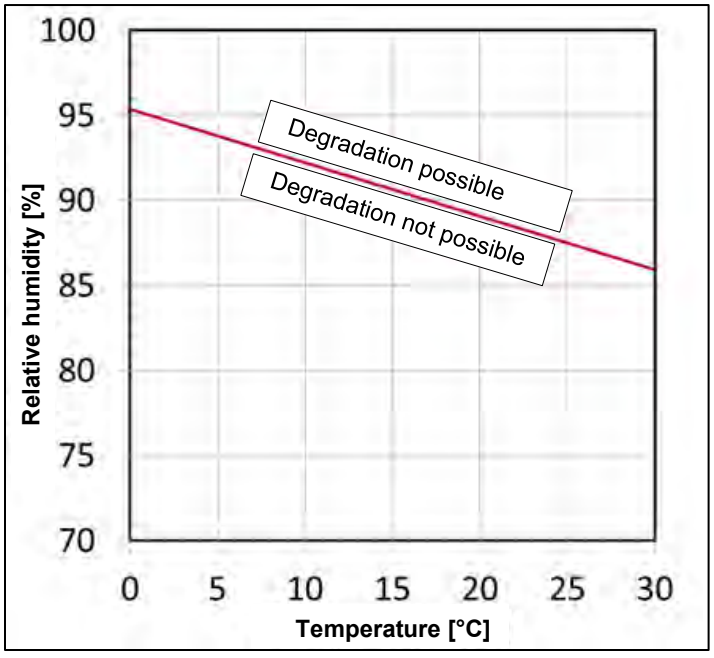

Figure 1 : Limit curve of the rel. pore RH related to the temperature of a 10 mm thick wood layer, which must not be exceeded as a daily average. Translated from German [7].

However, these limit values are also steady state and can therefore already lead to a formal failure of a component even by short-term moisture peaks exceeding the limit values. In practice, however, these short-term exceedances do normally not lead to problems if the moisture can subsequently dry out again quickly enough. For this reason, Fraunhofer-IBP is currently developing a transient wood decay model that is intended to close the gap between the temperature-dependent long-term limit values from WTA and the real behaviour as far as possible [13].

In the case of wood-based materials, the applicable limits often do not refer to the begin of decay, but to the strength properties of the materials. As a rule, structurally relevant wood-based materials must not exceed a moisture content of 18% by mass [12, 14] to ensure that the strength properties actually correspond to the declaration.

So far, there are hardly any reliable limit values for non-load-bearing natural fibre insulations. The 18% by mass limit does not actually apply in this case, but in practice it is used regularly due to the lack of alternatives. Since some fibre materials may be less resistant to moisture than solid wood, the WTA limit values [7] are not generally appropriate. This brings problems for manufacturers and planners if the materials are to be used in application areas where higher moisture contents can occur. This includes, for example, the use in flat roofs and external thermal insulation composite systems (ETICS), but also the application near the outside of building components, where high RH can occur, especially at night or in the winter months. On the other hand, there is also fibre insulation, which is more resistant than solid wood [8, 15]: they are often protected from access by the fungi by hydrophobic agents that, so to speak, coat the fibre surfaces. In other cases, mainly for fire protection reasons, the materials also contain salts or other substances that have the side effect of preventing the rotting process (e.g. cellulose fibre containing boron salts).

The current research project therefore focused, among other things, on the development of a transient evaluation model for natural fibre insulation materials, which considers the different specifications of these materials compared to solid wood and is intended to provide a reliable evaluation basis for manufacturers and planners.

2 Field tests

The backbone of the investigations carried out in the project was a 1:1-scale field test. This was carried out at the Holzforschung Austria (HFA) test house in Stetten (Austria). The core of the test was to monitor the real climatic conditions (temperature, humidity) in differently designed and aligned exterior walls for at least one year under real, transient climatic conditions. In addition, various in-situ heat flux measurements were performed. These recordings were later used for the simulation-based comparison of the results from the

laboratory measurements on thermal conductivity as well as for the evaluation of the determined limit values of the durability tests.

2.1 Location

The test house of Holzforschung Austria (Figure 2) is located directly at the HFA site, Gewerbegebiet 6, AT-2100 Stetten (48°21'57.6 "N 16°21'33.0 "E, 169 m a.s.l.).

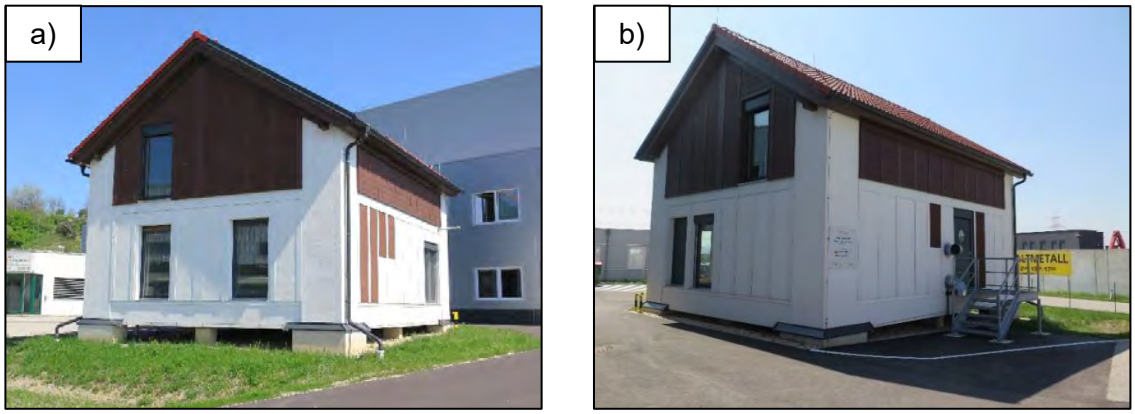

Figure 2 : Test house of Holzforschung Austria in AT-2100 Stetten.
a) South-west view.
b) North-east view.

The annual average outdoor temperature at this location is about 10.8 °C and the average relative humidity is 70% to 75% with predominant northwest and southeast winds. The terrain is rather flat. Wind speeds of up to 16 m/s can occur. The annual average of global radiation (direct + diffuse) is 136.5 W/m² with an average daily maximum of 350 W/m² in June and 63 W/m² in December [16]. The exterior walls are oriented exactly to the north, east, south and west directions. On the east side, the hall of the Akustik Center Austria (ACA) is in the immediate vicinity of the test house. In all other directions, no obstacles influence the facades of the building (Figure 3).

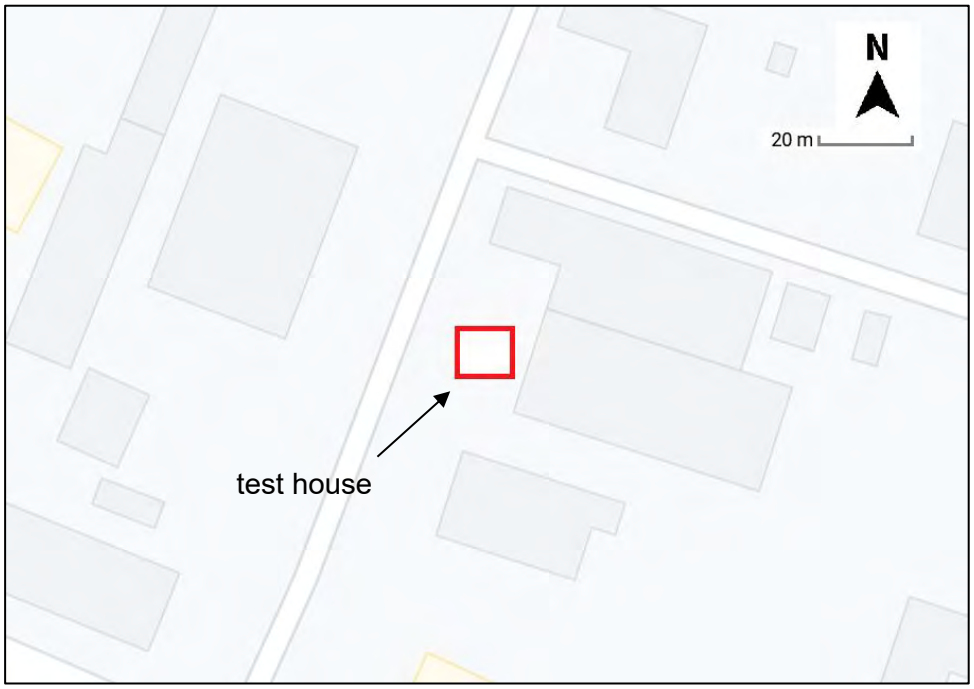

Figure 3 : Location and surroundings of the test house (source: maps.google.com).

2.2 Wall constructions and variants

2.2.1 Basic variants (north and south facades)

For the field test, various wall elements were installed on the main facades (N and S) of the test house and equipped with sensors. All wall assemblies were timber frame construction with varying cavity insulations, façade systems and render surface colours. Figure 4 shows a rough overview of the south and north walls of the test house including position numbering, cavity insulation and façade design of the variants. A total of 5 materials with several product variants were used for the cavity wall insulation:

- Fibreglass (no product variation)
- Wood fibre (wood fibre mat, wood fibre blow-in insulation)
- Cellulose (no product variation)
- Sheep wool (λ_{10dry} = 0.039 W/mK, λ_{10dry} = 0.04 W/mK)
- Straw (no product variation)

The facade was applied in three different variants:

- Render facade with EPS ETICS (luminosity=79, luminosity=17)
- Render facade with wood fibre ETICS (luminosity=79, luminosity=17)
- Ventilated larch wood facade

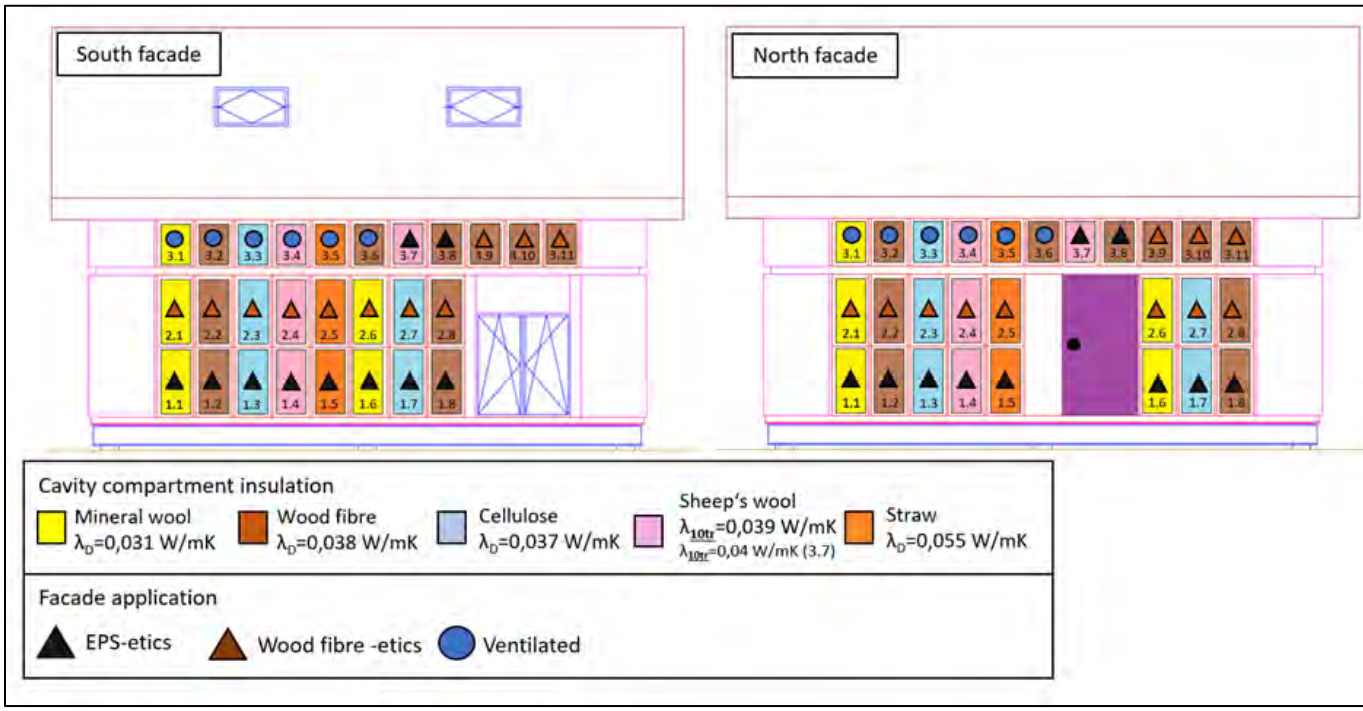

Figure 4 : Facade views south and north with element numbers as well as cavity insulation and facade systems.

In the case of wood-fibre ETICS elements, a variation in density and manufacturing process was also considered:

- Dry process, ρ = 140 kg/m³, λ_D = 0.04 W/mK, d = 100 mm
- Dry process, ρ = 110 kg/m³, λ_D = 0.037 W/mK, d = 100 mm
- Dry process, ρ = 180 kg/m³, λ_D = 0.043 W/mK, d = 100 mm
- Wet process, ρ = 265 kg/m³, λ_D = 0.048 W/mK, d = 60 mm

Figure 5 and Figure 6 show a photograph of the two finished facades after installation of the various wall elements with the different surface colours and facade systems.

Figure 5 :Photo of the south facade.

Figure 6 : Photo of the north facade.

Figure 7 and Figure 8 show all variants in the build-up in detail with the relevant variables (cavity insulation, exterior cladding, facade system and surface colour).

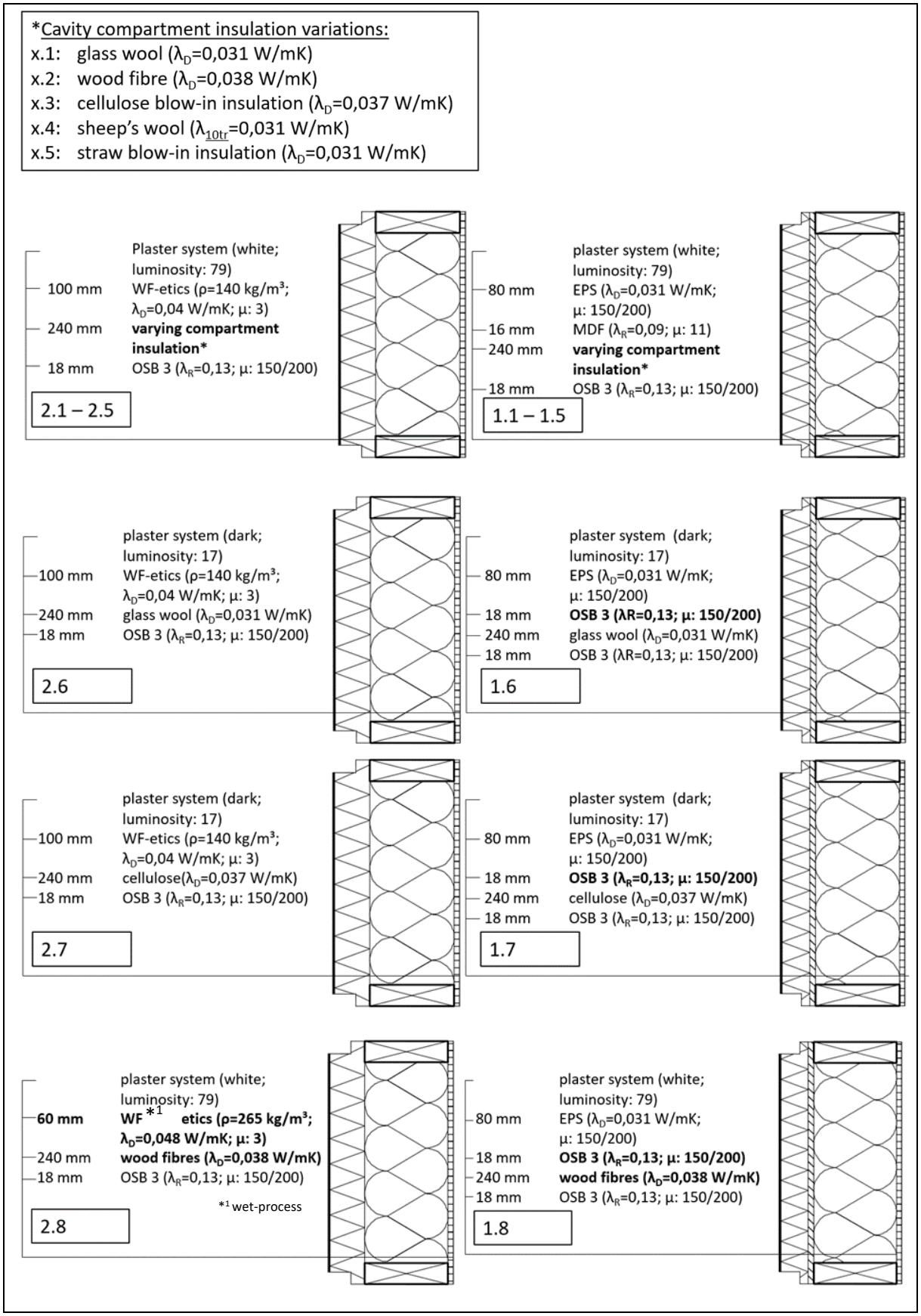

Figure 7 : Build-up and element numbers of the wall elements in the field test (rows 1 and 2).

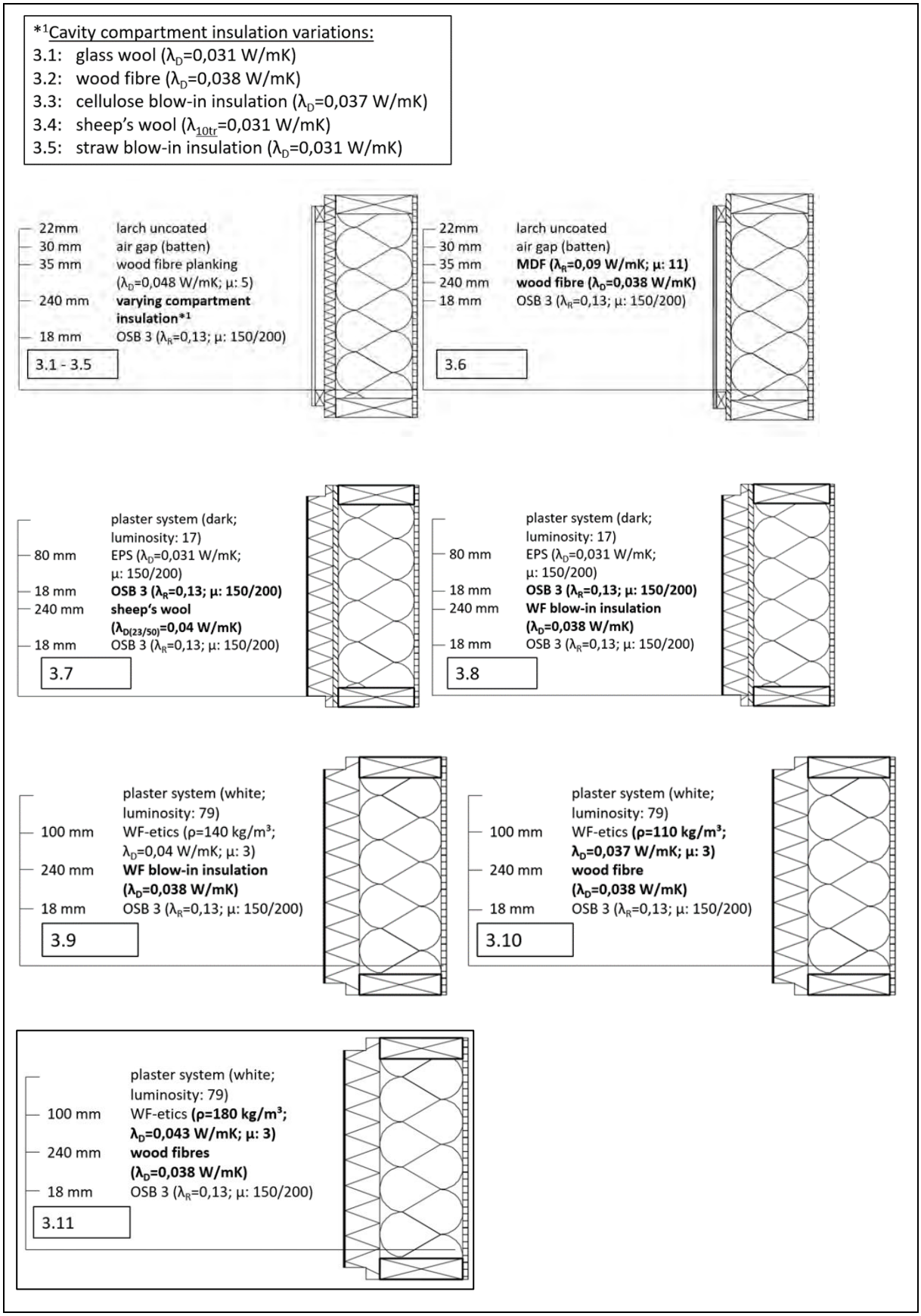

Figure 8 : Build-up and element numbers of the basic variants in the field test (row 3).

To reduce the thermal and hygric interaction of the adjacent elements to a negligible minimum, the element joints were separated with an appropriate hygric and thermal insulation (Figure 9). For thermal separation, a 50 mm thick, circumferential insulation fleece was used. The hygric insulation was ensured by a suitable, vapor-tight adhesive tape.

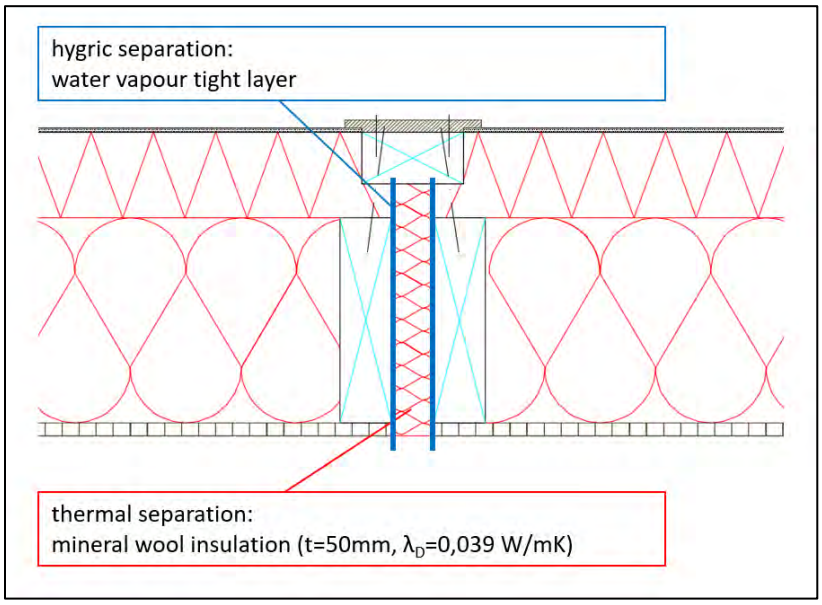

Figure 9 : Design of element joints with thermal and hygric separation.

2.2.2 Special variants (west facade)

In addition to the basic variants, four special additional variants were defined, and set on the west side of the test house (Figure 10 and Figure 11).

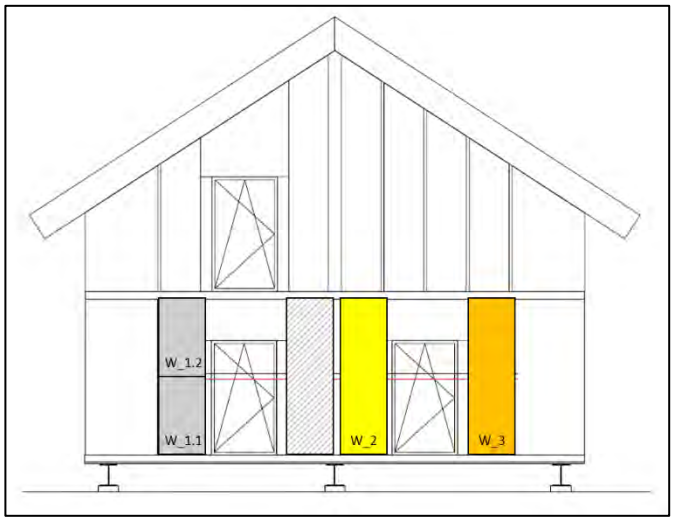

Figure 10 : Element positions on the west side

Figure 11 : Photo west facade

The respective build-up of the special variants is shown in Figure 12. The variants W_1.1 and W_1.2 are masonry elements with wood fibre ETICS facade. Variant W_2 is a special

renovation structure with exterior cladding made of airtight foil laminated gypsum fibre boards. The W_3 structure is based on natural materials, in which the 280 mm straw-chip insulation was inserted using a press-in process. This process ensures that the individual pieces of chopped straw remain preferably parallel to the plane of the wall. Due to this method, a minimization of the thermal conductivity, normal to the wall plane is expected.

The thermal and hygric insulation of the wall element joints was also carried out on the west façade in the same way as for the basic variants according to Figure 9.

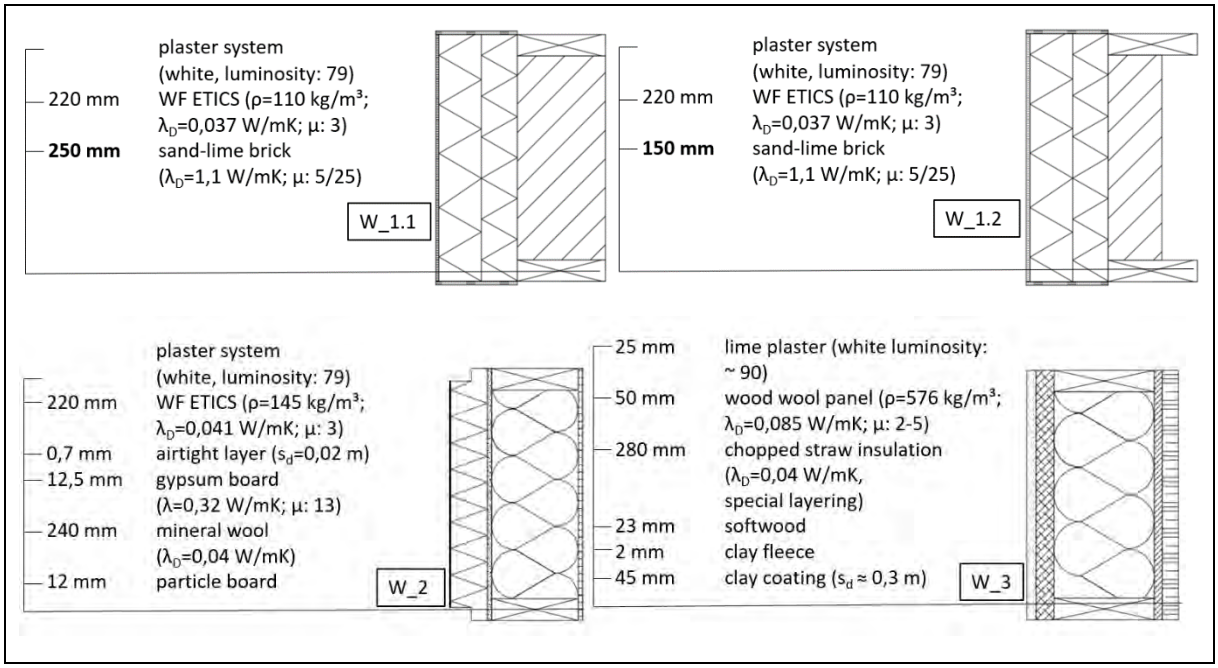

Figure 12 : Build-up and element numbers of the special variants in the field test (west facade).

2.3 Measurement and sensors

2.3.1 Outdoor climate

The recording of the ambient climate around the test house in Stetten was carried out using Ahlborn FHAD 46-C4AG sensor (temperature, humidity, air pressure), FMA-510 Meteo Multigeber (wind direction, speed) and Ahlborn FLA 613 GS sensor (global radiation) (Figure 13). These measurement instruments were mounted on the freestanding flat roof of the Akustik Center Austria (ACA) at the test house site (Figure 14). The measured ambient climate data were recorded using a data logger (Ahlborn ALMEMO 2890) at 10-minute intervals. The ambient climate was recorded from 16.12.2021 till 31.01.2022.

Figure 13 : Individual components of the weather station

Figure 14 : Weather station on the roof of the ACA in Stetten

2.3.2 Component and internal climate

Various types of sensors were used to record the climate inside the wall structure. An overview of sensor positions and types is given in Figure 15 Depending on the build-up, the cavity temperatures were measured at two or three relevant positions in the component. The measurement was carried out using NTC sensors and thermocouples (NiCr). For all basic variants in frame construction, as well as for the special variant W_3, the temperature was measured on the outside of the interior cladding (position: "i"; sensor: NTC). On the outside of the cavities temperature and RH were recorded (position: "a"; sensor: NTC/capacitive). For all elements with ETICS, the temperature was recorded between the render and insulation layers (position "P"; sensor: NiCr). For the structures with wood fibre ETICS, the humidity was additionally recorded at this position (sensor: balsa - see chapter 2.3.2.2).

Parallel to the climate recordings in the building component and in the outdoor area, the indoor climate was recorded in the ground floor and upper floor of the test house. The T/RH combination sensors were used on both floors at a height of approx. 1.50 m (floor distance) which recorded the temperature (NTC) and humidity (capacitive) respectively. In addition, the near-surface temperature was recorded at a distance of 10 cm from the wall surface on the north and south sides of both floors.

The winter target temperature in the interior of the test house was 22 °C. During the summer months, the interior was not actively cooled. The exterior shading was continuously active at that time to protect the interior from excessive solar radiation gains. There were no interior

loads until 10/19/2021. From this day on, the humidity in the interior was controlled between 60% to 65% RH to apply a high humidity load during the second cold period.

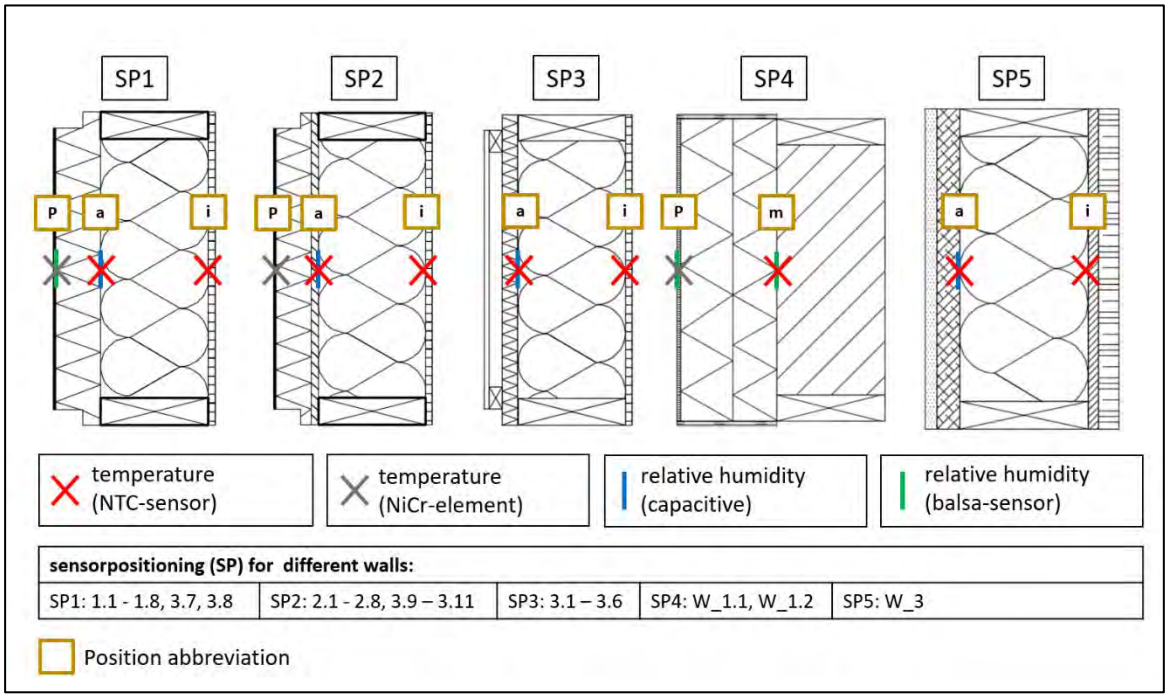

Figure 15 : Overview of sensor positions and types in the component cross-section. Details of corresponding wall element numbers and position abbreviations.

2.3.2.1 Simulation-based measured value correction

In the course of the recording, a simulation-based temperature comparison at measurement position "a" revealed that the frontal insertion of the sensor (Figure 16) leads to an increased temperature directly at this position due to a thermal bridge effect at large temperature differences between the exterior and interior (Figure 17). At a surface temperature difference of about 29 K between the interior and exterior surfaces in March 2021, the simulated and measured temperatures differed by as much as 4 K. The measured temperature differed from the simulated temperature. Whereby the measured temperature showed the higher value.

The effect of this thermal bridge was underestimated, since the expected influence is negligible when viewed over the whole component. Since in this case measurements were taken directly at the position where the thermal effect is maximum and the sensor head itself is firmly connected to the bridge (no contact resistances), this led to the deviations described above.

The simulation models of the main variants on the north and south sides showed very good agreement with the heat flow measurements carried out (see chapter 4.3). Using the simulation models of variants 1.1 and 2.1, the temperature curve at measurement position "a" was corrected. These variants were chosen because they showed the best agreement between heat flow measurement and simulation. They also have the lowest U-value of the comparison variants. Therefore, the lowest temperatures are to be expected at position "a" for these variants. Therefore, the adjustment of the relative humidity based on these correction

temperatures was on the “safe side” for each main variant (1.1 - 1.5 and 2.1 - 2.5). The correction of the relative humidity was carried out variant-specifically. For this purpose, the measured course of the water vapor partial pressure was related to the corrected temperature course in each case. In the case of variants with significantly higher U-values, this may result in a sbright overestimation of the relative humidity.

For the ventilated variants, as well as for variants W_2 and W_3, no simulation-based measured value correction could be performed. These variants were therefore omitted from the evaluation of the climatic conditions.

Figure 16 : Frontal installation of the combination sensors (measuring position "a").

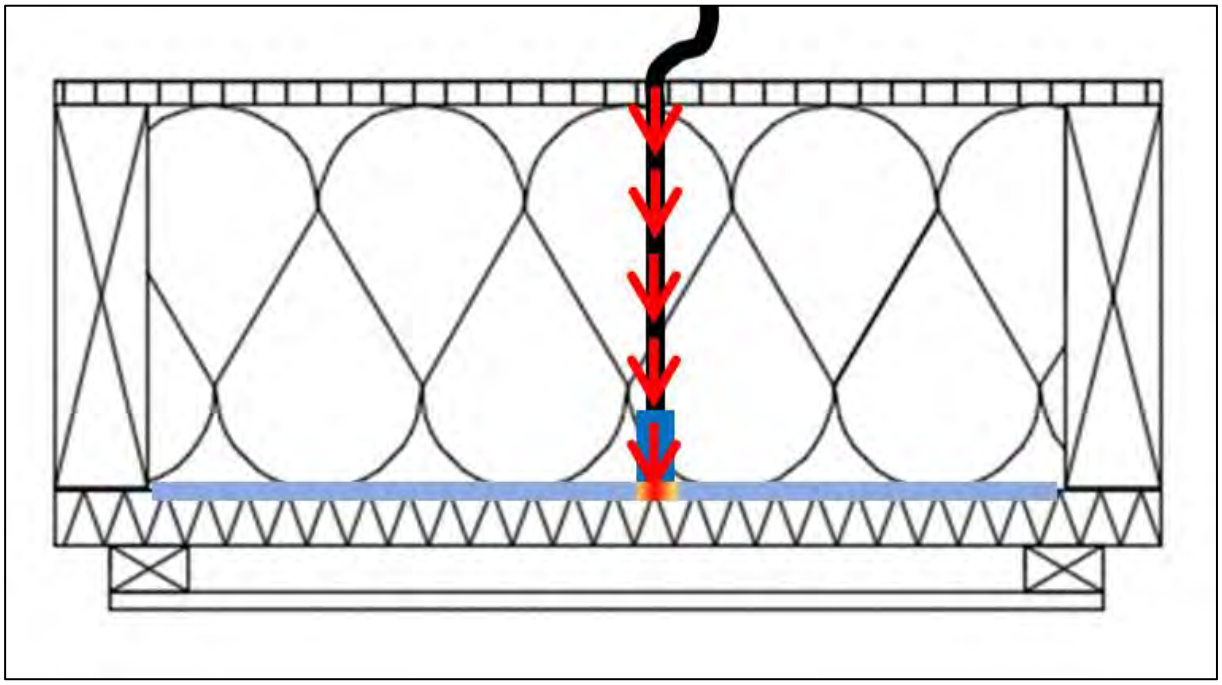

Figure 17 : Schematic sketch of the thermal bridge effect due to frontal installation.

2.3.2.2 Humidity recording by means of balsa wood sensor

The RH in the pores between the render and the ETICS insulation layer (position: "P") was measured with specially made balsa sensors (Figure 18) in combination with a temperature measurement (NiCr). In principle, this was a resistance measurement, as it is also performed for wood moisture measurement. This method is based on the dependence between the moisture content (and temperature) and the ohmic resistance of different types of wood. Since the moisture content of a hygroscopic material is dependent on the ambient climate (equilibrium wood moisture content), there is also an indirect dependence of the ohmic resistance on the ambient climate. In this case the dependence was instrumentalized to calculate the relative humidity at the respective measuring position on basis of the temperature and the ohmic resistance.

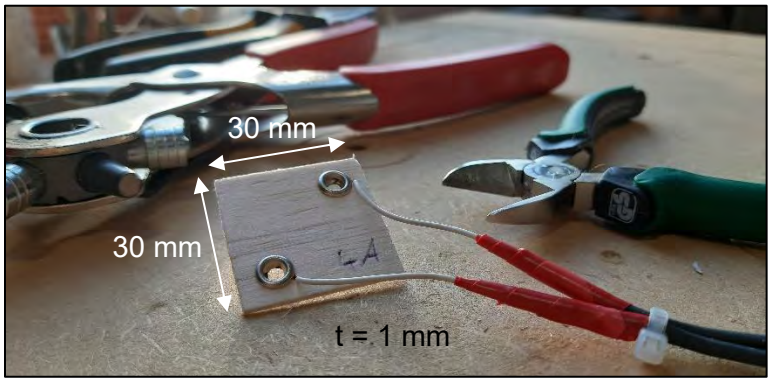

Figure 18 : Balsa sensor with dimensions

To ensure a fast response of the ohmic resistance (or the moisture content) to the transient, fluctuating ambient humidity conditions in the wall structure, very thin balsa wood samples were used (d = 1 mm). Using a total of 8 sensors, a calibration representative for all balsa sensors was performed in the climatic chamber at various climatic conditions (1 °C, 5 °C, 10 °C, 15 °C, 20 °C, 25 °C, 30 °C, 40 °C, 50 °C each with 20%, 30%, 50%, 80%, 90%, 95% RH). Each climate was held for at least 1 hour. The last 20 minutes of each climate interval were used for evaluation. The result of the calibration was the average isotherms of relative humidity as a function of ohmic resistance (Figure 19). With the help of these isotherms, the relative humidity beneath the render layer in the building component should be calculated with sufficient accuracy in the range between 60% RH and 100% RH.

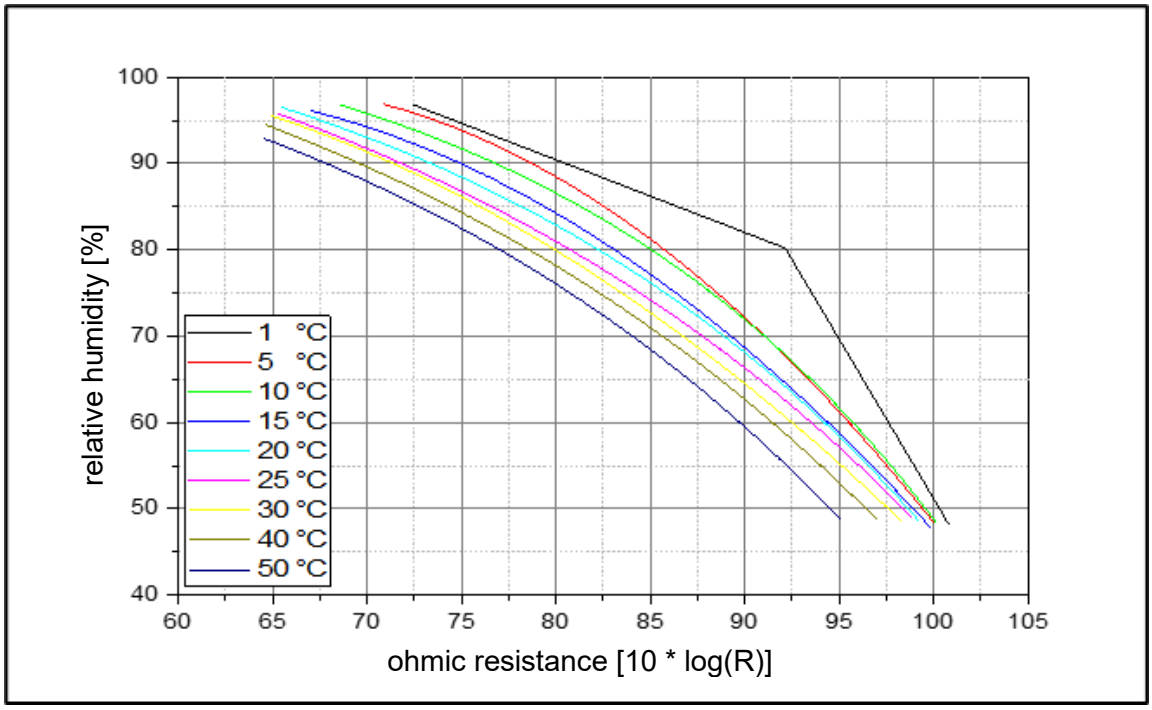

Figure 19 : Isotherms of relative humidity as a function of ohmic resistance

2.3.3 In-situ heat flow measurement

In addition to the climatic recordings, heat flow measurements were carried out on the test wall structures from October 2021. The measurements were divided into seven variant constellations. In each of these constellations, the heat flows of ten to twelve elements were recorded in parallel to ensure direct comparability between the variants. The heat flow meters were applied to the interior cladding. Figure 20 shows an example of the measurement setup at constellation 1 with ten measurement points / variants. To enable optimum contact between the heta flow meters and the OSB interior cladding, each plate was coated with thermal paste (λ = 6 W/mK) (Figure 21).

Figure 20 : Measurement setup of a heat flow measurement with heat flow meters and surface temperatures (constellation 1).

Figure 21 : Heat flow meter with applied thermal paste (λ = 6 W/mK).

In parallel, the external and internal temperatures were recorded at the wall surfaces (outside→ temperature beneath the render layer), as well as near the surface (distance approx. 10.5 cm) (Figure 22, Figure 23). The exact sensor scheme depending on the façade variant is shown in Figure 24.

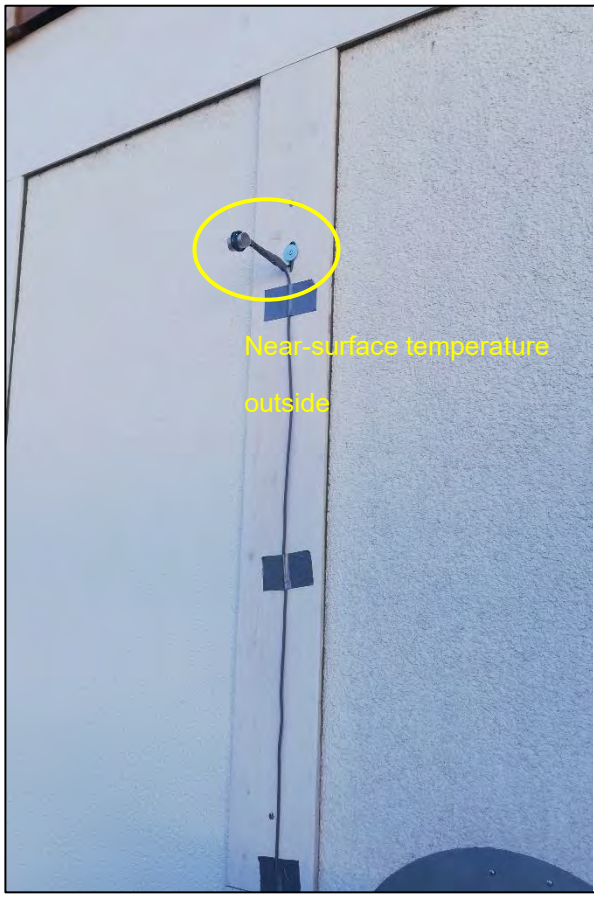

Figure 22 : Near-surface temperature sensor on the outer surface with radiation shield made of aluminium.

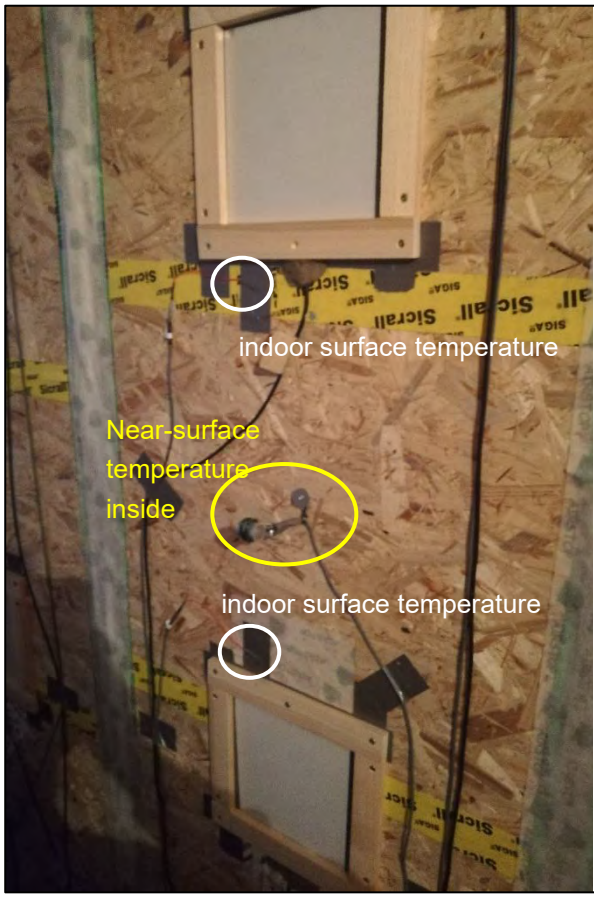

Figure 23 : Sensors on the inner surface of the test elements: near-surface temperature, surface temperatures and heta flow meters.

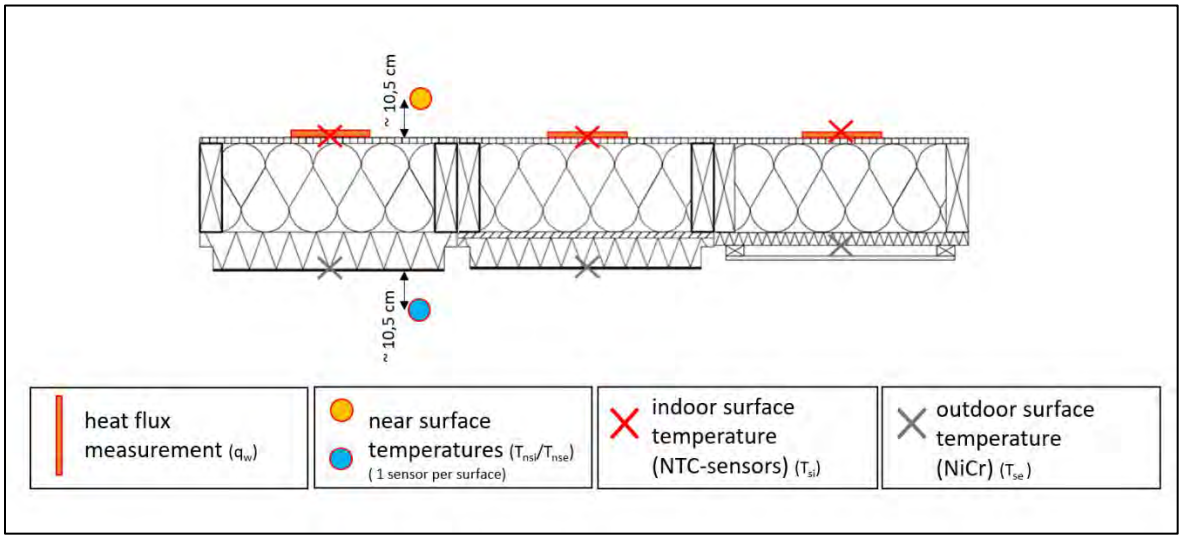

Figure 24 : Applied sensor scheme depending on the facade design of the measured variants.

From the recordings, the dynamic heat transfer coefficient (Λ-value) was calculated according to Equation 1 and used for qualitative comparison of the build-up variants.

$$\Lambda = \frac{q_w}{T_{si} - T_{se}} \quad (1)$$

$\Lambda \rightarrow heat\ transfer\ coefficient\ of\ the\ wall\ \left[\frac{W}{m^2K}\right]$

$q_w \rightarrow\ average\ measured\ heat\ flux\ considering\ the\ whole\ measurement\ period\ \left[\frac{W}{m^2}\right]$

$T_{si}, T_{se} \rightarrow surface\ temperatures\ (interior, exterior)\ [K]$

In addition to the comparison of build-ups with different insulation materials (cavity insulation, ETICS insulation), also orientation variants (north and south), façade variants (ventilated / WDVS), and colour variants (render colour) were compared. Table 1 lists the different constellations and their focus (comparison variables).

Table 1 : Overview of the heat flow measurement constellations K1 to K7, each with date, runtime and those variables on which the focus is placed during the comparison.

	Date [from-to]	**Runtime [h]**	**Comparison variables**
K1	13.10.21-24.10.21	264	- ETICS system (wood fibre, EPS) - comparison of insulation materials in the cavity (mineral fibre, wood fibre, cellulose blow-in insulation, sheep wool, straw blow-in insulation).
K2	28.10.21-08.11.21	264	- Facade design (ETICS, ventilated) - Wood fibre ETICS density (140 kg/m³ - 180 kg/m³)
K3	09.11.21-20.11.21	264	- Render paint (HBW 79 / HBW 17) - Wood fibre ETICS Density or manufacturing process (140 kg/m³ - 240 kg/m³ or dry process and wet process)
K4	26.11.21-07.12.21	264	- Comparison of orientation for ETICS facade (north, south)
K5	08.12.21-19.12.21	264	- Comparison of orientation for ventilated variants (north, south) - Comparison of insulation materials in the cavity (wood fibre, sheep wool, straw blow-in insulation, wood fibre blow-in insulation) - Comparison of wood fibre ETICS density (140 kg/m³ / 110 kg/m³ / 180 kg/m³)
K6	22.12.21-02.01.22	264	- Comparison of alignment for ventilated and ETICS variants (north/south) - special structures (W_2, W_3)

K7	05.01.2022- 01.02.2022	648 h	- ETICS system (wood fibre, EPS) - comparison of insulation materials in the cavity (mineral fibre, wood fibre, cellulose blow-in insulation, sheep wool, straw blow-in insulation) - Special constructions (W_2, W_3) - Period (264 h, 672 h or comparison K1 and K7)

2.4 Aim of the field tests

The aims of the field investigations can be summarized as follows:

1. Collection of measurement data on a real-scale building for qualitative comparison of the considered variants among each other with regard to hygrothermal performance (thermal conductivity, durability)
2. Comparison of the results from the laboratory tests on thermal conductivity with the empirically measured data from the field investigation.
3. First practical application of the developed wood decay prediction model to empirical measurement data.

At 1.) Unlike in the laboratory, the whole range of influencing parameters influences the individual component behaviour during a field test on a real scale. This also includes those that are not recorded (e.g. occurring turbulent flows/vortexes, reflections due to the environment, etc.). These effects were not recorded in the present study. The influence of these random variables is nevertheless included in the recorded measured values. The field test is therefore a good method for making comparative statements about the hygrothermal performance of the underlying component variants in the real application case, in which many influencing variables overlap that cannot be reproduced in their entirety in the laboratory.

At 2.) The comparison of the laboratory tests with the empirically measured data allows insights into the applicability of the λ-values (thermal conductivity) determined in the laboratory to the real application.

At 3.) Based on the newly developed model for the prediction of wood decay, predictions are made for wood or cellulose decay in the different variants of the field test. For comparison, a selection of insulation samples are taken from the elements and visually examined for wood decay fungi.

3 Durability of natural fibre insulation materials

3.1 Laboratory tests for durability

3.1.1 Description of experiments

In test series in the laboratory, wood fibre materials were compared with solid wood (Figure 25). They were inoculated with various wood decay fungi and exposed to different combinations of relative humidity and temperature. The following materials were investigated:

- Fibre insulation board, wet production process, 160 kg/m³ [A in Figure 25]
- Fibre insulation board, dry prod. process without hydrophobic agent, 150 kg/m³ [B].
- Fibre insulation board, dry prod. process with hydrophobic agent, 110 kg/m³ [C].
- Cellulose fibre, 50 kg/m³ [D].
- Pine sapwood, reference (*Pinus sylvestris*) [E].

The specimen size was 50 mm x 50 mm with 40 mm thickness for the insulation materials and 10 mm for the reference wood specimens. The specimens were provided with three holes of about 6 mm diameter to fit the dowels incubated with fungal culture. For each material, 84 specimens were examined.

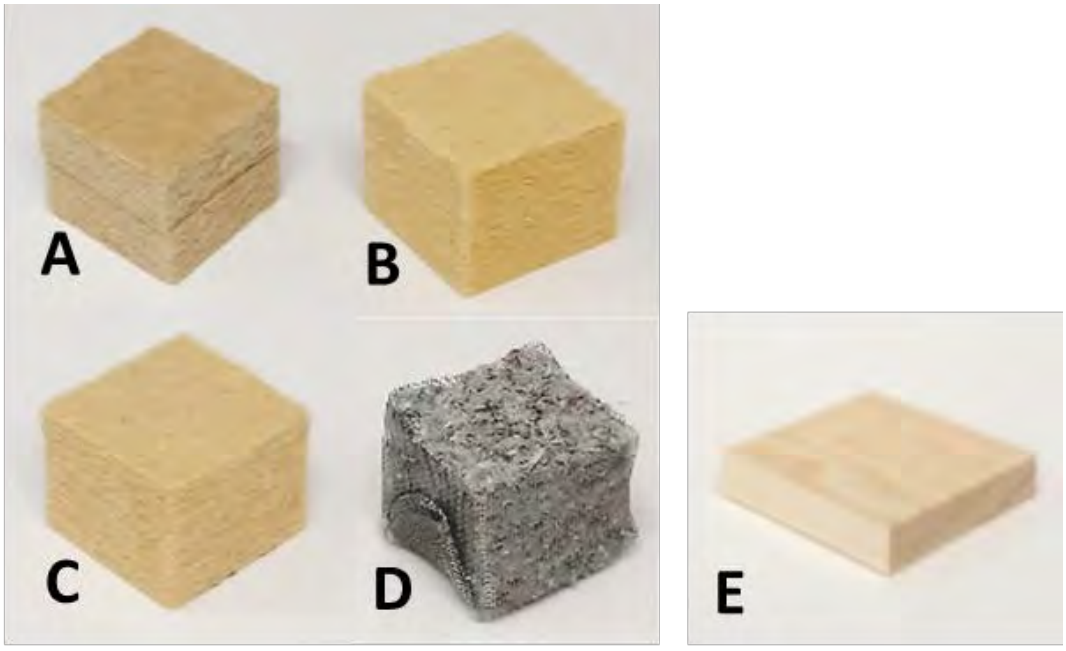

Figure 25 : Investigated wood fibre insulation materials (left) and reference pine-sapwood (right).

First, the specimens were dried in a drying oven at 60 °C with continuous ventilation with pre-dried air for 48 hours, and then the dry mass was determined. In many investigations such as [5, 17, 18] and also according to some standard procedures (e.g. EN 113-1 [19]), the wood samples are dried at 103 °C for 24 hours. Since it cannot be excluded that such high temperatures in fibre insulation materials could change the material properties and thus effect the resistivity against wood decay fungi, a lower temperature with a longer duration is used here. This procedure was already proven to be applicable for the determination of hygrothermal material parameters in the IBP laboratory.

The following species of wood decay fungi were used:

- *Coniophora puteana*. Common standard test fungus with high decomposition potential; causes brown rot.
- *Trametes versicolour*. common standard test fungus; causes white rot.
- *Schizophyllum commune*. According to literature, high affinity for fibrous materials; causes white rot.

For inoculation of the test specimens, the fungi were first grown on malt extract agar. 1 cm long "dowels" of untreated softwood were placed on the mycelium (without contact to the agar) and incubated for four weeks (Figure 26). After sterilization with gamma radiation, the specimens were first conditioned in the target climates until equilibrium moisture content was reached and then provided with one dowel per organism, i.e. a total of three dowels per specimen.

Figure 26 Preparation of infected wooden dowels (left: *Schizophyllum commune,* top right: *Coniophora puteana*, bottom: *Trametes versicolour*) and specimen "inoculated" with dowels.

Subsequently, they were incubated in incubation units (tightly sealed box, cf. Figure 27) for a maximum duration of 12 months under the following climatic conditions:

- 97% RH at 10 °C, 15 °C, 25 °C and 30 °C
- 100% RH at 10 °C and 15 °C

To adjust the moisture contents, trays filled with suitable liquids were placed in the incubation units. Potassium sulfate salt solution (K_2 SO_4) was used for 97% RH and distilled water for 100% RH.

Figure 27 : Incubation unit with inoculated specimens. The tray filled with salt solution or distilled water is located under the metal grid.

Three test specimens were taken at defined intervals and weighed to determine the sorption moisture. They were then dried again at 60 °C for two days and the mass losses were determined. The times at which the samples were taken are shown in

Table 2. The samples of the reference specimens made of pine-sapwood were also tested for comparison at boundary conditions at which a significant loss of mass is to be expected based on previous data from the literature: at the higher temperatures of 25 and 30 °C in combination with 97% RH, and at high relative humidity of 100% RH also at 15 °C.

Table 2 : Climates and sampling for mass loss determination of the fibre insulation specimens.

Climate		Sampling after
Temperature	RH	
10 °C	97%	6, 8, 10, 12 months
	100%	4, 6, 8, 10 months
15 °C	97%	5, 7, 9, 12 months
	100%	3, 5*, 7, 10* months
25 °C	97%	4*, 6* weeks and 2*, 3*, 5*, 8* months
30 °C	97%	3*, 5*, 7*, 10* weeks and 4*, 6* months

* additional sampling of the reference pine sapwood specimens

3.1.2 Results

The insulation samples, incubated at 25 °C and 97% RH and not inoculated with fungi (correction samples), showed only minor mass losses after 7 months. The highest mass losses occurred in the dry insulation board without hydrophobic agent with 2.4 % by mass. Only the mass of the reference pine-sapwood, remained unchanged during the incubation period (Table 3). The reasons for the mass losses of the fibre specimens could not be investigated further within the project. But one can assume, that either volatile compounds were outgassed from the insulation materials or that additives, introduced during production, were dissolved by the moist environment during incubation.

In any case, this loss of mass, which is not caused by biogenic degradation, must be considered for the evaluation of the results of the incubated specimens. Therefore, the material specific correction values in Table 3 are used and subtracted from the mass losses of the inoculated samples. Figure 28 shows an example of the tests carried out at 25 °C and 97% RH.

Table 3 : Mass losses of insulation and wood samples not inoculated with fungi (correction samples) after 7 months of incubation at 25 °C and 97% RH.

Material	**Mass loss [%]**
Wet fibre board without hydrophobic agent	0,7
Dry fibre board without hydrophobic agent	2,4
Dry fibre board with hydrophobic agent	1,1
Cellulose fibre with boron salts	0,5
Pine sapwood (Reference)	0,0

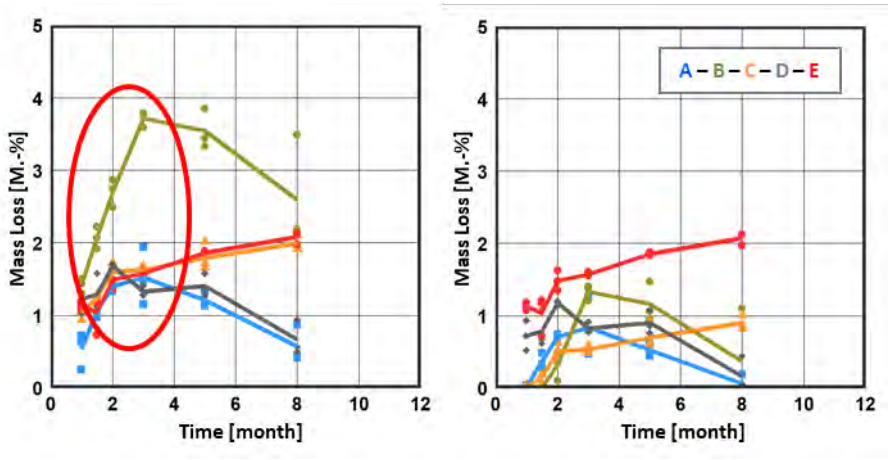

Figure 28: Mass losses of the samples incubated at 25 °C and 97% RH total (left) and corrected by the mass losses from Table 3 (right). (A = wet process; B = dry process without hydrophobic agent; C = dry process with hydrophobic agent; D = cellulose; E = pine sapwood).

The unrealistic “decreases” in mass loss (mass gains) between months 3 and 8 in Figure 28 could be explained with a typically large variance at biological measurements. Here about 1.5% by mass seem to apply. Therefore the range up to 1.5% by mass is used as uncertainty range of the measurement and indicated in rad in Figure. 29 and Figure. 30.

Another experimental uncertainty results from the RH control at 97% by means of a saturated K_2SO_4 solution, as described in section 3.1. Due to the temperature dependence, a RH of 98.2 ± 0.8% is obtained at 10 °C, 97.9 ± 0.6% at 15 °C, 97.3 ± 0.5% at 25 °C, and 97.0 ± 0.4% at 30 °C [20]. The target relative humidity could therefore not be adjusted exactly but varies between approx. 97.0 and 98.2 depending on the temperature.

The results of the laboratory tests are shown in Figure 29 and Figure 30. At 97% RH and temperatures of 10 °C, 15 °C, 25 °C and 30 °C no or only marginal mass lass was observed. Apart from a single outlier value (wet insulation board without hydrophobic agent) at 15°C after about 6.5 months), all mass losses remained below 1.5% by mass. Even at temperatures of 25 °C and 30 °C, which are favourable for fungal growth, the maximum mass losses of 1.5% by mass were within the range of measurement inaccuracy and in all cases below the determined mass loss of the reference pine sapwood samples.

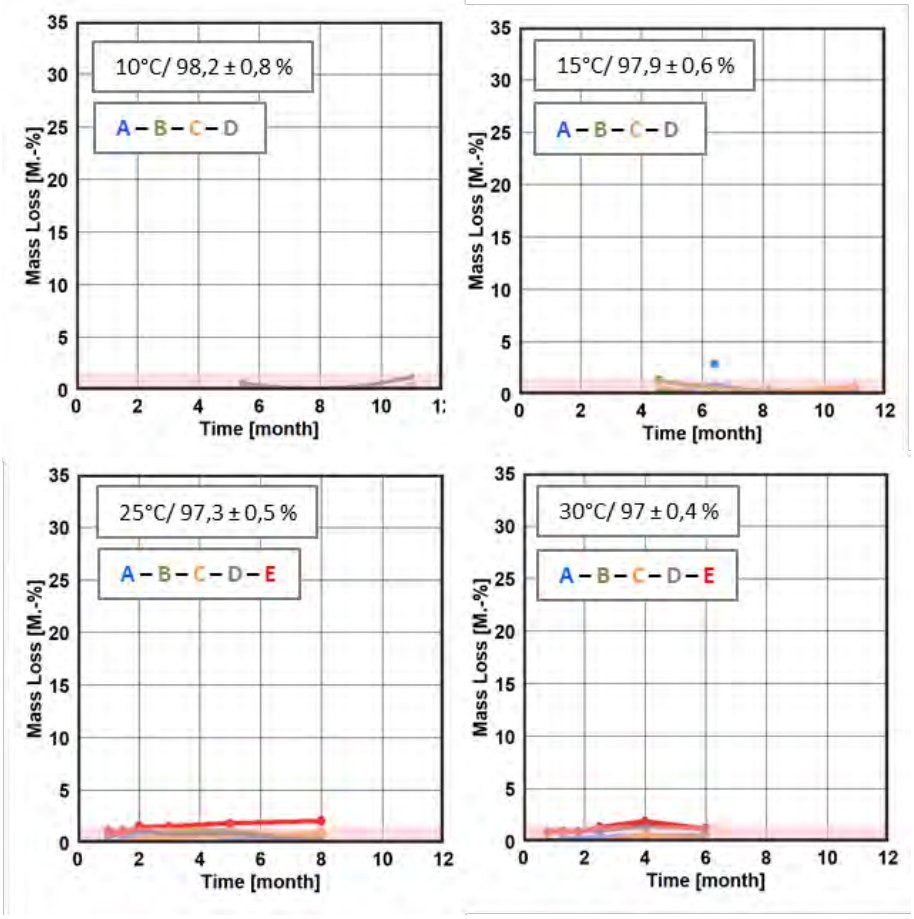

Figure 29 : Corrected mass loss of the samples incubated at 25 °C and 97% RH (A = wet process; B = dry process without hydrophobic agent; C = dry process with hydrophobic agent; D = cellulose; E = pine sapwood).

At 100% RH and 10° / 15°C, the cellulose fibre ("D" in graphs) did not show any mass loss at any time. The two dry insulation bords without and with hydrophobic agent (B and C) showed minor mass losses over time. The impregnated insulation material performed slightly better than the non-hydrophobized one. However, both insulation boards showed lower mass losses than the pine-sapwood reference. Only the wet insulation board without hydrophobic agent showed higher mass loss than the pine sapwood reference at 100% RH and 10°C / 15°C.

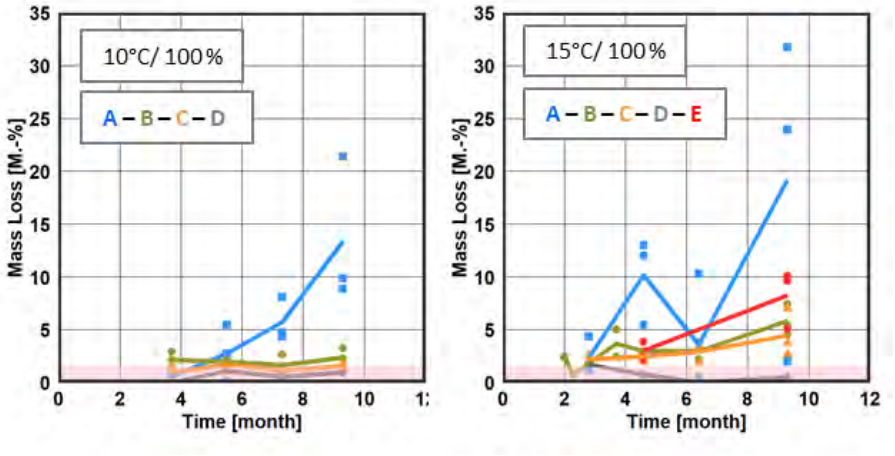

Figure 30 : Mass losses of the tests conducted at 10 °C and 15 °C and 100% RH.
(A = wet process; B = dry process without hydrophobic agent; C = dry process with hydrophobic agent; D = cellulose; E = pine sapwood).

It should be noted that in the present investigation, hardly any mass loss was observed at 97% RH at 10 and 15 °C, respectively. However, in [17] at 97% and [18] already at 94% RH significant mass losses were reported. This discrepancy is found throughout the literature: some authors state that no mass loss is possible at such humidity levels, while others already measure it. But often they also point out the uncertainty of RH control, the occurrence of dew water during the tests as well as possible other sources of moisture that could cause higher humidity contents in the specimens than the equilibrium moisture content at the targeted RH.

A comparison with further information from literature in Table 4 shows that studies with incubation and additional nutrient supply produce the greatest mass losses of 6 to 15% by mass per month (studies 3 to 8 in the table). At incubation without additional nutrient supply the mass loss remains significantly lower with per month only 1 to 4% by mass (studies 9 to 11). Even lower mass losses of 0.03 to 0.6% per month were measured in the tests without inoculations in which "normal" establishment of fungi via spores (tests 1 and 2) was waited for - although extremely high wood moisture contents of 40 to 70 M-% were reached. However, the test conditions also differ with respect to other test parameters such as temperature, humidity and the ratio of fungal mass to specimen mass. Also the species of fungi as well as the wood specimens types differed. The used softwoods, grown slowly in cold climates, are considered more resistant than those grown faster in warm climates. Therefore, each constellation may lead to different results, which makes a uniform interpretation very difficult.

Table 4 : Comparison of investigation methods and wood degradation rate. The wood degradation rate is calculated based on the investigation results of literatures (No. 1-9) and from the investigations conducted in this project (No. 10-11). For intuitive comparison, the wood degradation rate is shown with gradually more intense colour scalar.

No.	Wood type	Wood decay fungi type	Incubation	Specimen size [mm]	Temperature	RH	Wood rot rate [% by mass / month]	Source
1	*Tsuga canadensis* (Canadian helmlock) 40% by mass	not determined	Exposed to untreated room air	50 x 60 x 20	28 ° C	~ 100%	0.03	[21]
2	*Tsuga canadensis* (Canadian helmlock) 70% by mass			50 x 60 x 20		~ 100%	0.6	
3	*Pinus densiflora* (Japanese red pine)	*Fomitopsis palustris*	Laid on the grown mycelium on agar	n.s.		n.s.	15.0	[22]
4	*Cryptomeria japonice* (Sickle fir)			5 x 5 x 20		n.s.	9.8	[23]
5	*Cercidiphyllum japonicum* (Japanese cake tree)			5 x 5 x 20		n.s.	13.7	
6	*Picea* sitchensis Sitka spruce)			20 x 20 x 100		~ 100%	13.0	[24]
7		*Trametes versicolour*				~ 100%	8.6	
8	*Picea abies* (spruce)	*Coniophora puteana*	5 x 5 mm² mycelium with agar placed on top of samples.	7 x 15 x 50		100%	6.2	[17]
9	*Pinus densiflora* (Japanese red pine)	*Fomitopsis* palustris	After establishment of mycelium on samples separated from agar.	20 x 20 x 20		100%	4.4	[25]
						97%	0	
10	*Pinus syrvestri*	*Coniophora puteana, Trametes versicolour, Schizophyllum commune*	Plugged with dowels already established by a fungi	40 x 40 x 10	15 ° C	100%	1.0	current
11					30 ° C	97%	0.2	

*WG = water content

While a significant external nutrient supply in building materials is unlikely, the presence of small amounts of mycelium cannot be excluded in individual cases. The incubation scenario,

chosen for the current project, therefore seems more reasonable than the test procedures without any incubation, but closer to real life than the results of the investigations with additional nutrient transfer.

The delay until the start of mass loss is also difficult to quantify. Here, in some studies, only a mass loss of 5% by mass is considered significant, while other studies preferred 3% by mass. However, in the current project, a more careful limit of 1.5% by mass was chosen to indicate start of decay.

3.2 Limit curves and development of a transient prediction model

From the laboratory tests temperature- and moisture-dependent limit curves (limit isopleths) for natural fibre insulation materials of different resistance. These are based on the results, previously obtained at IBP in the context of [26] as well as on the principal shape of fungal isopleths determined for mould fungi within [27]. Based on the lower limit isopleths, from which wood decay fungi can just begin to grow, the growth rate can then be indirectly predicted via the mass losses relevant for the assessment using the transient prediction model WUFI® Decay, which is currently under development.

3.2.1 Previous research on minimum growth requirements.

Figure 31 shows the range of limit curves representing the minimum growth conditions for wood decay fungi according to the results of the investigations carried out at IBP in 2016 [26], according to the results from Viitanen [28] and the curve currently used for design purposes according to WTA guideline 6-8 [7]. All limit curves refer to the growth conditions of decay fungi in pine or spruce sapwood.

The area below the gray limit curve according to Viitanen [28] was initially indicated by the author as permanently safe for avoiding mass loss in softwood by decay fungi. However, at that time, from corresponding standards, typically a mass loss of 5% or more was considered significant. That means, when interpreted more precisely, that below the curve, not no material loss at all, but no more than 5% by mass is to be expected. Accordingly, Viitanen also provided somewhat lower curves in later publications to ensure no growth at all.

Based on the studies of Viitanen, a temperature-dependent limit curve (green dotted line) for design purposes was established for timber construction design by hygrothermal simulation in WTA guideline 6-8 in 2016 [7]. This limit curve, developed in [29] contains recognizably higher safeties than the original curves mentioned before. Since the course of fungal isopleths is normally not linear, a typically shaped isopleth curve (green solid line) was supplemented.

The area between the two dark blue curves represent the examined conditions in [26].The lower curve stands for the highest tested conditions where no wood decay fungal activity

(detected by increase in CO_2 concentration) was yet detectable. The upper curve then shows the conditions where first fungal activity was measurable. The shaded area was not investigated in more detail - so the actual lower limit curve should probably be somewhat higher than the lower dark blue curve, nevertheless this will be used as a basis for further investigations as a lower limit with additional security.

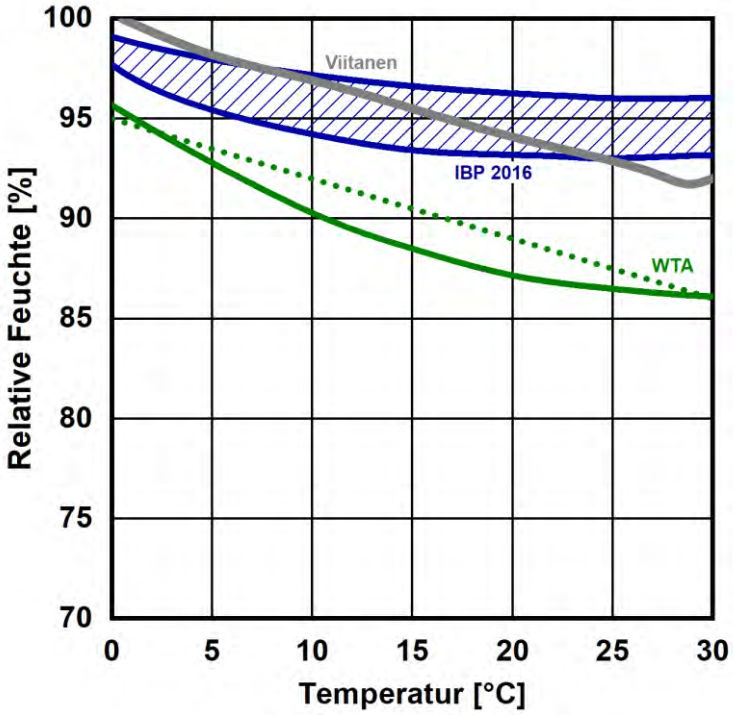

Figure 31 : Minimum combinations of temperature and relative humidity indicated as necessary for the degradation of solid wood in various sources.

Since already in the project In2EuroBuild [30] it was found that some wood fibre insulations are as or even more resistant to fungal attack than solid wood, it is assumed that this curve is also suitable and can be used as a limit curve for such natural fibre materials.

3.2.2 Determination of limit curves for natural fibre insulation materials

The reference wood test specimens measured as part of the current project confirm the reliability of the limit curve for solid wood from the previous IBP project from 2016. Material degradation was not detected in any case for the conditions lying below the lower dark blue limit curve - on the contrary, this was even not the case for some temperature and RH combination lying significantly above the limit curve, even over several months. The difference to previous investigations [28] and reason for the more favourable results could lie, among other things, in the fact that the inoculation was not performed by a direct transfer of mycelium parts (together with some growth medium), but by a transfer of overgrown softwood dowels, which were previously laid on top of the mycelium in the petri dish without contact to the growth

medium. This has two effects: no additional nutrients are transferred and the ratio of fungal mass to specimen mass is lower. The lack of growth medium may retard the initial growth, and the lower ratio of fungal mass to specimen mass reduces the mass loss. Therefore it can be assumed that each experimental scenario results in slightly different durations until start of the wood decay and in different mass loss rates.

For the initial growth, however, previously used test scenarios should be on the safe side, since in these cases already living mycelium is brought into contact with the test specimen, while in real life, the fungus must first germinate before it can grow. Accordingly, the lowest limit curve for the growth of wood decay fungi on solid wood can once again be regarded as validated with the new results and can be used both to define the safe area below this limit curve and to predict growth with the new model above the limit curve. For the investigated wood-fibre insulation materials with equal or higher resistance than solid wood, this curve can therefore also be used - accordingly, it is shown in Figure 32 as the "ThermNat II" curve.

However, not all the materials investigated are more resistant than wood. A non-hydrophobic wood fibre insulation board produced in wet process proves to be less resistant than wood, at least at the higher relative humidity of 100% (see Figure 30). It is noticeable, however, that the same board at 97% RH exhibits less mass loss than wood at all but one measurement point (Figure 29). This raises the question of how this material can be treated. So far, the model system assumes that one material is either always more durable or always less durable than another but does not behave differently at different RH. To represent this behaviour in the model, separate curves would be required for each material with the corresponding measurement effort. It is therefore decided to currently stick to the analogy mentioned above and to classify the wet-process panel uniformly as less resistant to wood decay fungi than the solid wood. Since no suitable measurement levels are available here, the ThermNat I curve was set to the level of the WTA curve to be on the safe side. In this case, the limit values are significantly lower at 30 °C, where degradation already starts from 86% RH. Although this is unrealistically low, further, and more detailed investigations would be required to be able to give more realistic progressions. Therefore, this low level currently remains without alternative until further findings are available. Nevertheless, even this limit curve is still significantly higher than the previously available limit value of 18% by mass, which is independent of temperature.

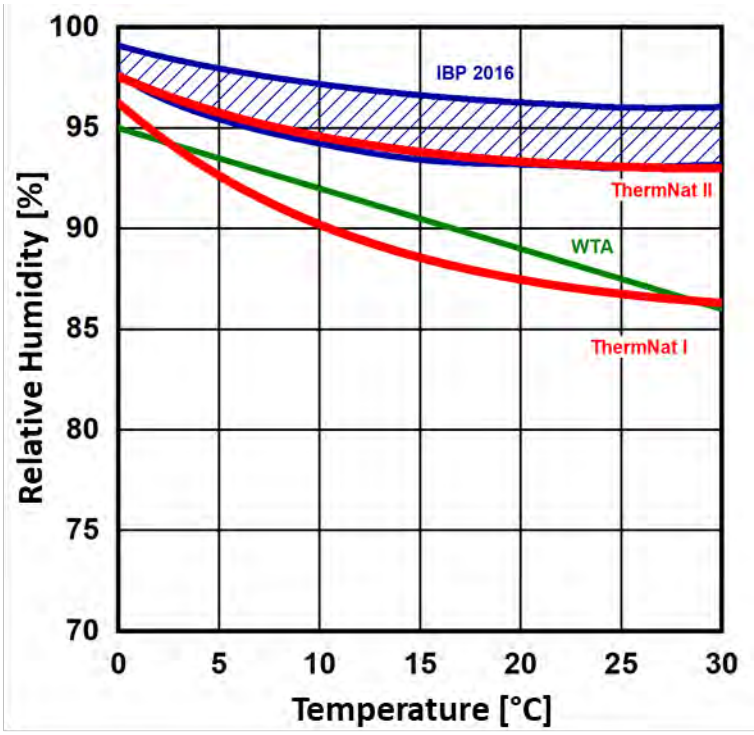

Figure 32 : Newly determined limit curves for solid wood and equally resistant or more resistant natural fibre insulation materials (ThermNat II) as well as lying on the “safe side” for less resistant natural fibre insulation materials (ThermNat I). The limit curves from the IBP 2016 investigations [26] (blue) and the limit curve from the WTA data sheet 6-8 (green) are also provided for comparison.

3.2.3 Wood decay prediction model WUFI® Decay based on Biohygrothermal mould prediction model WUFI® Bio

For the assessment of mould growth on interior surfaces of building components, a physical-empirical model was developed at Fraunhofer IBP [27] which predicts the germination of a fungus spore and the subsequent development of the fungal mycelium as a function of temperature and RH, their duration of exposure, and the nutrient quality of the surface material. The germination and growth conditions do not refer to a single fungal species but summarize the critical growth conditions of typical fungal species isolated on building component surfaces on the safe side. The first part of the prediction refers to the uptake, release and storage of moisture from the model spore based on the moisture-variable diffusion resistance of the spore wall and its moisture storage function, until the temperature-dependent critical limit water content is reached at which the spore can germinate. The parameters of the model spore (Figure 33 top) were determined in such a way that the germination duration of can be represented in the physical model. The limit water content is derived for the respective nutrient quality from the temperature-dependent minimum relative humidity according to the laboratory experiments (Figure 33 bottom). After germination has taken place, the simulation switches to

the second part with prediction of mycelial growth. As soon as germination occurred, the model assumes the presence of a living mycelium, which can develop further accordingly.

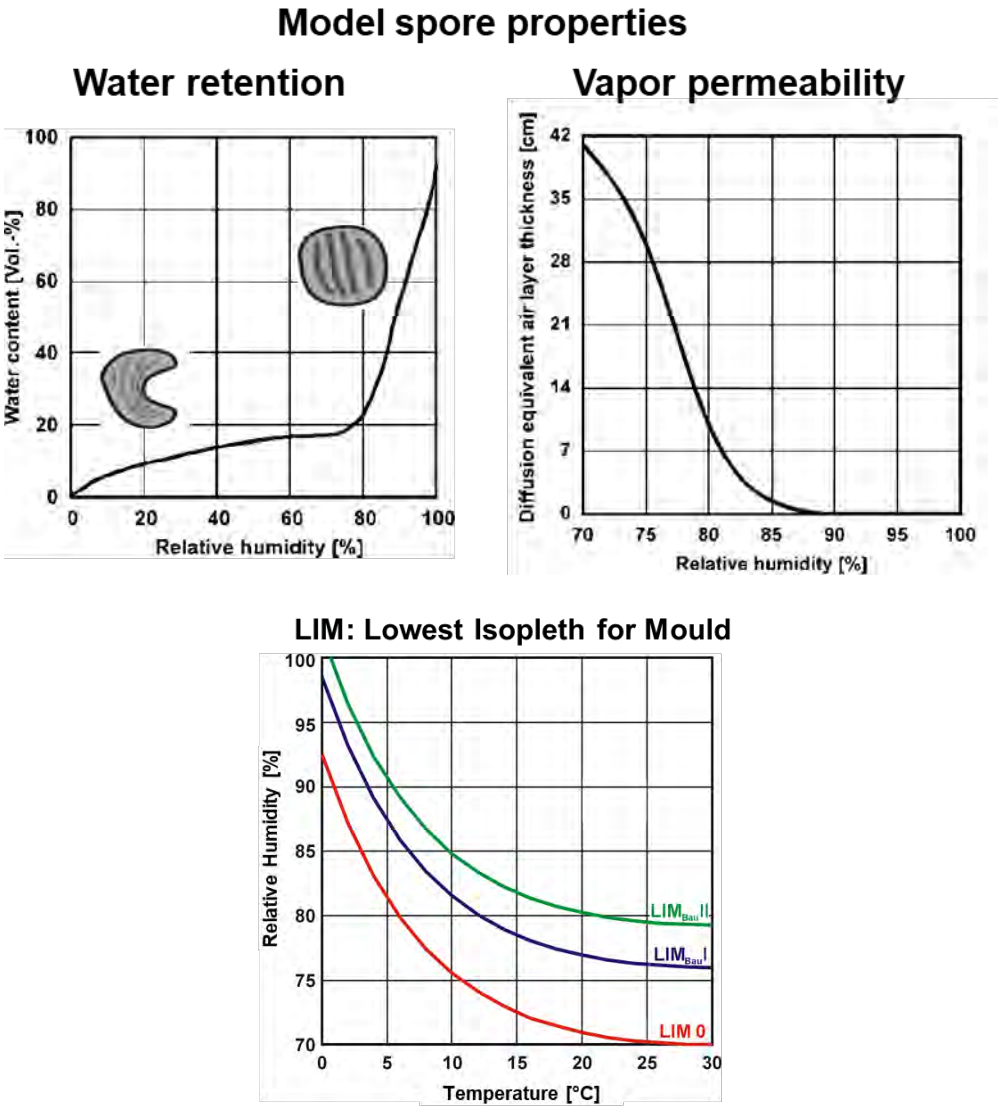

Figure 33: Sorption isotherm (top left) and diffusion resistance of the spore wall (top right) of the fungal spore of the mould prediction model WUFI® Bio. “Lowest Isopleth for Mould" (LIM) limit curves for materials with different susceptibilities depending on the nutrient supply level (Class 0 for optimal growing medium and Classes I and II for biodegradable and non-degradable building materials, respectively).

The Biohygrothermal Model as well as the mathematical-empirical VTT model of Viitanen [31] have already been regularly used and proven in practice for around two decades. They enable a significantly more reliable prediction of the mould risk than steady, temperature-dependent limit curves or only moisture-dependent limit values, such as the 80% RH for the evaluation of thermal bridges in winter, established in many standards.

Already in project [26] it was shown that clear analogies exist between the growth of mould and wood decay fungi, even if the wood decay fungi require a higher moisture level than mould fungi, at least at higher temperatures [32]. Accordingly, the WUFI® Bio model was used as the basis for a new model to predict the growth of wood decay fungi WUFI® Decay. For this purpose, the limit curve for the growth of wood decay fungi in solid wood, described above was first used. Unlike mould, the growth of wood decay fungi takes place inside the materials and is accordingly not directly observable under the microscope. For the detection of initial growth activities, therefore, in [26] CO_2 concentration was used. Subsequent mycelial growth also cannot be quantified in the same way as for mould for the same reasons. Instead, the mass loss of the wood is used. Both effects can only be observed later during the growth of decay fungi than spore germination and mycelial growth during the growth of mould fungi. The first activities of the decay fungi are often not visible at all. Nevertheless, the analogy in principle remains: the delay until the establishment of the fungus in the material (initiation phase) and the subsequent material degradation. Both can be represented by the existing systematic:

1.) Diffusion resistance and sorption isotherm of the spore determine the moisture uptake until the critical humidity level is reached at which the fungus is sufficiently established in the material.
2.) Subsequent proceeding of wood decay depending on nutrient quality, temperature, and humidity.

The calibration of the two effects is done on a double basis: for the duration of the initiation phase (duration until the first mass loss) the model in [17] provides a calculation approach that enables the determination from temperature and relative humidity for any boundary conditions. In the WUFI® Decay approach, this delay is represented by the diffusion resistance of the fungal spore, which slows down humidification and drying accordingly and only switches to the second phase of the mass loss calculation when the specific required water content is exceeded. While the mould growth model predicts the growth of the fungal mycelium in mm, the Decay model predicts the mass loss as a percentage of the existing mass. To achieve agreement with the measured mass losses from the current lab tests, a suitable conversion is required.

Currently, the conversion is determined with a factor of 35 mm / 1% by mass so that it covers the mass losses from the most critical material in most critical climate conditions (pine sapwood at 15 °C and 100% RH) on the safe side. This seems reasonable, since mass losses should usually be avoided in absolute terms in practice, and this factor still yields lower growth than the approach from [17]. For all other materials except the wet insulation board, and the other climates, the prediction remains on the safe side. For the wet insulation board, the correspondingly lower limit curve ThermNat I with the same conversion factor is considered. It covers the initial mass losses at 15 °C and 100% RH still on the safe side but shows somewhat lower losses compared to the later measurements. These slightly lower values after several months seem acceptable, since larger mass losses shall not be tolerated anyway (an

evaluation in a range of higher mass losses is therefore only of little practical relevance) and at the other, lower humidity levels, the predicted mass loss is higher than the measured one.

In summary, it can be stated that the method described in [26] and verified and further developed in the current project is still clearly on the safe side compared with the measurement results, but nevertheless also clearly extends the application limits of the materials compared to the previously available evaluation criteria. Further experience can now be gained with the new approach in comparison with laboratory tests and real life analyses and it can be further refined where necessary. Additional investigations would appear to be particularly useful for the lower limit curves of the particularly resistant materials, some of which exhibit significantly lower mass loss than solid wood - but also regarding the speed of degradation in the moisture range around 97% RH, where the prediction is currently still quite far on the safe side.

3.2.4 Comparison of the models with the experimental results

Using the defined ThermNat I and ThermNat II limit curves and the growth parameters described above, the wood degradation processes are now recalculated under the climatic conditions investigated and compared with the test results.

Figure 34 shows the comparison of the prediction with the measurement results. The wet panel without hydrophobic treatment was assigned to class ThermNat I (less resistant than wood) according to the measurement results. The dots represent the individual measurement results and the solid line the mean values of the three test specimens in each case. The bright blue dashed line corresponds to the predicted mass loss from the prediction model. The comparison shows that, especially at the lower temperatures and humidities, the mass loss starts earlier and increases significantly more than in the test. At the higher temperatures of 25 and 30 °C and 97% RH, the start of the mass loss is well represented and the subsequent increase is again clearly higher than the measured data.

The other natural fibre insulation materials as well as the reference wood (pine sapwood) are calculated with the "ThermNat II" limit curve (dashed red line). The mass loss starts after about 1-2 months for the different climatic conditions - slightly earlier for the low temperatures, and similar at the higher ones. As already mentioned, the predicted mass loss is only slightly higher at the higher humidity of 100% RH, but further on the safe side at the lower one of 97% RH.

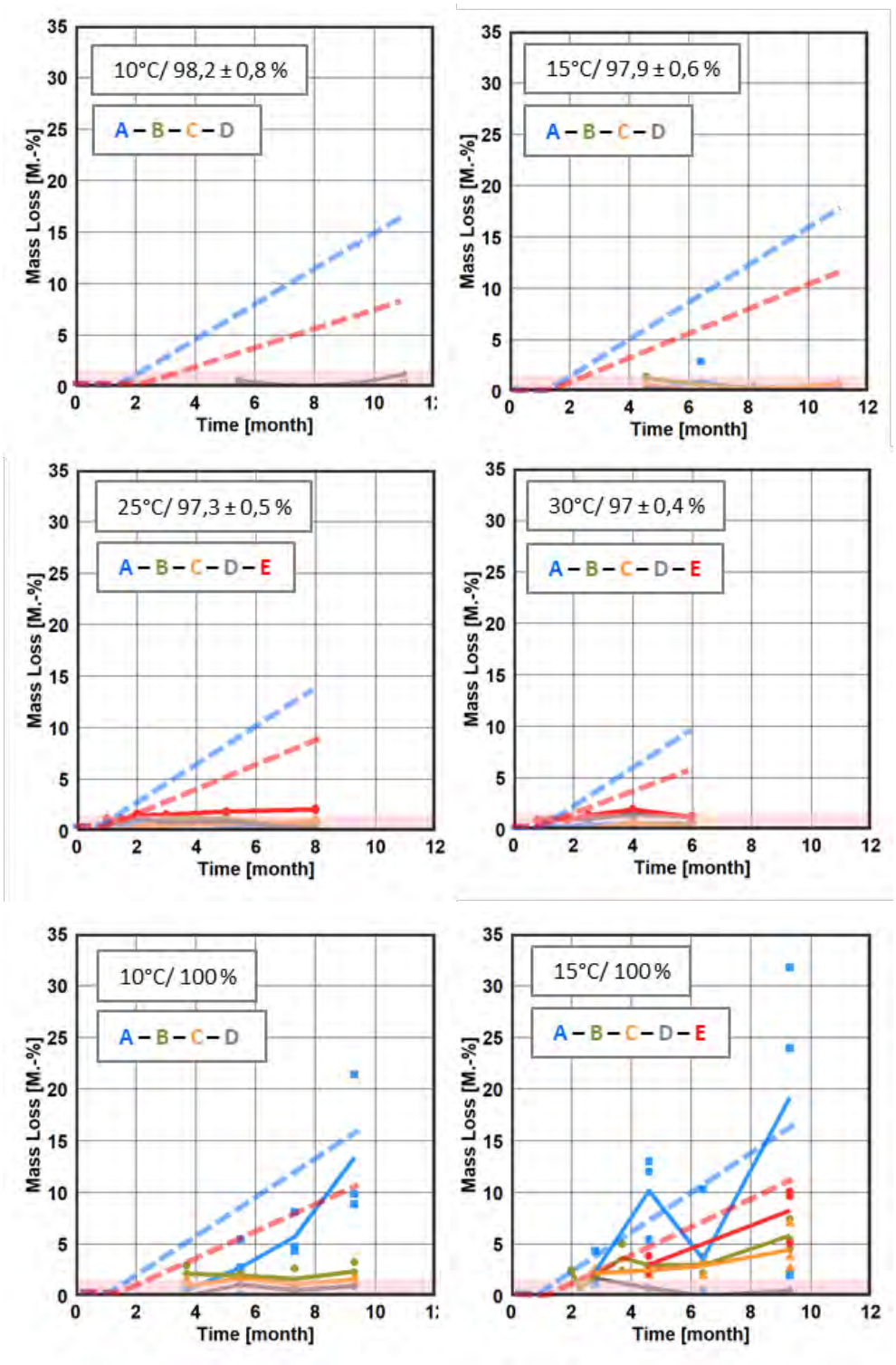

Figure 34: Comparison between prediction (blue for ThermNat I and red dashed line for ThermNat II) and measurement (points and mean curves) of mass losses of the different natural fibre insulation materials and the reference wood. (A = wet board; B = dry board without hydrophobic agent; C = dry board with hydrophobic agent; D = cellulose; E = pine sapwood).

In Figure 35 the prediction with the two newly determined limit curves is compared to the results according to the model of Viitanen [17]. This can be used for solid wood, but according to his own statement, it should only be used for the evaluation up to the start of the degradation process, but at most to a limited extent for the prediction of subsequent mass degradation. The mathematical-empirical Viitanen model also considers the factors time, temperature, and relative humidity based on laboratory tests. In the extensive laboratory studies conducted as part of his dissertation, the critical fungus studied was *Coniophora puteana* on Swedish pine sapwood [32]. Here, the predicted mass losses based on this model are shown in Figure 35 as bright green lines. The degradation rate after Viitanen is in all cases significantly higher than the mass losses predicted by the new approaches. As already mentioned, the faster mass loss with Viitanen is probably due to the use of more fungal mass in relation to the specimen mass in his experiments (see chapter 3.1.2).

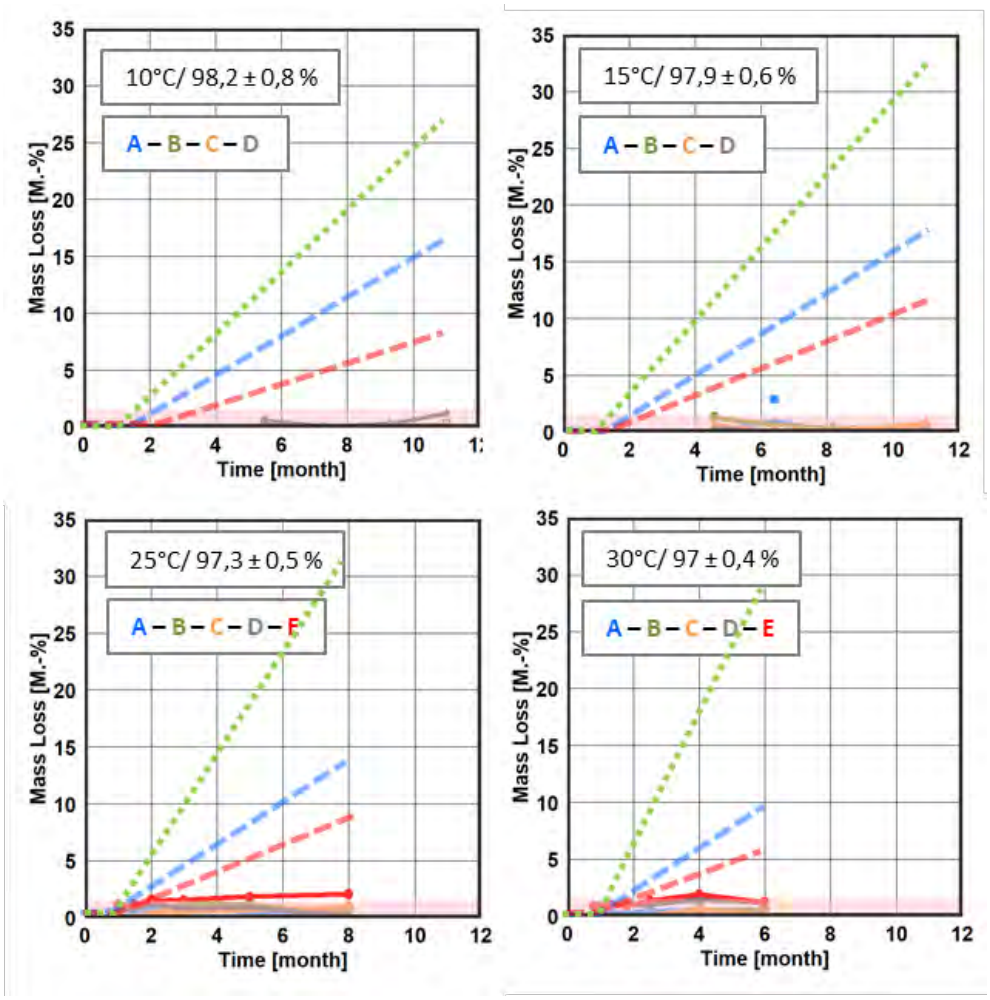

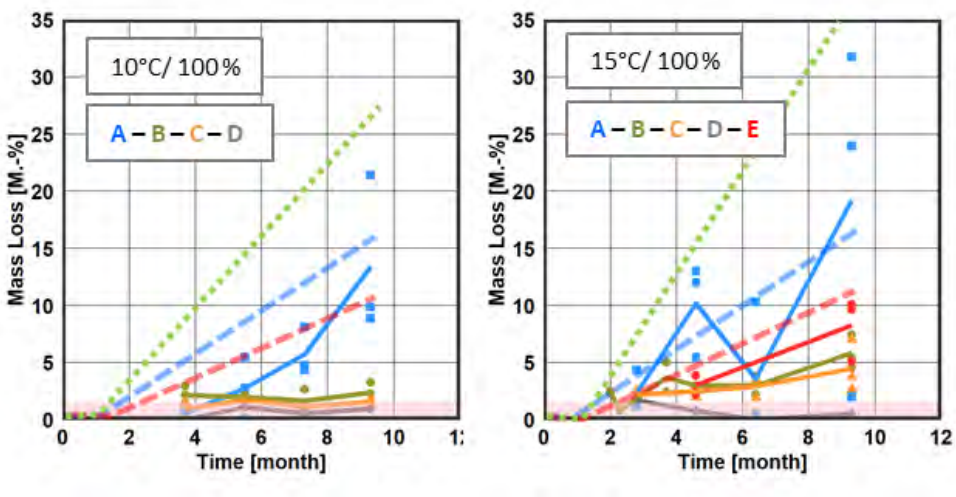

Figure 35: Comparison between prediction according to the new model (blue and red dashed line) and Viitanen's model (green dashed line) and measurement (points and mean value curves) of the mass losses of the different natural fibre insulation materials and the reference wood (A = wet board; B = dry board without hydrophobic agent; C = dry board with hydrophobic agent; D = cellulose; E = pine sapwood)

The results of the reference wood samples prove that the model of Viitanen is in principle well suited and still clearly on the safe side compared with the decay progress to be expected in real terms. Rather, lower growth, as represented by the red dashed line, is to be expected. Thus, even natural fibre insulation materials show lower mass losses than the Viitanen model would predict for wood. Just like the new approach, Also the prediction according to Viitanen is further on the safe side in the lower moisture range compared to the measured data than at the higher moisture contents.

With the new approach, this discrepancy was to be expected for the less resistant materials according to curve ThermNat I due to the systematics of the model. To enable a finer differentiation for the rather untypical material behaviour, correspondingly more extensive investigations would be required, but since the material proves to be particularly sensitive to degradation at the higher humidity levels, it nevertheless seems reasonable to remain cautious here at present.

In general, the question arises whether individual curves should be determined for individual materials in the case of deviating behaviour. If it is assumed that one material is either always more sensitive or always less sensitive than another, "unnecessary" safety buffers may result in individual cases; however, these could be tolerated in benefit of the simple approach, if necessary, and would keep the testing effort for additional certainty to a minimum. And also this approach still allows for somewhat higher RH than the prediction according to Viitanen [32] for the reference wood.

3.3 Evaluation based on field test

In the following section, the climatic data (temperature, humidity) recorded in the field test according to chapter 2 are compared with the proposed limit curves proposed in chapter 3.2. The recorded temperature / RH combinations shown on the outside of the cavity (measuring position "a") are those corrected according to chapter 2.3.2.1.

3.3.1 Climatic conditions in the component cavities

Figure 36 shows the daily mean temperature / RH combinations on the outside of the cavity (position “a”) of selected north-facing wall elements. For the variants with wood fibre and cellulose insulation (N 1.2/N 2.2 and N 1.3/N 2.3), the relevant limit curve for these insulation materials (ThermNat II) is not exceeded. Only regarding the combination of cellulose insulation and EPS ETICS (N 1.3) a short-term exceedance (1 day) occurs, which can be considered negligible. In the case of the EPS variants, an MDF cladding is applied on the outside between cavity and ETICS (cf. Figure 7). Since there is currently no alternative assessment method for such board materials, the limit value for wood-based materials of 18% by mass would apply, which would correspond to a RH in the pores 90% for the MDF. In variant N 1.3, the daily mean values of the RH in the cavity at the beginning of the measurement are often above 90% RH. An exceeding of the limit value of 18% by mass in the MDF cladding can therefore not be excluded.

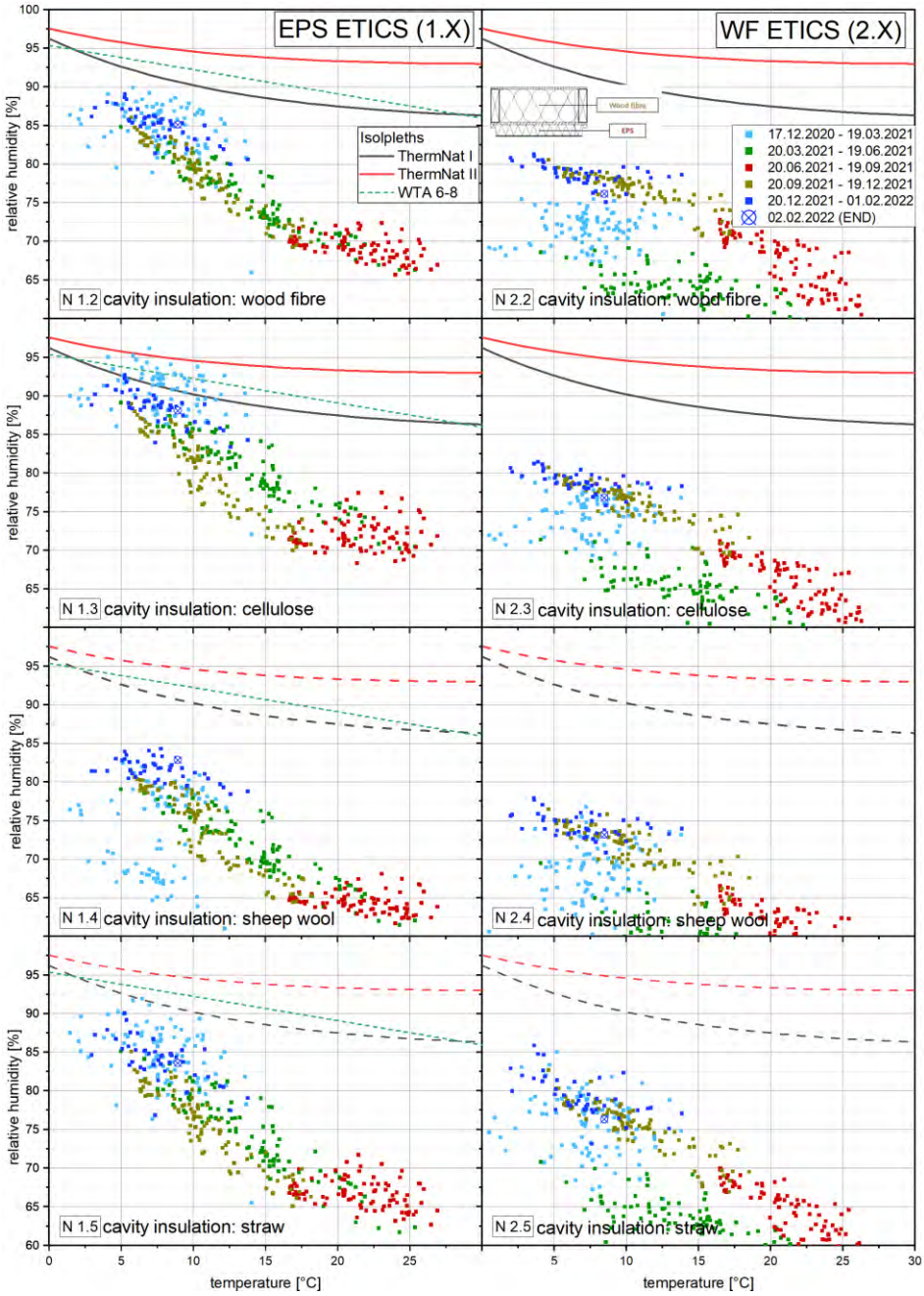

Figure 36: Temperature / RH combinations (24 h average of the measured values) on the outside of the cavities (position "a") of 8 selected structure variants of the north facade with limit curves ThermNat I and ThermNat II (for sheep wool and straw indicated by dashed lines for orientation).

In the case of the sheep wool and straw variants (N 1.4/N 2.4 and N 1.5/N 2.5), there is likewise no significant exceeding of the proposed limit curves in any case. It should be noted here, however, that these normally apply to wood and cellulose fibre insulation materials. For reasons of comparability of the RH level, the curves are plotted in addition. As in the case of the wood panel materials (see above), corresponding durability tests would be useful also for sheep wool and straw in the future to improve design quality and safety.

Figure 37 shows the daily mean values of the same test variants on the south facade. In all cases higher temperatures coincide with lower relative humidity. The higher temperature is caused by the significantly increased solar radiation compared to the north facade. This causes an increased temperature on the render surface, which in the present measurements led to short-term temperature peaks up to 67.5 °C (dark render) and 44 °C (bright render). Overall, the variants on the south side are even less critical than the identical variant on the north side. All daily mean values are for the most part far below the proposed limit curves and the WTA design limit.

Both, Figure 36 as well as Figure 37 show that the variants with exterior wood fibre ETICS (WF ETICS) have a significantly lower RH level than the respective EPS comparison variant. This again shows that the high vapor permeability and the low s_d-value of the WF ETICS result in a reduced RH level in the structure. Also Figure 38 confirms this aspect. Here, in addition the s_d-values of the variants are provided. Depending on the variant, these amount to 6 m (N 1.8 - OSB + EPS ETICS), 3 m (N 1.2 - MDF + EPS ETICS) and 0.3 m (N 2.2 - WF ETICS). In the case of the north-facing structure with OSB cladding and EPS ETICS, the daily mean values are again significantly higher than in the variant with MDF cladding. As for MDF (see above), there are no material-specific isopleth models for OSB available now. Therefore, again the limit of 18 by mass (90% RH in the pores) for OSB) would apply here [7]. Since the daily mean values often exceed these values, the structure would not be considered suitable during planning. In the variant with wood fibre ETICS (N 2.2), the daily mean values are far below the limits described in chapter 3.2 for wood fibre and cellulose insulation materials (ThermNat I and ThermNat II).

In general, the increased vapor permeability of wood-fibre-based ETICS systems can be of advantage for both the durability of the materials, as the wood decay risk is lower due to the reduced RH level in the structure and the thermal performance, as the thermal conductivity remains also lower at lower moisture levels.

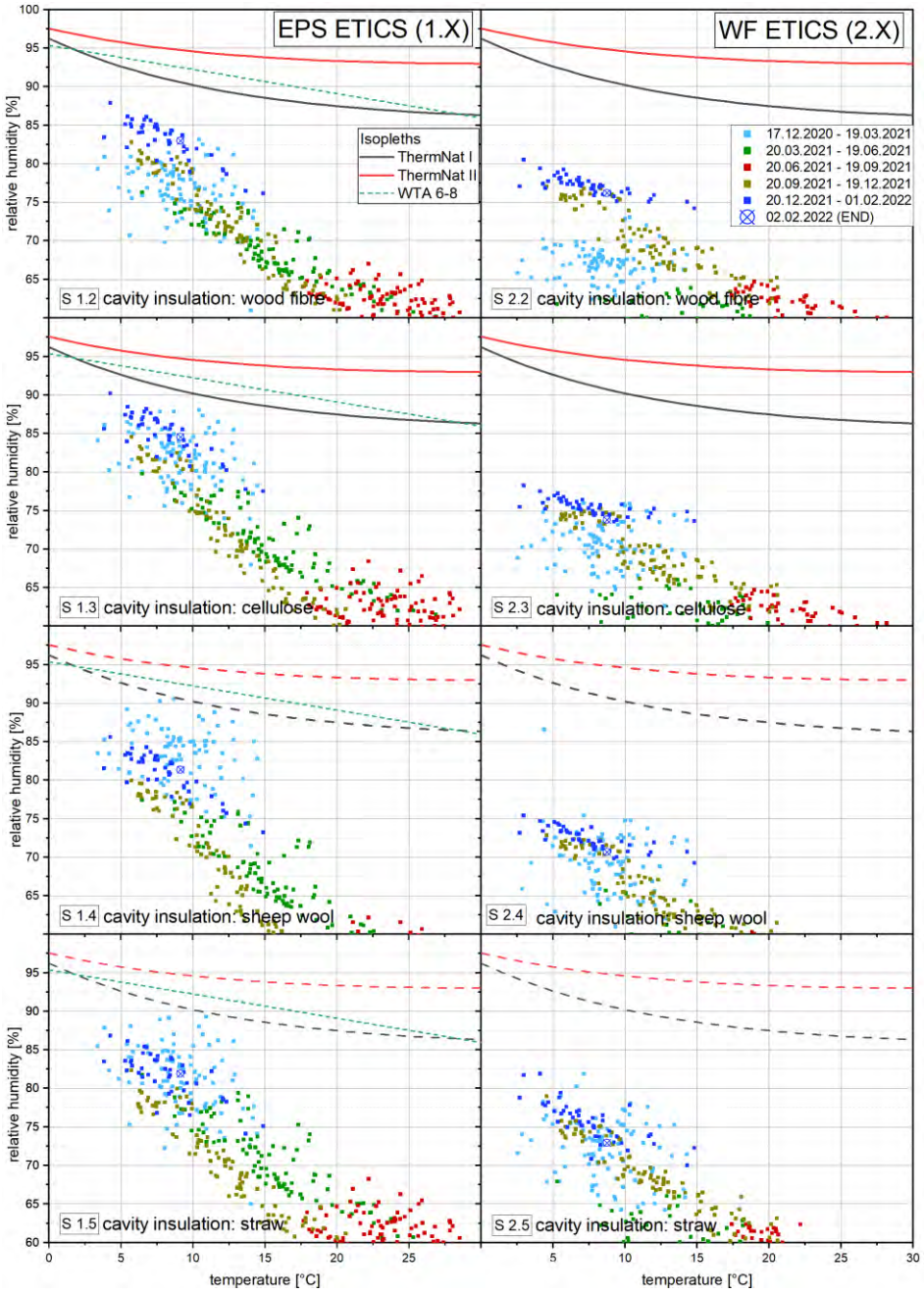

Figure 37: Measured temperature / RH combinations (24 h average) on the outside of the cavities (position “a”) of 8 selected variants of the south façade with limit curves ThermNat I and ThermNat II (for sheep wool and straw indicated by dashed lines for orientation).

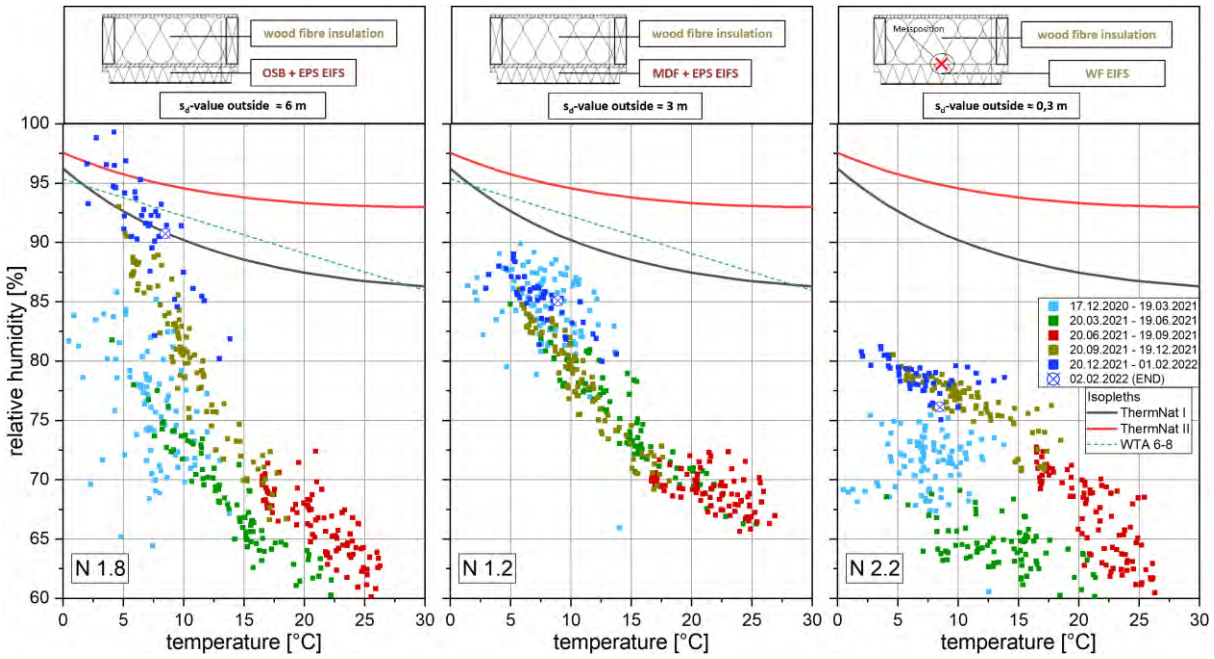

Figure 38 : Measured Temperature / RH combinations (24 h average) on the outside of the cavities (position "a") with wood-fibre insulation and different outer cladding / facade systems with varying s_d-values.

3.3.2 Climatic conditions in the wood fibre ETICS

3.3.2.1 Wood fibre board from the dry production process with hydrophobic treatment

In Figure 39 the temperature / RH combinations in the wood-fibre ETICS beneath the exterior render (position P) of the north facade are plotted as daily average. One could directly see that in both cases (bright (HBW approx. 79) and dark render (HBW approx. 17)) the limit curves are exceeded regularly in winter between 17.12.2020 and 19.03.2021. The render was applied in mid-November 2020, when the daily mean temperature and the global radiation sum were already at late autumnal levels. The render therefore dried a longer period of time, and the RH in the wood-fibre ETICS was correspondingly increased. In the case of the dark render variants, the RH drops much faster in spring (green dots) than in the case of the bright renders and decreases to a level of below 60% RH in the summer of 2021. The drying of the render layer thus appears to proceed much faster here. In the case of the bright-coloured render, the RH remains at a level between 65% and 70% also in summer 2021. In the following winter (20.12.2021 - 01.02.2022), the daily average rises again to a level of over 90% RH, with slightly higher values beneath bright compared to the dark render. In both cases, the daily average values no longer exceed the proposed limit curves during this period.

The transient prediction of the expected material decay at the climate conditions according to Figure 39 is shown in Figure 40 and Figure 41.

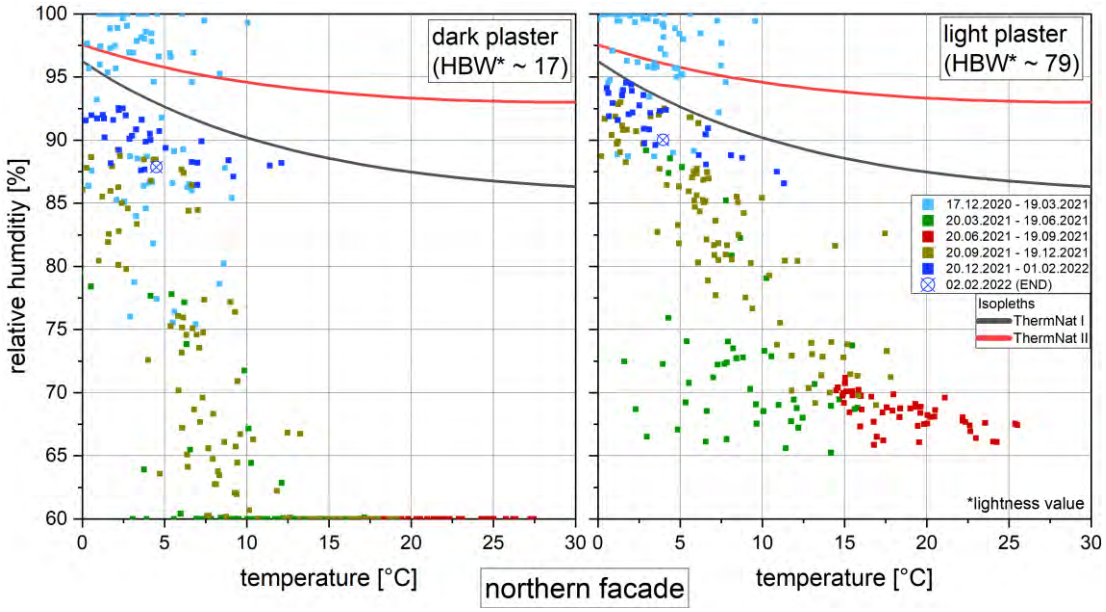

Figure 39: Measured Temperature / RH combinations (24h average) in the hydrophobic wood fibre ETICS (dry production process, density according to data sheet: 140 kg/m³) beneath the render layer (measuring position "P") for the variants with dark (left) and bright (right) render colour on the north facade. The arithmetic mean values of the measurements for the variants N 2.6 and N 2.7 (left) and the variants N 2.1 to N 2.5 (right) are shown.

The temperature and humidity curves shown here as hourly values confirm the explanations given above on the drying and humidification behaviour of the two different colour variants. In this diagram, it can be seen even better that the RH remains visibly longer at a level > 90% (> 2000 h) after the start of the measurement on 07.12.2020 below the bright render variants. In the case of the dark render variants, a steady decrease in relative humidity can already be observed from approx. 1000 h after the start of measurement.

In both cases, the limit temperature dependent water content is exceeded after about 800 h (ThermNat II). In the case of a bright-coloured render, the exceedance is higher and lasts for a longer period than with the dark render. After about 1000 h, the model predicts decay fungi growth, which rises more steeply and lasts longer in the case of bright-coloured render than in the case of dark render, where the spore water content drops again much earlier due the more distinct drying behaviour.

In the following fall/winter (after approx. 7000 h), the spore water content remains far below the limit water content. Accordingly, the prediction model does not describe any further growth. The predicted total of mycelial growth is approx. 35 mm (white render) and approx. 13 mm (dark render). The predicted mycelium growth in [mm] is currently in analogy to WUFI® Bio only an evaluation “indicator”, which describes whether wood decay can take place at all (mycelium growth > 0 mm), as well as for the qualitative comparison between different strong wood degradation levels.

As described in chapter 3.2.2 the predicted material degradation is converted according to the current draft status of the model by a factor of 1 M.-% / 35 mm from the "mycelium growth".

The final conversion factor can still deviate somewhat from the current one. Thus, a maximum material loss of 1% by mass has to be expected on the safe side.

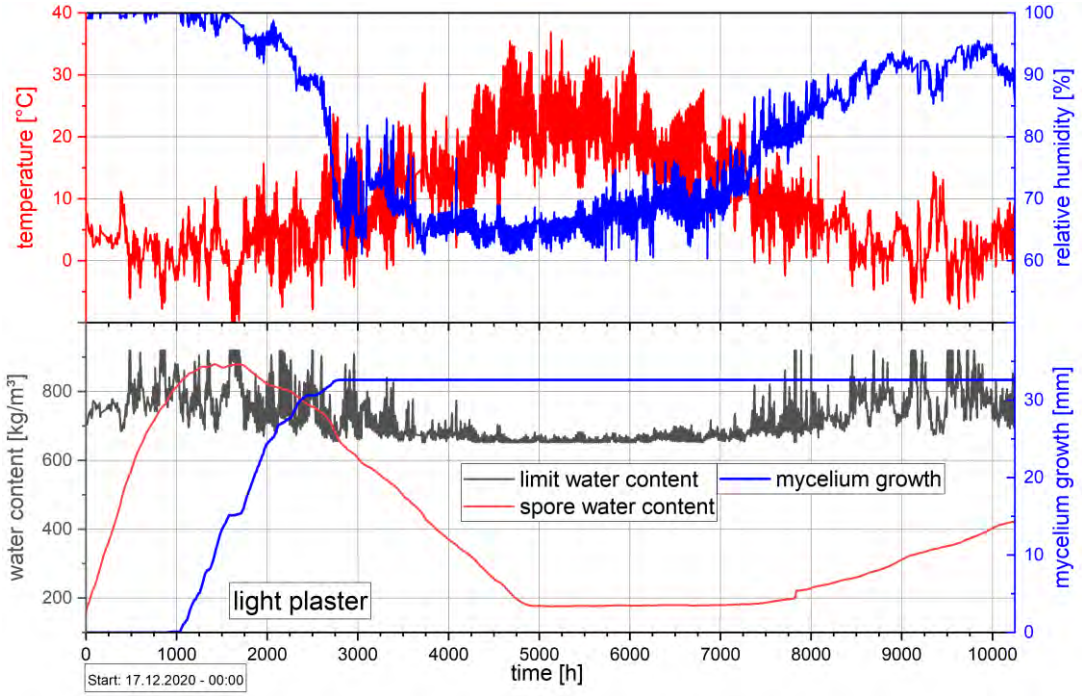

Figure 40 : Measured temperature and RH in the hydrophobized wood fibre ETICS (dry production prcess, density according to data sheet: 140 kg/m³) beneath the bright render over the whole test period (top) with temperature depending limit water content (ThermNat II), spore water content and resulting mycelium growth (bottom).

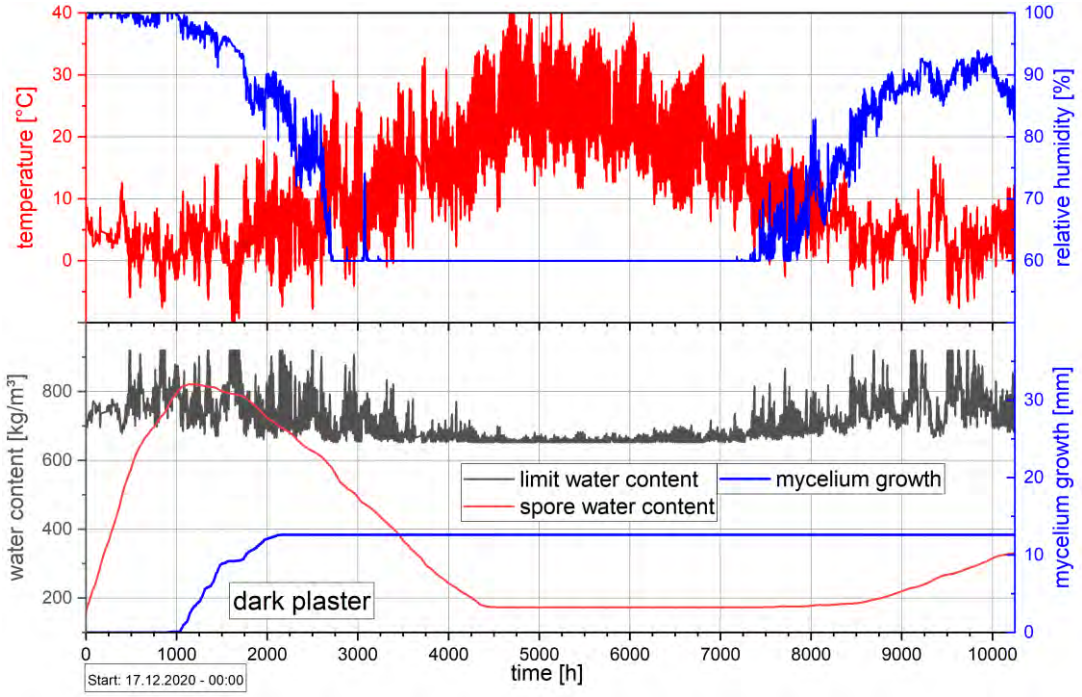

Figure 41 : Measured temperature and RH in the hydrophobized wood fibre ETICS (dry production process, density according to data sheet: 140 kg/m³) beneath the dark render over the

whole test period (top) with temperature depending limit water content (ThermNat II), spore water content and resulting mycelium growth (bottom).

Figure 42 to Figure 45 show photos of the opened measurement points on the north facade of one bright and one dark render (position P) after the end of the test period. Altogether five measuring points with white render and two measuring points with dark render were opened and examined for the occurrence of mycelium, visible to the naked eye. The photos are representative for all opened variants: No mycelium growth was observed in any case.

Figure 42 : Opened measuring position P at variant N 2.3 (bright-coloured render) after the test period. No fungal mycelium visible.

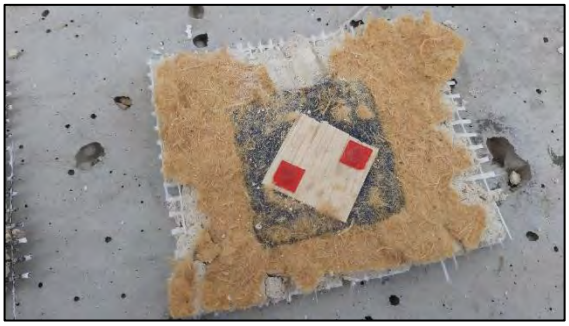

Figure 43: Removed render layer of variant N 2.3 (bright render) with Balsa sensor and wood fibre residues. No fungal mycelium visible.

Figure 44: Open measuring position P at variant N 2.6 (dark render) after the test period. No fungal mycelium visible.

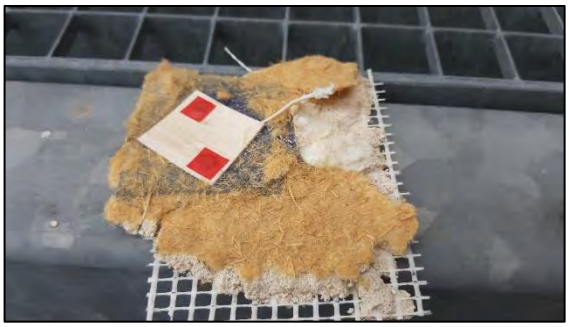

Figure 45 : Removed render layer of variant N 2.6 (dark render) with Balsa sensor and wood fibre residues: No fungal mycelium visible.

The mycelial growth predicted on the safe side by the prediction model based on the climatic records has thus apparently not or not yet taken place in real life or is not visible to the naked eye. This is not surprising and has the following reasons, among others:

- Freshly applied render systems lead to increased pH values on the wood fibre ETICS→ inhibits wood decay fungi
- reduced oxygen availability beneath the render layer in the rather dense material
- the measured values are strongly related to the position → only a few mm deeper, the level of relative humidity could already be lower. Due to the tests, the conditions in the

laboratory and thus also in the prediction model tend to be related to average moisture levels in somewhat thicker layers (~ 5-10 mm).

- the prediction model includes certain safeties, which are caused by the uncertainties of the laboratory tests, but are of course also intended, since it is to be used as a tool for component design in the long term.

Figure 46 shows the temperature / RH combinations below the bright and dark render on the south facade. As expected, the differences between the two colour variants are more distinct than on the north facade due to the much higher direct solar radiation on the south side. In the case of the dark variant, only a few daily mean values at the beginning (17.12.2020 - 19.03.2021) exceed the relevant limit line (ThermNat II). Already in spring (green dots), the humidity level here falls below 60% RH, while below the bright-coloured render, even in the summer period (red dots), the humidity level is still above 60% RH on many days. In both cases, the drying behaviour of the render is noticeably faster than on the north side due to the more favourable solar radiation balance and the resulting increased surface temperatures.

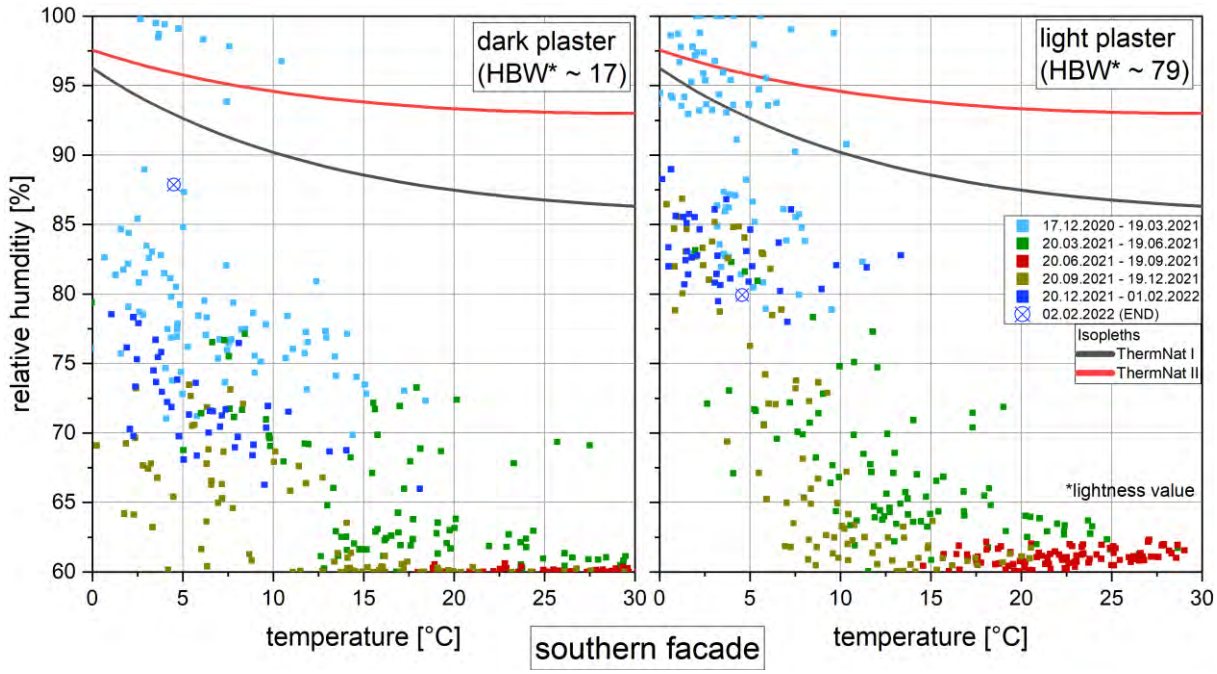

Figure 46 : Measured temperature / RH combinations (24h average) on the ETICS made of hydrophobized wood fibre (the dry production process, density according to data sheet 140 kg/m³) beneath the render (position P) for the variants with dark (left) and bright (right) render on the north facade. The measured values for variant S 2.6 (left) and the arithmetic mean values for variants S 2.1 to N 2.5 (right) are shown.

3.3.2.2 Wood fibre board from the wet production process without hydrophobic treatment

The daily mean values of the temperature / RH combinations in the non-hydrophobic wood-fibre ETICS from the wet production process (N 2.8 north side, bright render) are shown in Figure 47. Regarding the RH, it is noticeable that the daily mean values differ from those observed for the hydrophobic material from the dry process. In contrast to the latter, at the

beginning of the test period (17.12.2020 - 19.03.2021), no daily mean value was at the dew point limit (100% RH). In this case, the isopleth ThermNat I (black line) is used as limit curve, since in the laboratory test the wood fibre product from the wet process was more sensitive than solid wood (chapter 3.1.2). However, it cannot be ruled out that the resistance of individual products from the same manufacturing process may also differ depending on other factors such as density, raw material and, if necessary, additives. In [15] for example, a wet insulation board was more durable than solid wood. Many values exceed the ThermNat I limit curve. Over the rest of the test period (20.03.2021 - 02.02.2022), a lower moisture level than in the case of the variants with dry insulation boards is observed here. In summer, the moisture drops below 60% RH for a longer period. Figure 48 shows, among other things, the hourly values of relative humidity at measurement position P plotted over time. Here one can see even better that the humidity never reaches 100% RH. In the second cold period (after approx. 7000 h), the RH remains permantently below 90% RH. Certain properties of the non-hydrophobic board from the wet process thus apparently cause a recognizably lower humidity level compared to the hydrophobic dry insulation boards. It is assumed that amongst others, moisture absorption and liquid transport reach a higher level due to the missing impregnation. Condensation can thus be better absorbed and redistributed to the inside of the panel. The moisture peaks at the board surface could thus be reduced.

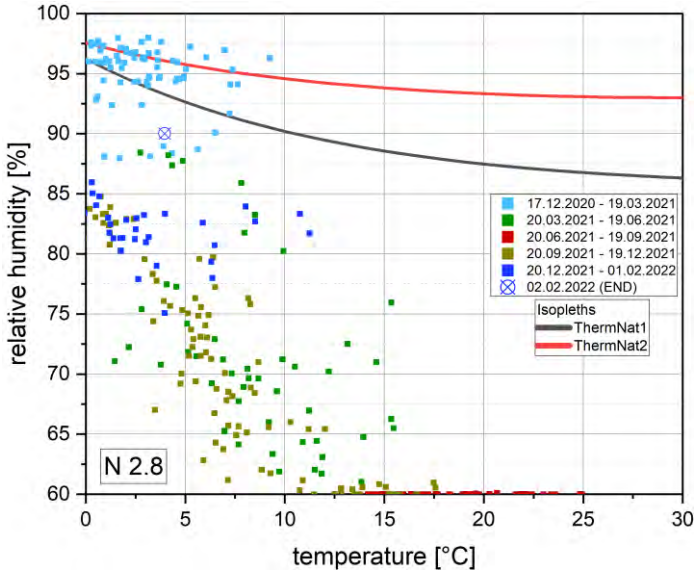

Figure 47 : Measured Temperature / RH combinations (24h average) in the ETICS made of non-hydrophobic wood fibre (wet process, density according to data sheet: 265 kg/m³) beneath the render layer (position P). Measured values of variant N 2.8 (bright-coloured render) are shown.

At the bottom part of Figure 48, the limit water content according to the relevant isopleth ThermNat I, the spore water content and the predicted mycelium growth are plotted for the measured climatic conditions in the ETICS for variant N 2.8. Since ThermNat I is relevant, the limit water content is recognizably lower than in the previous cases (see Figure 40). Due to the lower RH level, the spore RH also increases only very slowly and exceeds the limit water

content only for a short period (2600 h - 2800 h). The model predicts mycelium growth of about 1 mm during this period, a very low level at which material degradation might just begin in the worst case. In the following winter, the spore water content remains well below the limit water content due to the relatively low humidity level. Further mycelial growth is accordingly not predicted by the model.

Although the considered wood fibre board from the wet process was assumed and evaluated here as more sensitive than the materials from the dry process with the limit curve ThermNat I based on the laboratory tests (see chapter 3.1.2), a much lower mycelial growth is nevertheless predicted than for the comparative variants from the dry process. This is probably due to the higher moisture absorption and transport capacity of the wet-process products without hydrophobic agent, which leads to more moisture storage and redistribution than in the dry-process products and thus counteracts rapid changes in relative humidity. The relative humidity usually remains even below the lower limit line.

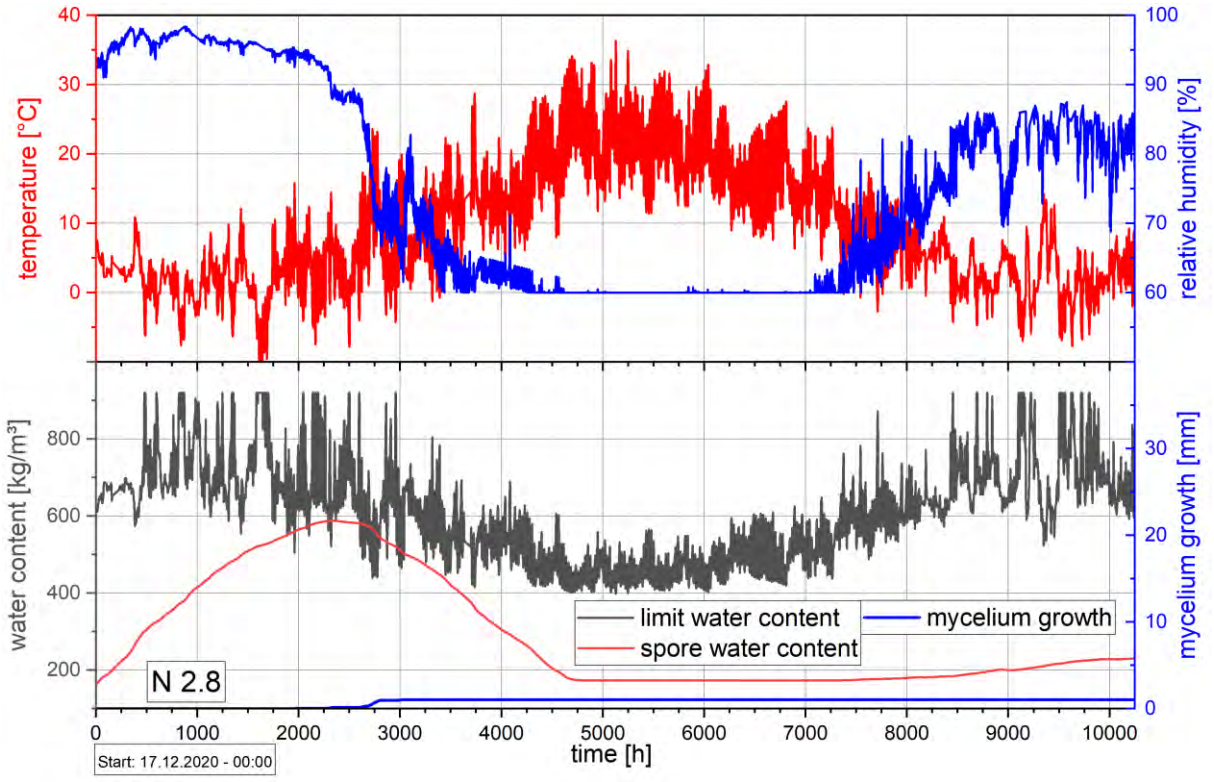

Figure 48 : Measured temperature and relative humidity in the non-hydrophobized wood fibre ETICS (wet production process, density according to data sheet: 265 kg/m³) beneath the bright-coloured render over the whole test period (top) with temperature depending limit water content (ThermNat I), spore water content and resulting mycelium growth (bottom).

Also during the visual inspection after the test period (see Figure 49 and Figure 50), no mycelium was visible on the softwood fibre board.

Figure 49 : Opened measuring position P at variant N 2.8 (bright-coloured render) after the test period. No fungal mycelium visible.

Figure 50 : Removed render layer of variant N 2.8 (bright-coloured render) with Balsa sensor and wood fibre residues. No fungal mycelium visible.

3.3.2.3 Wood fibre ETICS on humid lime silica brick masonry

The temperature / RH combinations in the masonry on the west side (W 1.1 and W 1.2) are shown at different positions as daily averages in Figure 51. The moisture content of the bricks was determined by the kiln-drying method prior to the start of the measurement and was between 4% by mass and 6% by mass in the condition as delivered from the factory. At a density of 2000 kg/m³, this corresponds to 80 l/m³ - 120 l/m³. For these variants, the render was applied at the beginning of March 2021 shortly before the start of spring.

Regarding the measured daily mean values, both variants show very similar results. In the case of the thicker masonry variant (25 cm, W 1.1), the daily mean values at both measuring positions are at a slightly higher level. In both variants, the daily mean values between masonry and ETICS (measuring position m) do not exceed the relevant limit curve (ThermNat II). The clearly recognizable decrease in the moisture level at the positions from spring to fall 2021 (20.03.2021 - 19.09.2021) results from the drying processes in the masonry. The renewed increase in relative humidity starting in fall is due to the increase in moisture load in the test house starting on 10/19/2021 (see Chapter 2.3.2) in combination with slightly lower indoor temperatures.

On the render side (measuring position P) of the ETICS, the relevant limit curve (ThermNat II) is exceeded in both cases on several days at the beginning and end of the test period. After rapid drying of the render in spring, the RH settles at around 60% to 70% RH in the summer months. Due to the moisture in the masonry, the humidity level is higher in summer than at the same time in the north-facing variants in wood frame construction, despite the more favorable radiation balance on the west side. Even in the second winter (dark blue dots), both variants have critical daily mean humidity levels above the limit line of up to 100% RH. This is due to diffusion of the masonry moisture to the outside of the building component.

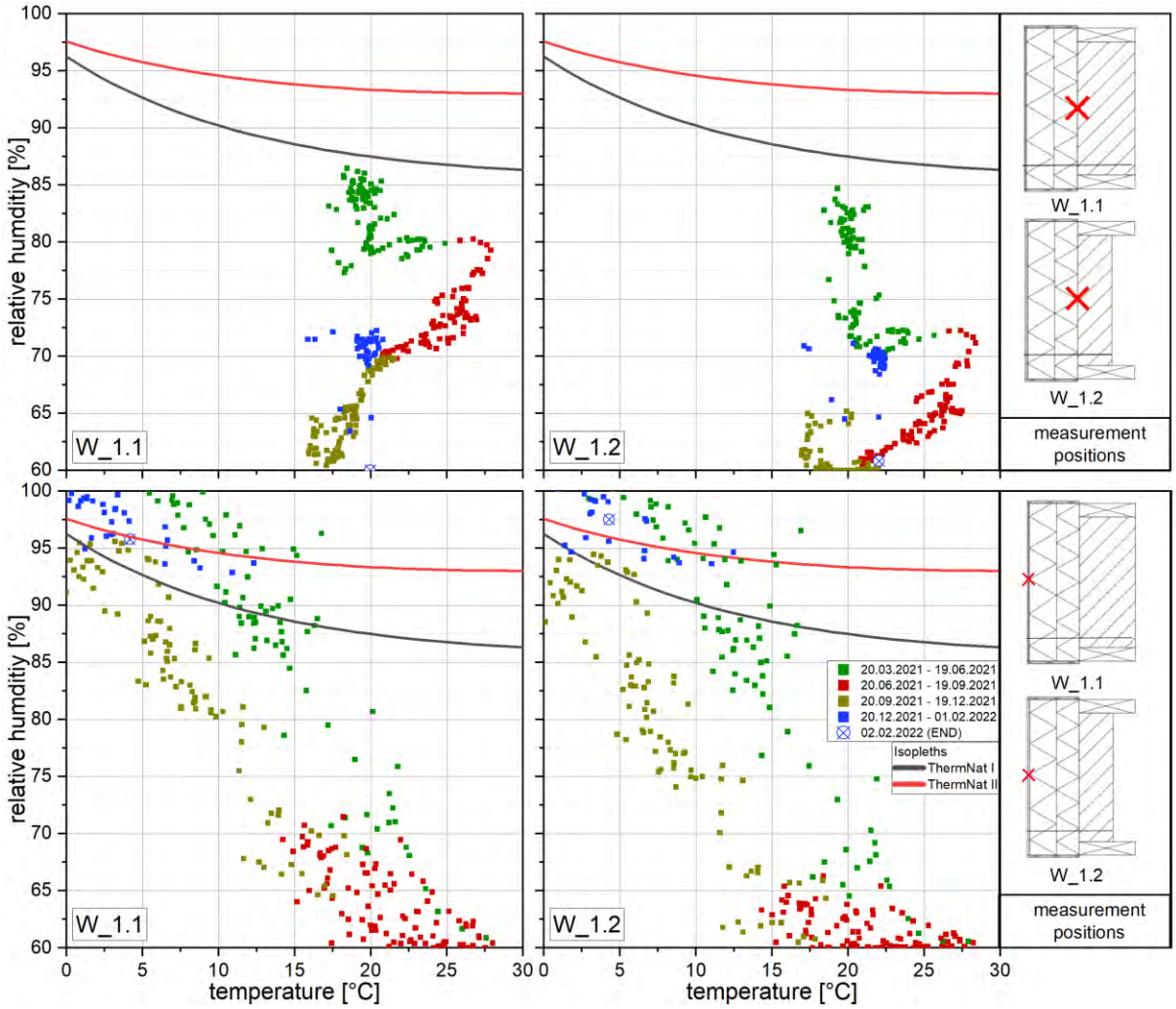

Figure 51 : Measured temperature / RH combinations (24 h average) in the hydrophobized wood fibre ETICS (dry production process, density according to data sheet: 110 kg/m³) beneath the render layer (measuring position P - bottom) as well as inside the component (measuring position m - top) for the variants on 25 cm (left) and 15 cm (right) thick lime silica brick manysonry on the west facade.

The transient wood decay prediction of ETICS on masonry based on the limit curve "ThermNat II" are shown in Figure 52 and Figure 53. With regard to the course of the relative humidity, both variants show once again a faster drying phase in spring (approx. between 2400 h and 3500 h) compared to the cases with render application in winter, as well as a higher humidity level in summer. After about 3200 h, the spore content exceeds the limit water content and the model predicts mycelial growth in both variants (W 1.1: ≈ 5 mm; W 1.2: ≈ 3 mm). In the following summer months, the growth stops due to the low humidity level. In fall 2021 (after about 7000 h), the humidity level on the ETICS rises again and even reaches values up to 100% RH in the following winter. Subsequently, also the spore water content rises in both variants. In variant W 1.2, the limit water content is exceeded at the end of the test period. Accordingly, a further mycelium growth of the mycelium is predicted. In variant W 1.1, the spore water content is just below the limit water content at the end of the test period. Since the measurement had to be

stopped at this point, no further values are available later. It cannot be excluded that the model would predict further mycelial growth for variant W 1.1 in the following period.

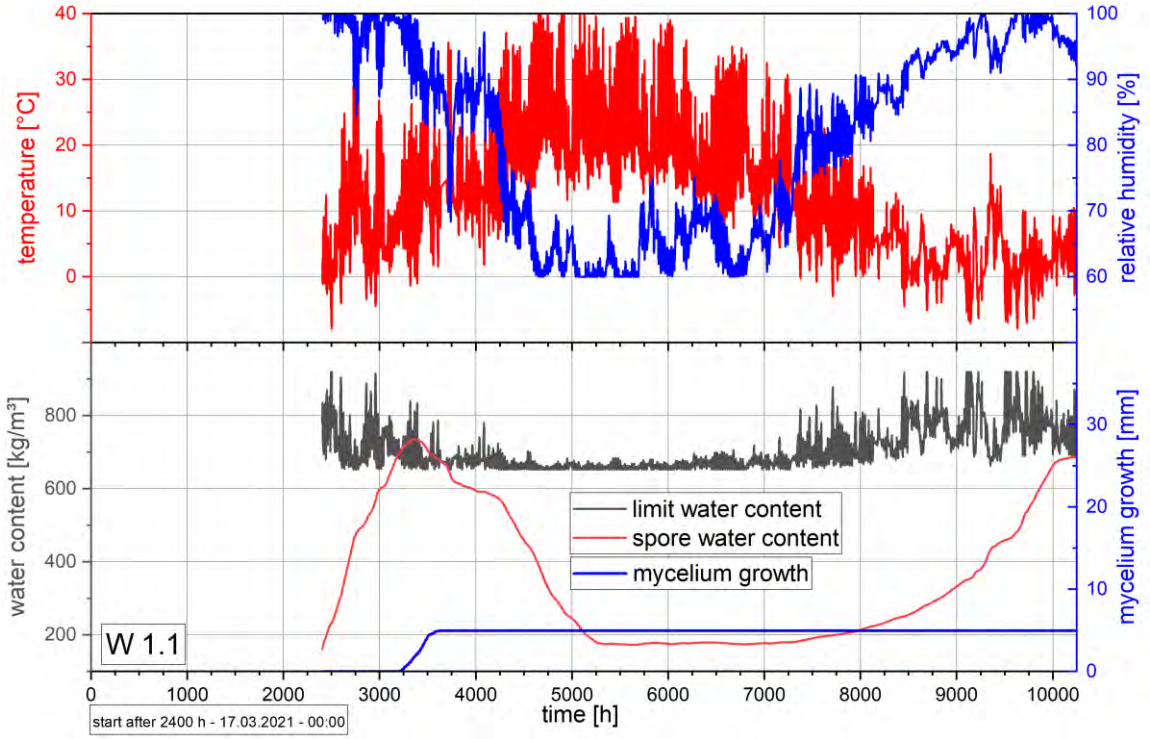

Figure 52 : Measured temperature and relative humidity in the hydrophobized wood fibre ETICS (dry production process, density according to data sheet: 110 kg/m³) beneath the render layer (position P) for the variant on 25 cm thick lime silica brick masonry on the west facade (top) with temperature depending limit water content (ThermNat I), spore water content and resulting mycelium growth (bottom).

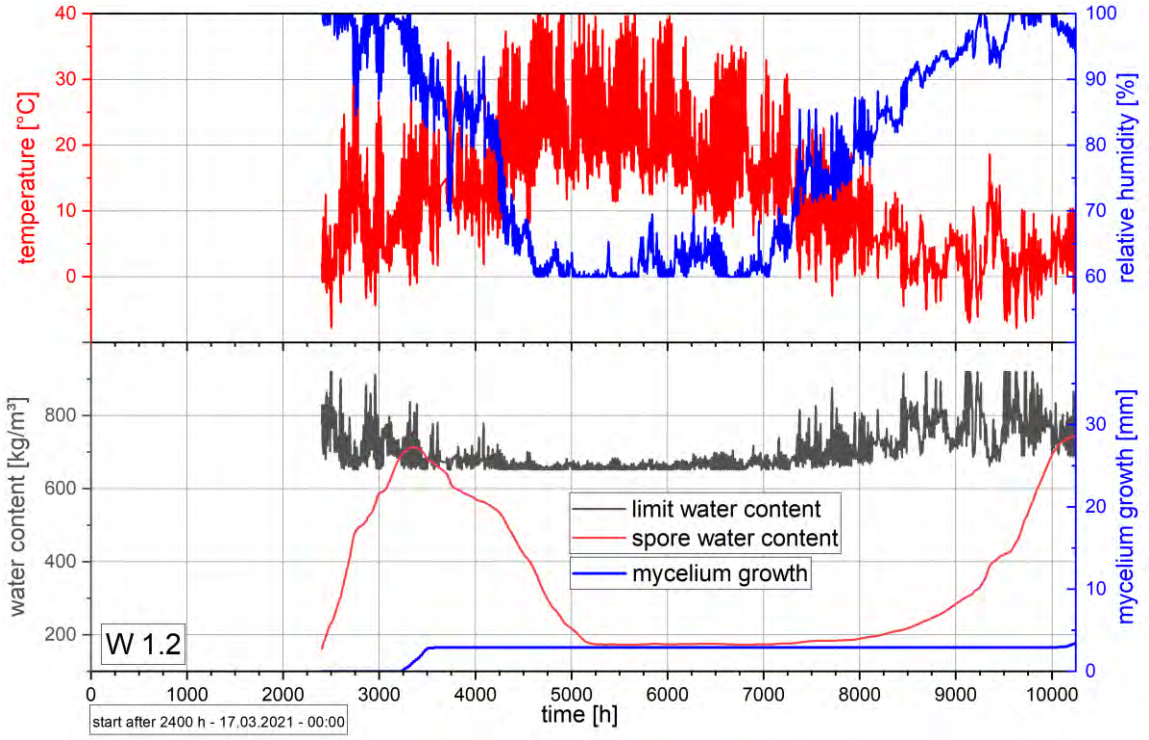

Figure 53 : Measured temperature and relative humidity in the hydrophobized wood fibre ETICS (dry production process, density according to data sheet: 110 kg/m³) beneath the render layer (position P) for the variant on 15 cm thick lime silica brick masonry on the west facade (top) with temperature depending limit water content (ThermNat I), spore water content and resulting mycelium growth (bottom).

3.4 Conclusions and outlook

3.4.1 Laboratory tests, limit values and prediction model

The results of the laboratory tests show that wood and natural fibre insulation materials can be both more susceptible and more resistant to infestation by wood decay fungi than solid wood. It is therefore not necessary to apply more cautious limits for these materials than for wood. Some products even appear to be significantly more resistant.

Based on the laboratory results, new limit values for wood and natural fibre insulation materials as well as a transient prediction model could be developed. For the pine-sapwood reference samples, the laboratory results demonstrate that previously determined limit curves and models in [17, 26] for degradation by wood decay fungi are valid and in some cases even more on the safe side than expected. Accordingly, the ThermNat II limit curve for wood and more resistant fibre insulation materials determined during the project lies higher than those published before. Nevertheless, uncertainties still remain, and the transient model predicts mass degradation analogous to [26] starting at 10 °C above 95% and at 30 °C above 93% RH. For the ThermNat I curve, the limits are lower: at 30 °C, degradation already starts at 86% RH. Based on the current state of research, this seems unrealistically low. However, further and

more detailed investigations would be required in order to be able to give more precise progressions here. Therefore, this low level currently remains without alternative until further findings are available. Nevertheless, this limit curve is still clearly higher than the limit value of 18% by mass, which is known to be of limited suitability, and at a similar level to the limit curve of the WTA guideline 6-8 [7] which, however, has been so far reserved only for solid wood applications. The two new limit curves are shown in Figure 32.

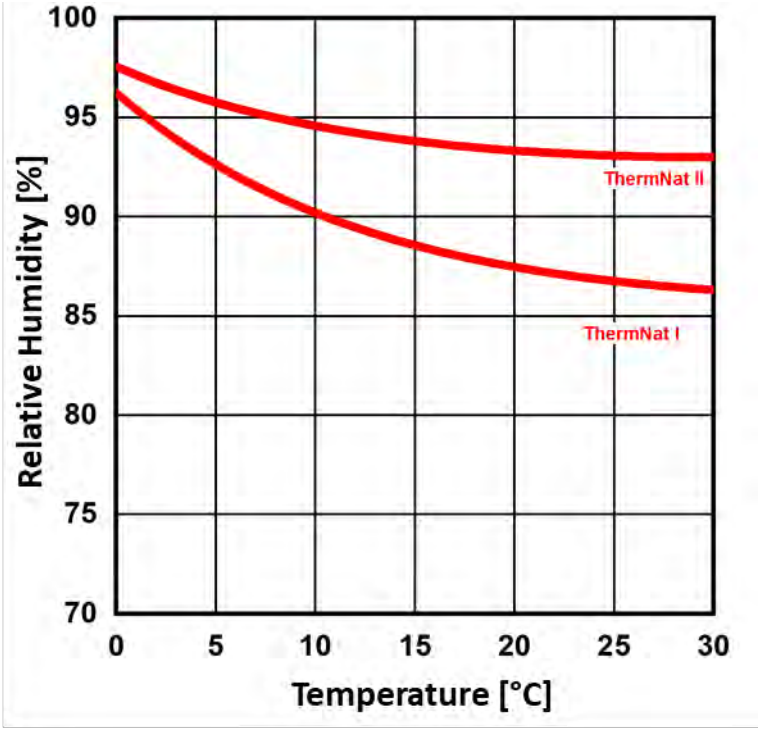

Figure 54: Newly determined limit curves for solid wood and equal or more resistant natural fibre insulation materials (ThermNat II) and for less resistant natural fibre insulation materials (ThermNat I).

With the prediction model developed for wood fibre insulation (described in chapter 3.2.3), the decay conditions received in the laboratory tests can be reproduced well and with sufficient safety.

The field tests also showed that no damage to the materials is to be expected, at least over the test period, despite the occurring at least temporarily high moisture contents. Here it became clear that limit curves alone are not useful for evaluating such situations: After render application, the two limit curves were exceeded in many cases at the interface between insulation material and render. Thus, based only on a steady-state limit curve and without transient assessment, some systems would have "failed." With the transient assessment, however, it then emerged that the exceedances usually do not last long enough to allow infestation or material degradation. In the worst cases, a low mass loss is predicted, while this was not observable in real life in the field tests. However, no more detailed investigations, e.g.

microscopic examinations, could be carried out within the project, as it is generally difficult to detect any mass losses in field tests and nearly impossible to do so in case of only marginal losses.

3.4.2 Findings from the field tests

The moisture conditions in the cavity insulation are generally rather uncritical. This is particularly true if the exterior ETICS is vapor permeable. In this case, the cavity insulation materials remain at a particularly low moisture level, at which both the thermal properties are favourable, and no durability risks must be feared. With a vapor retarding EPS insulation in the ETICS, the moisture levels remain somewhat higher or degrade somewhat more slowly. But here, too, critical moisture contents can only be observed to a small extent and in the short term.

The situation is somewhat different in ETICS insulation materials themselves when rendered and on masonry. Generally, high moisture contents result after application of the render, which however, often degrade within the first year in timber frame construction. In the case of southern orientation and rather dark colours, this happens particularly quickly, and correspondingly more slowly in the case of brighter colours and northern orientation. To accelerate drying, the walls should ideally be rendered early in the spring, which minimizes the moisture load in the first winter.

In the case of masonry with construction moisture, drying takes considerably longer due to the much higher quantity and storage capacity compared to the render layer. In this case, care must be taken to ensure the lowest possible construction moisture and good protection of the masonry against rain prior to installation of the ETICS to avoid unnecessary loads on the systems. The problem of the construction moisture becomes even more acute with thicker masonry, which can absorb correspondingly more moisture. Some manufacturers guarantee that their systems and insulating materials can withstand such high initial moisture levels temporarily without damage. In case of doubt, products from such manufacturers should therefore be preferred. In the case of renovation of existing buildings, a lower level of masonry moisture can be assumed, which relativizes the problem described above. Nevertheless, it is at least recommended to check the masonry moisture before applying the ETICS.

When using the non-hydrophobized wet board, which was found to be somewhat more susceptible to degradation by wood decay fungi in the lab test, the field tests showed recognizably lower moisture contents at the critical position under the render than the hydrophobized dry-process boards. Thus, the higher hygroscopicity as well as the stronger liquid transport in this board lead to a lower moisture level on the cold side in winter. This partly compensates the higher sensitivity of the material: although it is somewhat less resistant, it also only achieves lower moisture contents for the same installation situation. More precise knowledge of the hygrothermal parameters of the material and its resistance to wood decay fungi would allow a more accurate analysis to determine the predominating aspects in the

installation situation. In the current investigations, it was found that the wet-process board showed, despite its higher sensitivity, a lower risk of wood degradation than the dry-process boards, due to the lower moisture levels which occurred during the field test.

3.4.3 Outlook: Practice validation and further differentiation

The ThermNat I and ThermNat II limit curves developed in the project for natural fibre insulation materials with different resistance levels and the transient prediction model enable an assessment of the application safety of the products investigated and show good and promising results in comparison with the laboratory and field tests carried out.

The new prediction model must now be further tested for practical suitability and further validated based on real constructions. Both well performing and damaged components need to be evaluated - the model should be able to reproduce both, whereby in case of doubt, damage should be indicated too early rather than too late. It should become clear whether, in addition to the uncertainties already mentioned, there is a need for change in other aspects or whether improvements are possible. After any further adjustments and a successful trial period, it can be used as a practical tool. The prediction results currently given with growth of mycelium in [mm] can be implemented with a further validated factor as a wood degradation indicator by mass loss [% by mass]. In addition, a traffic light scheme is to be introduced to provide planners with a simple orientation for the design of structures.

In perspective, it is desirable to further differentiate the proposed two classes, both on the side of the more sensitive materials and on the side of the more resistant ones since some materials are presumably significantly more resistant to wood decay fungi than sapwood. For individual materials that deviate significantly from the classes, it is also possible to define an individual curve. For this purpose, test scenarios will be developed that are as simple as possible. For insulation materials made of straw or sheep wool, only little knowledge is available so far, so that their assessment and applicability is particularly difficult: currently, neither of the two limit curves can be used for them.

This project did not take a closer look at the wood based cladding materials. However, it became clear that these usually have even higher moisture contents than the insulation and thus also tend to exceed the corresponding limit values regarding durability earlier. Since there are also very different products here, which presumably also have correspondingly different resistance to wood decay fungi, these materials should also be subjected to more detailed durability tests in the future. The Appendix summarizes the development and the further prospects for the prediction models.

4 Thermal conductivity of natural fibre insulation materials

Most natural fibre insulation materials can store moisture to varying degrees both via sorption and in liquid form. Both influence the measurement of thermal conductivity in the laboratory, since the materials are normally not measured completely dry, but with the equilibrium moisture content that occurs during laboratory conditioning. As a result, the thermal conductivity measurement may not only measure the pure thermal conductivity of the material, but also the redistribution of heat due to the so-called latent heat effects described already in the introduction. Moisture evaporates on the warm side, extracts heat there and then supplies it again during condensation on the cold side. If an undefined mixture of sensible (heat conduction) and latent heat transport (vapor transport with phase change) is found in the measurement, there is a risk of mixing both effects and misrepresenting the thermal behaviour of the materials. This is particularly the case if the latent heat transport is also added to the thermal conductivity and the latter is thus assumed to be higher than it actually is. This has often happened in the past. During the approval process, additional surcharges were usually introduced to account for the increase in heat loss due to moisture content. Thus, to achieve a realistic material characterization, a differentiation between the two effects is necessary. How this can be done by appropriately adapted laboratory tests or by a combination of laboratory tests and computational analyses using hygrothermal simulations is investigated in the following chapter.

4.1 Current handling of the design value

The so-called design value of thermal conductivity (λ_B - in Germany or λ_r – in Austria) is used for the energy design of a building. Since the thermal conductivity in the material in the installed state with a corresponding moisture content is usually higher than in the dry state (λ_{dry}), the design value is given an additional value. This surcharge value is, however, to a certain extent a political parameter, which is regulated differently in the national standards of the individual countries and for which no uniform definition exists. In Switzerland, for example, natural fibre insulation materials sometimes remain without surcharge, depending on the area of application [33] while in Austria this can be as high as 20% (in case of missing monitoring of the production process) [9]. It therefore seems useful to clarify which surcharge is appropriate in practice for energy measurements (no further consideration of latent heat) or hygrothermal simulations (with consideration of latent heat). A harmonization at the European level would also be desirable to eliminate country-specific differences that cannot be explained physically.

In Germany, the design value for wood fibre insulating materials is determined according to DIN 4108-4 by adding 5%, but at least 2 mW/mK, to the declared value (λ_D). This design value

is in good agreement with the thermal conductivities, measured in current and previous projects [34] on wood fibre insulation samples preconditioned at 80% RH ($\lambda_{80\%}$). Figure 55 shows the design values according to DIN 4108-4 in comparison to the values with 20% surcharge as well as to the measured thermal conductivity values in dry condition and at 80% RH. It becomes clear that the 20% surcharge is significantly too high and overstating the installation moisture content.

However, the surcharge for other natural fibre insulation materials in Table 5 of DIN 4108-4 is generally 11% for "other vegetable fibres without mineral binders" and 4% for sheep wool. For "loose cellulose fibres", reference is made to DIN EN ISO 10456, which, however, does not define a clear surcharge value. For a practical thermal design of a building with such materials, further investigations are therefore required to define the material-specific surcharges.

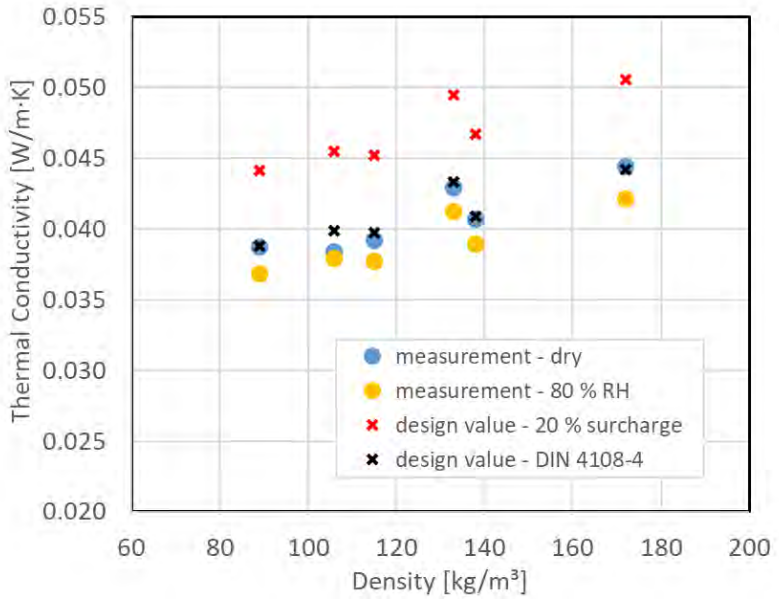

Figure 55 : Thermal conductivity of wood fibre insulation materials. Comparison with measured and design values.

As the recalculation of the thermal conductivity measurement has shown, the moisture-related increase of the thermal conductivity up to 95% RH is already implicitly included in the measurement of the natural fibre insulation materials, preconditioned at 80% RH (chapter 4.5). Furthermore, the simulation study of internally insulated exterior walls presented in [35] points out that the resulting R-value based on the thermal conductivity of the humid material measured in the lab ($\lambda_{80\%}$) is slightly lower than the R-value which results from a simulation during the heating period (October to April). This is true at least under Central European climatic conditions. The maximum RH in the simulated exterior walls with interior insulation with two different wood fibre materials (dry board, density 110 kg/m³ and wet board, density 160 kg/m³) only temporarily reach almost 100% RH on the exterior side under very critical conditions, while remaining below 80% RH in the middle of the insulation layer. These results already indicate that a surcharge of 20% could be clearly too high both for hygrothermal

material data and for application in thermal calculations. This aspect will be reviewed again in the evaluation of the field tests in the following chapter.

4.2 Results of the in-situ heat flow measurement

In the following, the results of the re-simulation of the in-situ heat flow measurement with the software WUFI® Pro 6 are presented. According to the manufacturer's specifications of the heta flow meters, the average ΔT should be > 20 K for assemblies with very low U-values to ensure a reliable measurement. Therefore, for the simulation adjustment, the 24h moving average values of the respective heat fluxes in the period between 11.01.2022 and 01.02.2022 were used. ΔT was on average about 20.5 K during this period. A detailed evaluation of all measurement constellations is presented in [36]. Furthermore, in [37] the thermal insulation potential of sheep wool and straw insulation is discussed in more detail on basis of the heat flow measurements on the ventilated variants.

In Figure 56 the simulation comparison with measurement of the variant with mineral wool and EPS ETICS facade is presented. There is good agreement between measured and simulated heat fluxes over the period considered. The average dynamic heat transfer coefficients (Λ_{dyn}) are on a very similar level with 0.101 W/m²K and 0.099 W/m²K, respectively. The simulation model thus leads to rather realistic results. Compared to the expected values, the Λ_{dyn} in the simulation is increased by 0.001 W/m²K (1%). When considering the heat fluxes from the simulation without latent heat effects (blue line), Λ_{dyn} with a value of 0.098 W/m²K corresponds exactly with the expected value. It can be concluded that these effects probably also led to the increase of the measured value by 0.003 W/m²K (3%) in the in-situ measurement.

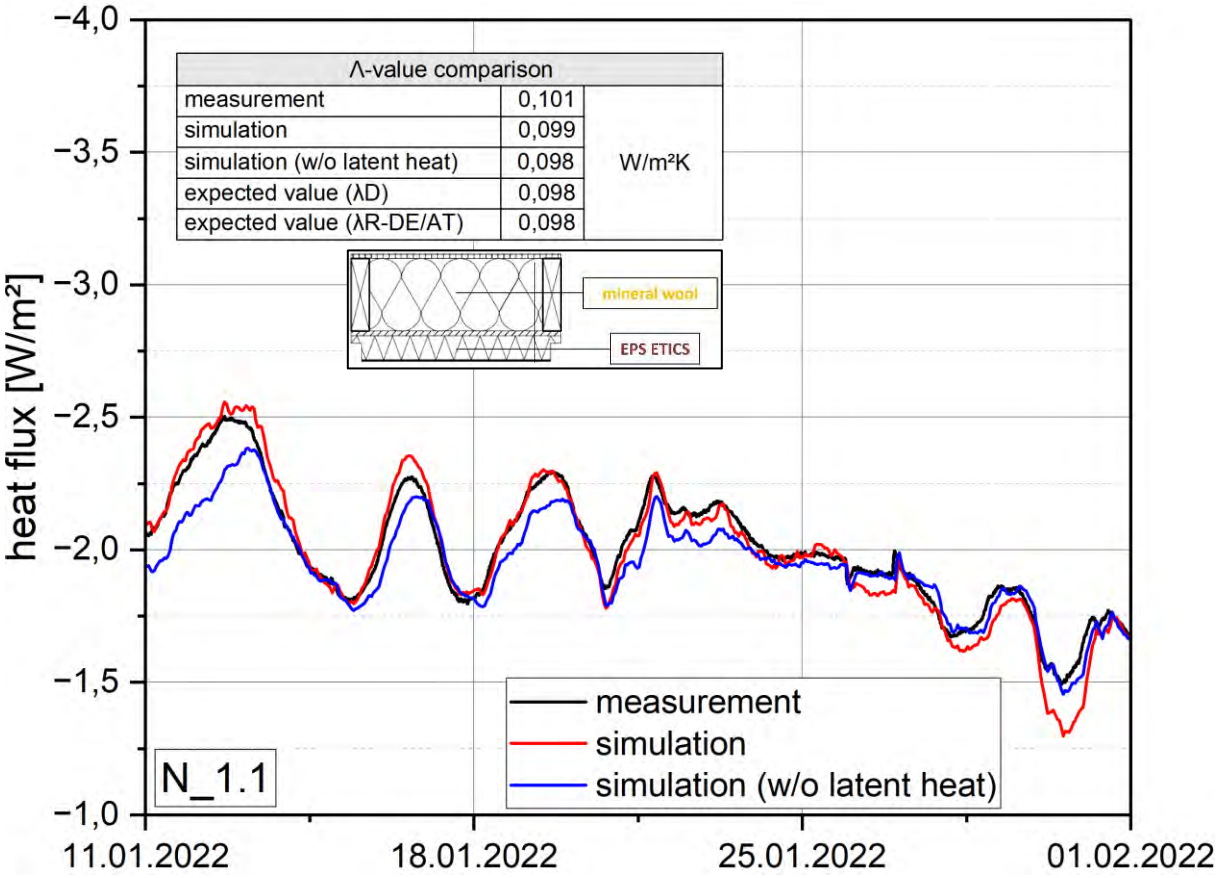

Figure 56 : Comparison between the measured and simulated heat flows (24h moving average) of the structure with mineral wool insulation and EPS ETICS (N 1.1). Tabular listing of the average dynamic heat transfer coefficients (Λ_{dyn}) in the measurement and simulation period, respectively, as well as their expected value calculated for the considered period on the basis of the manufacturer's data on nominal (λ_D) and design values (λ_r) of the insulation materials.

In comparison to this variant, the structure with mineral wool and wood fibre ETICS façade (N 2.1, Figure 57) also shows a relatively good agreement between simulation and measurement. The difference between the calculated Λ_{dyn} values based on the measured and simulated heat flows is with 0.004 W/m²K (3.7%) slightly larger than for the variant with EPS ETICS facade (1%). The heat transmission coefficient resulting from the simulation is higher than the expected values by +0.005 W/m²K (nominal value), +0.004 W/m²K (design value AT) and +0.003 W/m²K (design value DE), depending on the reference value. These differences are all higher than for the EPS variant. With deactivated latent heat effects, the corresponding simulated heat flows result in a Λ_{dyn} of 0.101 W/m²K, which corresponds exactly to the calculated expected value based on the nominal values. The increased heat flows in the simulation can therefore be attributed entirely to these effects. They are higher in this variant (wood fibre ETICS) than in the comparison variant with EPS ETICS. It can be assumed that at least a large part of the increased heat flux during the in-situ measurement is due to latent heat effects inside the WF ETICS.

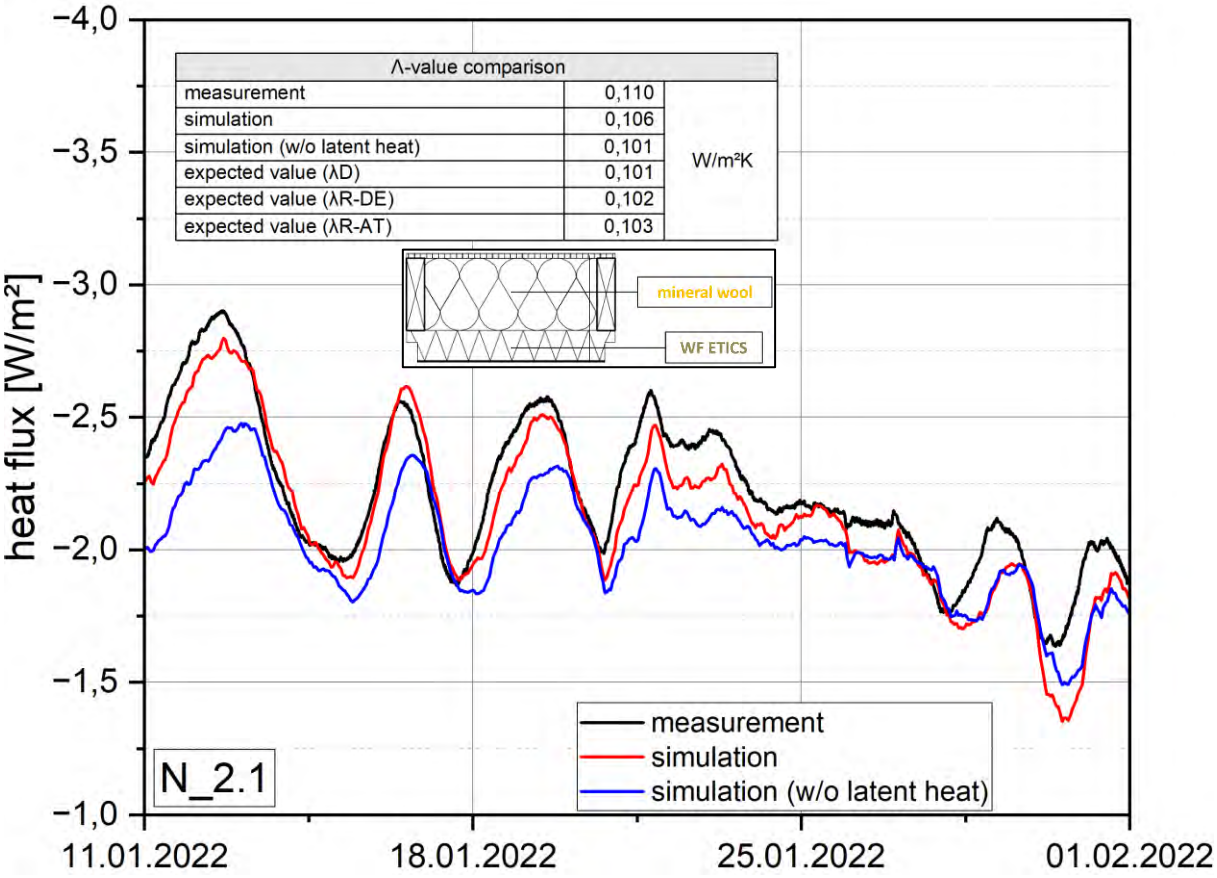

Figure 57 : Comparison between the measured and simulated heat flows (24h moving average) of the structure with mineral wool cavity insulation and WF ETICS (N 2.1). Tabular listing of the average dynamic heat transfer coefficients (Λ_{dyn}) in the measurement and simulation period, respectively, as well as their expected value calculated for the considered period on the basis of the manufacturer's data on nominal (λ_D) and design values (λ_r) of the insulation materials.

Figure 58 shows the simulation comparison of variant N 2.1 with wood-fibre cavity insulation and WF ETICS facade. Here, the simulated and measured heat flows also are relatively close to each other. The difference of Λ_{dyn} between simulation and measurement is 0.001 W/m²K (0.8% related to the measured value). Simulated without latent heat effects, Λ_{dyn} is 0.109 W/m²K, which, as with the variants described above (cf. Figure 56 and Figure 57), this corresponds to the calculated expected value based on the nominal values for this wall structure. As in the case of the previous variants, the difference between the Λ_{dyn} calculated on the basis of the nominal values and that obtained from the measurements can therefore also be explained here by moisture-related sorption processes in the wood fibre material and the resulting latent heat balance. Compared to the EPS ETICS variant with mineral wool cavity insulation (N 1.1, Figure 56), the share of the latent heat-related increase of Λ_{dyn} resulting from the respective simulations is 0.006 W/m²K higher. This amounts to +0.002 W/m²K (1%) for N 1.1 and +0.008 W/m²K (6.8%) for N 1.2.

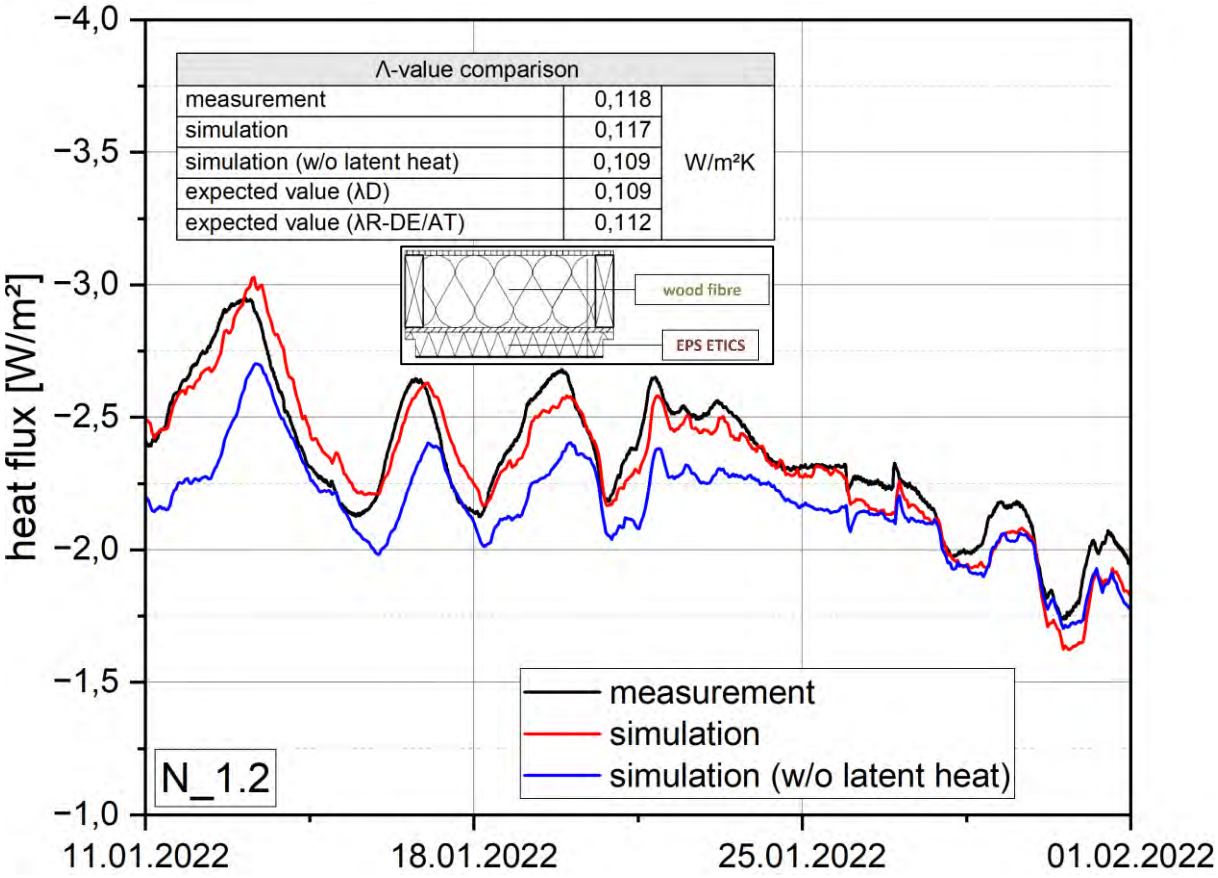

Figure 58 : Comparison between the measured and simulated heat flows (24h moving average) of the structure with wood fibre insulation and EPS ETICS (N 1.2). Tabular listing of the average dynamic heat transfer coefficients (Λ_{dyn}) in the measurement and simulation period, respectively, as well as their expected value calculated for the considered period on the basis of the manufacturer's data on nominal (λ_D) and design values (λ_r) of the insulation materials.

The simulation comparison of the construction variant with wood-fibre cavity insulation and WF ETICS facade (N 2.2, Figure 59) shows the same qualitative tendencies as already observed with respect to Figure 56 to Figure 58 described in detail. The share of the latent heat induced increase (in the simulations) of Λ_{dyn} is here even slightly higher than in variant N 1.2 and is +0.009 W/m²K (7.6%). The measured value of the dynamic thermal transmittance coefficient is +0.011 W/m²K (8.3%) higher than the Λ_{dyn} calculated on a nominal basis. It can be assumed that in this variant, due to the combination of two sorptive insulation materials (cavity and ETICS), the sorption-related latent heat effects are at a higher level than in the variants considered up to this point, in which either only the cavity insulation material (N 1.2), or only the ETICS (N 2.1), or neither of them (N1.1) consists of a sorptive material.

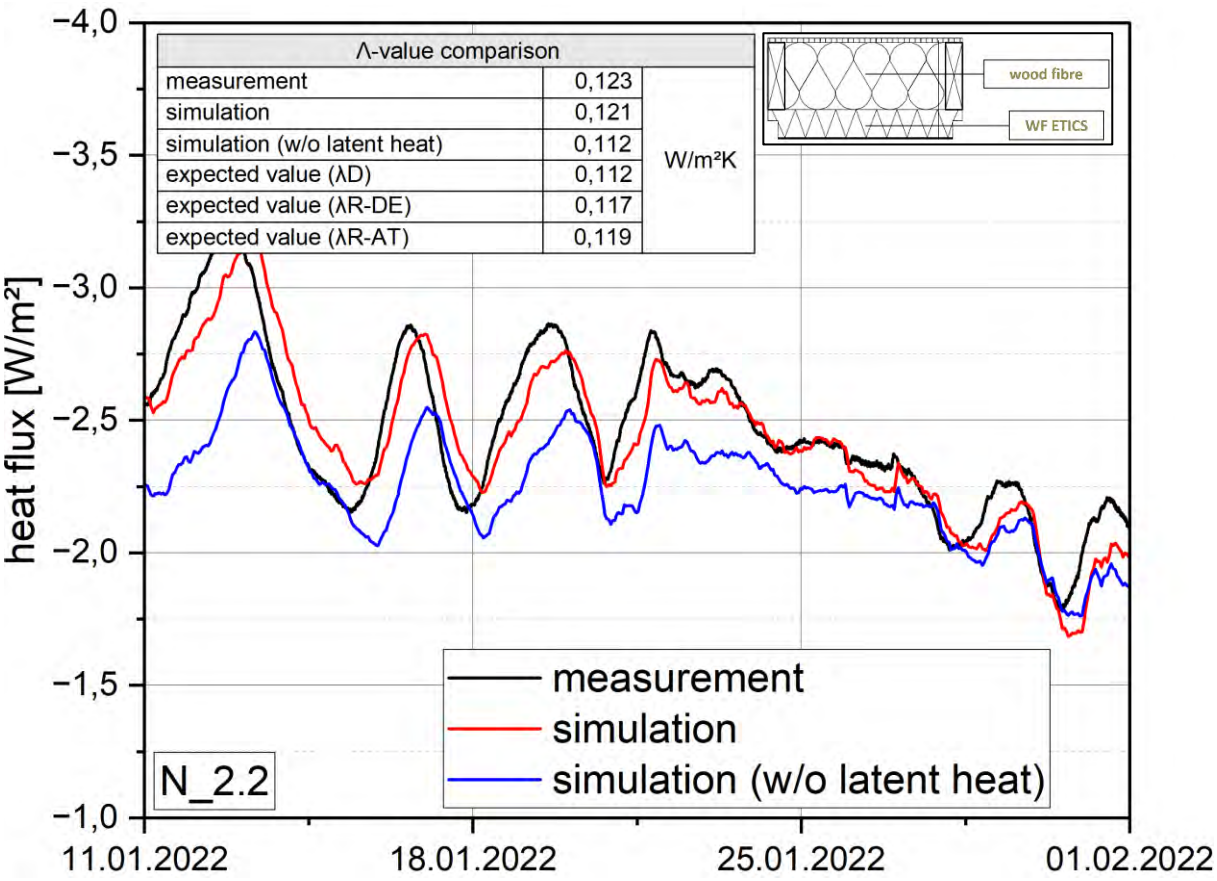

Figure 59 : Comparison between the measured and simulated heat flows (24h moving average) of the structure with wood fibre insulation and WF ETICS (N 2.2). Tabular listing of the average dynamic heat transfer coefficients (Λ_{dyn}) in the measurement or simulation period and their expected value calculated for the considered period based on the manufacturer's data on nominal (λ_D) and design values (λ_r) of the insulation materials.

The results described above with respect to Figure 56 to Figure 59 allow the conclusion that, due to sorption and desorption processes and the resulting positive latent heat balance, the measured heat flows were at a recognizably higher level than it would be expected based on the nominal and design values. This is particularly true for the considered variants with sorptive insulation materials (wood-fibre cavity insulation, wood-fibre ETICS). Sorption processes can also take place in the opposite direction, releasing thermal energy. [2]. From a physical point of view, all the energy stored in the structure in the form of latent heat during the colder half of the year is reversible and is released again in the warmer half of the year. This would reduce the heat fluxes during this period (→ reduced Λ_{dyn}). If such a phase is present in the heating season, this would increase the heat protection performance of the component during this period. It can therefore be assumed that the enthalpy-related heat losses can be recovered, at least in part. The annual average values of the dynamic heat transfer coefficients are thus certainly at a lower level than the values of Λ_{dyn} calculated on the basis of the in-situ measurement. Nevertheless, it cannot be assumed that all the latent heat stored in the insulation material is released during the heating period relevant for thermal insulation performance, but during the warmer half of the year. Therefore, a certain moisture surcharge

for the insulation variants considered here is certainly justified due to the latent heat losses. Whether the moisture surcharges for wood fibre insulation materials currently specified in ÖNORM EN ISO 10456 (AT) [38] or DIN 4108-4 (DE) [10] are realistic average values throughout the year, can unfortunately not be conclusively deduced from the outdoor measurements,. However, they indicate that the surcharge of 5% on the nominal value for wood insulation materials according to DIN 4108-4 is justified as an annual average. By contrast, an overall moisture surcharge of 20% on plant fibre insulation materials, as specified in ÖNORM B 6015-2, is clearly too high.

Figure 60 shows the simulation comparison of the construction variant with cellulose blow-in insulation and EPS ETICS. The difference between the Λ_{dyn} from simulation and measurement shows up higher here than in the variants considered so far (±0.014 W/m²K, 10.8%), with a higher Λ_{dyn} emerging from the measurements than from the simulation. The expected values are exceeded in the simulation/measurement by 0.008/0.022 W/m²K (nominal value), 0.005/0.019 W/m²K (design value DE) and 0.006/0.020 W/m²K (design value AT), respectively. Again, the exceeding in the simulation can be explained by latent heat losses. This is because when this effect is deactivated, Λ_{dyn} corresponds exactly to the nominal value-based expected value.

The comparison variant with wood fibre ETICS (Figure 61) tends to show comparable results. The deviations from the expected value described above are on a somewhat higher level than with EPS ETICS.

The exceedance of the expected value by the measurement-based Λ_{dyn} cannot be explained only by moisture-related effects. A determination of the density following the measurement showed that the optimum blow-in density was clearly exceeded in the constructions presented here and lies outside the approval range for the product at hand (75-90 kg/m³ instead of 40-65 kg/m³). If the density is too high (or too low), the thermal conductivity of the blow-in insulation material increases [39], which probably led to the somewhat more pronounced expected value exceedances in this test. In addition, it cannot be excluded that the water absorption potential in kg/m³ also increases with increasing density. Increased density results in a larger specific fibre surface area (m²/m³). The number of polar groups (OH groups), to which water can attach physisorptively [40] increases accordingly, allowing a greater absolute amount of water to be absorbed by the cellulose. [41]. The raw material of the blow-in insulation could also play a role [34]. However, many studies have shown that cellulose can show much better thermal insulation performance than in the present studies, when all reference parameters, including the required blow-in density, are met [42]. There for the increased blow-in density seems to be the main reason for the differences.

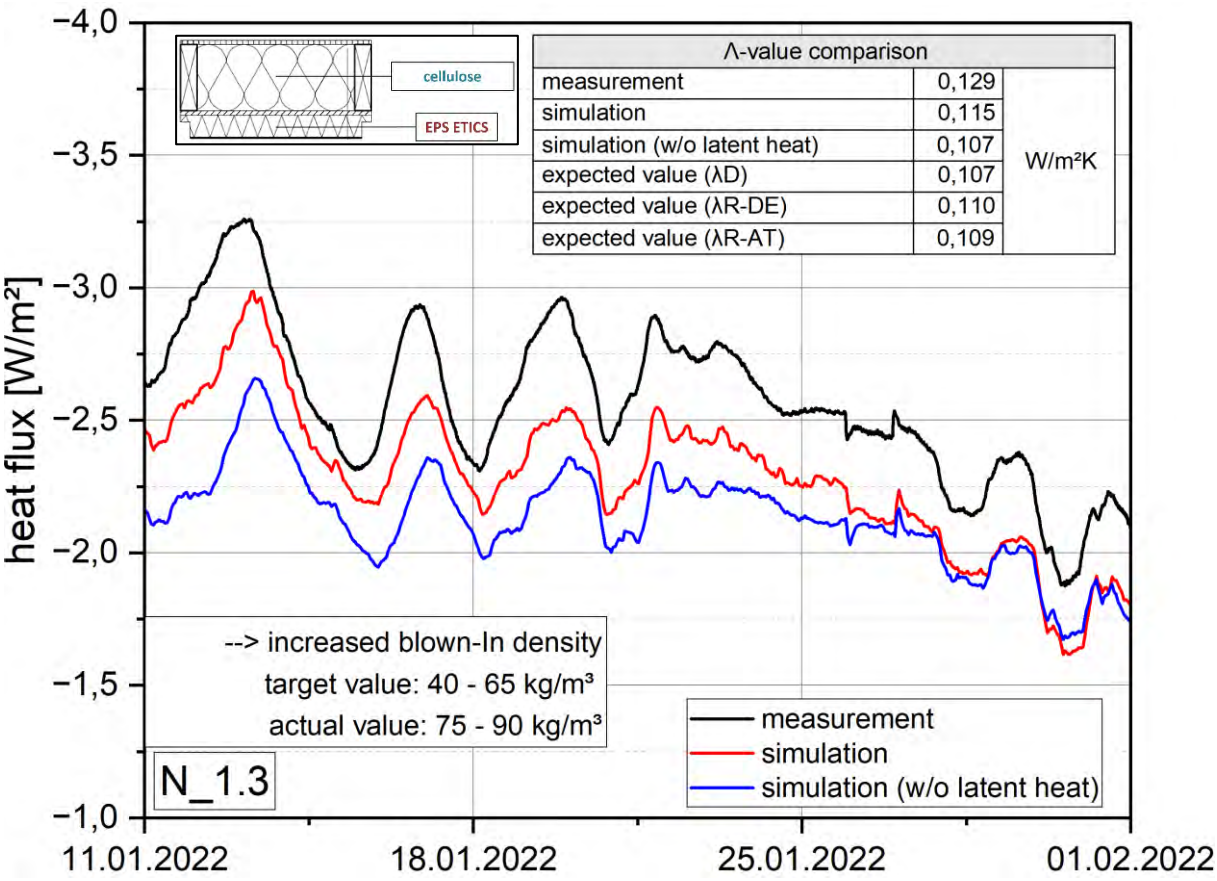

Figure 60 : Comparison between the measured and simulated heat flows (24h moving average) of the structure with cellulose blow-in insulation and EPS ETICS (N 1.3). Tabular listing of the average dynamic heat transfer coefficients (Λ_{dyn}) in the measurement or simulation period and their expected value calculated for the considered period based on the manufacturer's data on nominal (λ_D) and design values (λ_r) of the insulation materials.

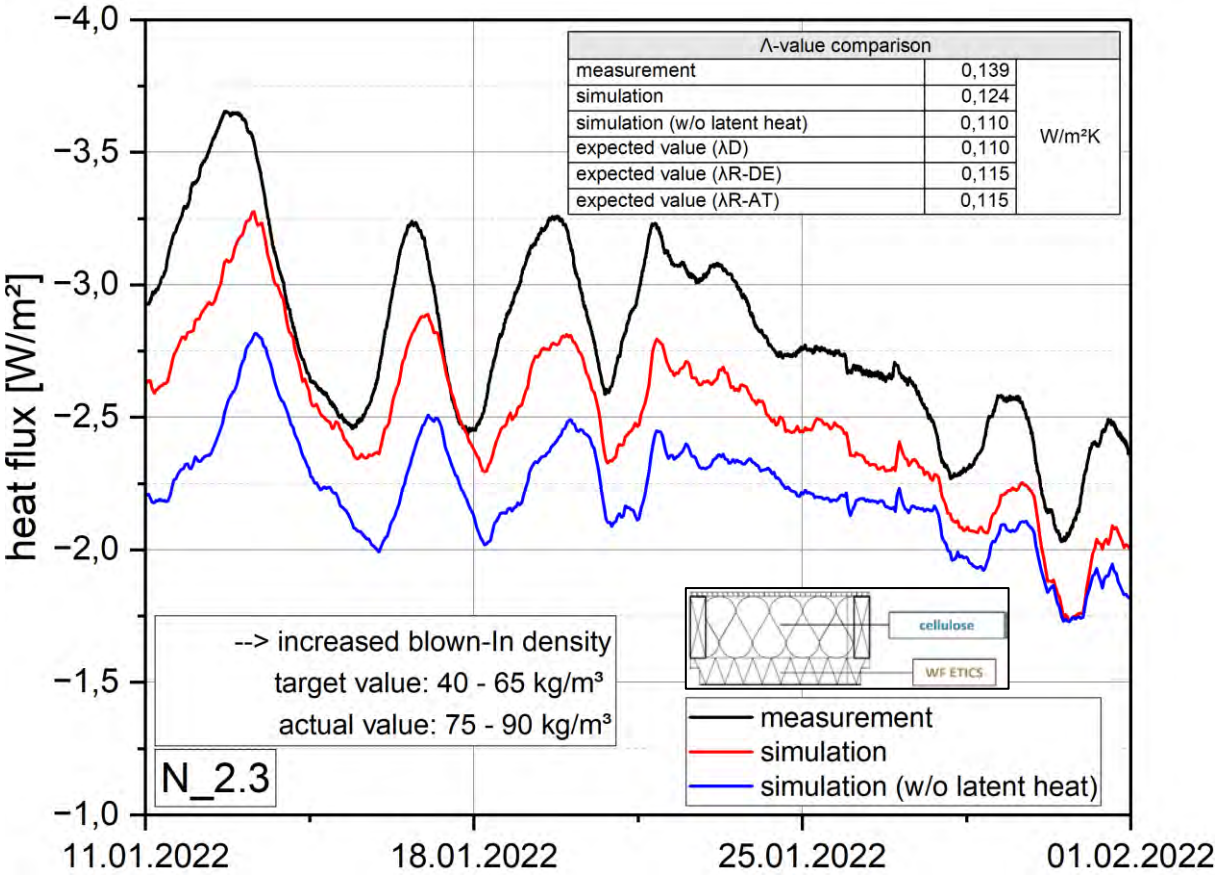

Figure 61 : Comparison between the measured and simulated heat flows (24h moving average) of the structure with cellulose blow-in insulation and WF ETICS (N 2.3). Tabular listing of the average dynamic heat transfer coefficients (Λ_{dyn}) in the measured or simulated period as well as their expected value calculated for the considered period based on the manufacturer's data on nominal (λ_D) and design values (λ_r) of the insulation materials.

The results from the simulation comparisons of the construction variants with sheep wool as cavity insulation are shown in Figure 62 (N 1.4, EPS ETICS) and Figure 63 (N 2.4, WF ETICS). In the case of EPS ETICS, there is no good agreement between simulation and measurement. The heat flows are slightly underestimated in the simulation ($\Lambda_{dyn,\ simulation}$ = 0.116 W/m²K, $\Lambda_{dyn,\ measurement}$ = 0.124 W/m²K). The measured moisture level (blue dashed lines) in the cavity averaged between 62% and 65% RH during the test period. On the outside of the cavity, the level was consistently > 80% RH. In the case of the construction variant with wood fibre ETICS, there is a good agreement between simulation and measurement ($\Lambda_{dyn,\ simulation}$ = 0.121 W/m²K, $\Lambda_{dyn,\ measurement}$ = 0.119 W/m²K). The relative humidity of the air during the test period was on average between 54% and 57% RH. The humidity level on the outside of the building remained < 75% RH.

In both cases, the dynamic heat transfer coefficients from the simulations without latent heat effects correspond to the nominal value-based expected values (0.111 W/m²K and 0.114 W/m²K). Since no product-specific hygrothermal data set was available for the sheep wool used, the data of a sheep wool from another manufacturer were used for the simulation. The

results from simulations and measurements suggest that this data set does not realistically represent the sorption properties of the sheep wool product used here in the higher moisture range. This results from the simulation of the EPS variant (N 1.4, Figure 62), the latent heat balance at the higher humidity level is too inaccurate, leading to an underestimation of the heat fluxes. The sorption properties are strongly product-dependent and are strongly influenced by the addition and concentration of various additives (e.g. insecticides, fungicides, hydrophobing agents, etc.) - accordingly, product-specific data sets would be required for a more accurate recalculation.

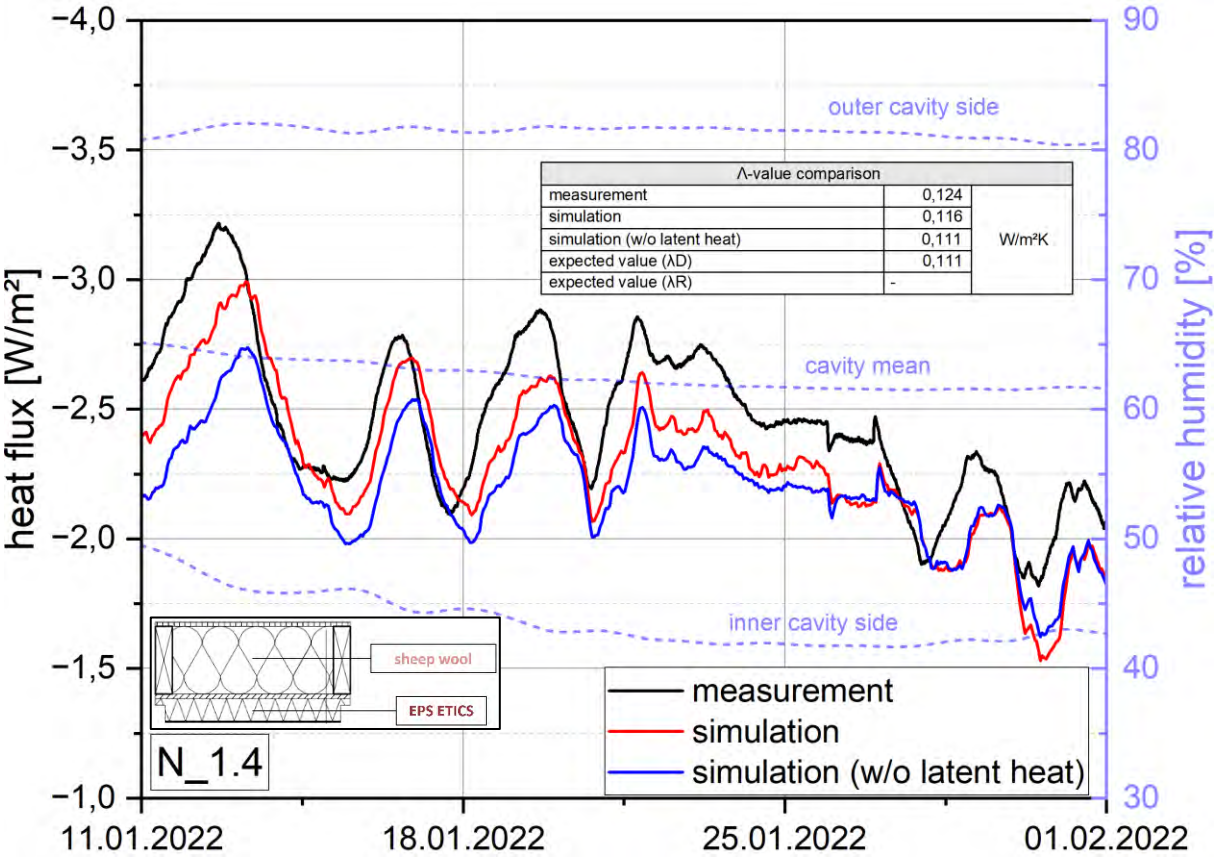

Figure 62 : Comparison between the measured and simulated heat flows (24h moving average) of the structure with sheep wool insulation and EPS ETICS (N 1.4), as well as the RH level at different locations in the cavity. Tabular listing of the average dynamic heat transfer coefficients (Λ_{dyn}) in the measurement and simulation period, respectively, as well as their expected value calculated for the considered period based on the manufacturer's data on the nominal value (λ_D) of the insulation materials.

Considering the deviation between the measured value-based and the nominal value-based dynamic thermal transmittance in each case, the result is an increased Λ_{dyn} of 0.013 W/m²K (+ 11.7%) for the EPS variant and an increased Λ_{dyn} of 0.005 W/m²K (+ 4.4%) for the WF variant. The results of the comparison therefore indicate in a broader sense that vapour permeable facade systems can not only be advantageous for the durability of exterior wall components (see Chapter 3.3.1) but can also make a positive contribution to thermal insulation performance due to the lower moisture content in the cavity.

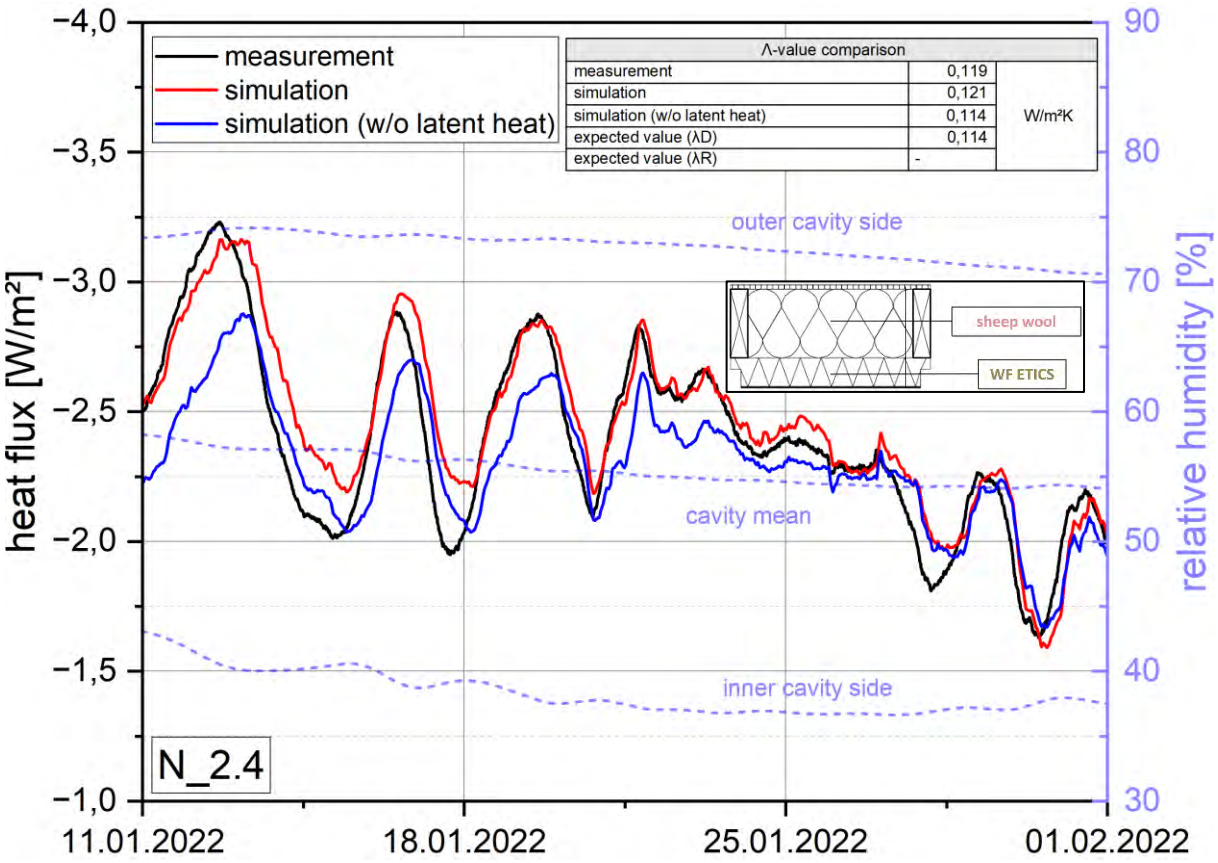

Figure 63 Comparison between the measured and simulated heat flows (24h mean value, sliding) of the structure with sheep wool insulation and WF ETICS (N 2.4), as well as the RH level at different locations in the cavity. Tabular listing of the average dynamic thermal transmittance coefficients (Λ_{dyn}) in the measurement and simulation period, respectively, as well as their expected value calculated for the considered period based on the manufacturer's data on the nominal value (λ_D) of the insulation materials.

In Figure 64 the results of the simulation comparison are plotted for the variant with straw blow-in insulation in the cavity and EPS ETICS facade. The measurements indicate a significantly lower dynamic thermal transmittance than would be expected based on the nominal values ($\Lambda_{dyn,\ measurement}$ = 0.129 W/m²K, $\Lambda_{dyn,\ nominal\ values}$ = 0.138 W/m²K). Assuming a constant thermal conductivity (moisture-independent, with latent heat effects) of the straw blow-in insulation of 0.055 W/mK (≙ λ_D), the heat fluxes in the simulation are significantly overestimated ($\Lambda_{dyn,\ simulation,\ 055}$ = 0.146 W/m²K). Assuming a constant λ of 0.044 W/mK, simulated and measured heat fluxes are relatively close ($\Lambda_{dyn,\ Simulation,\ 044}$ = 0.132 W/m²K), indicating that the nominal value (λ_D) of 0.055 W/mK of the straw blow-in insulation used here is too high.

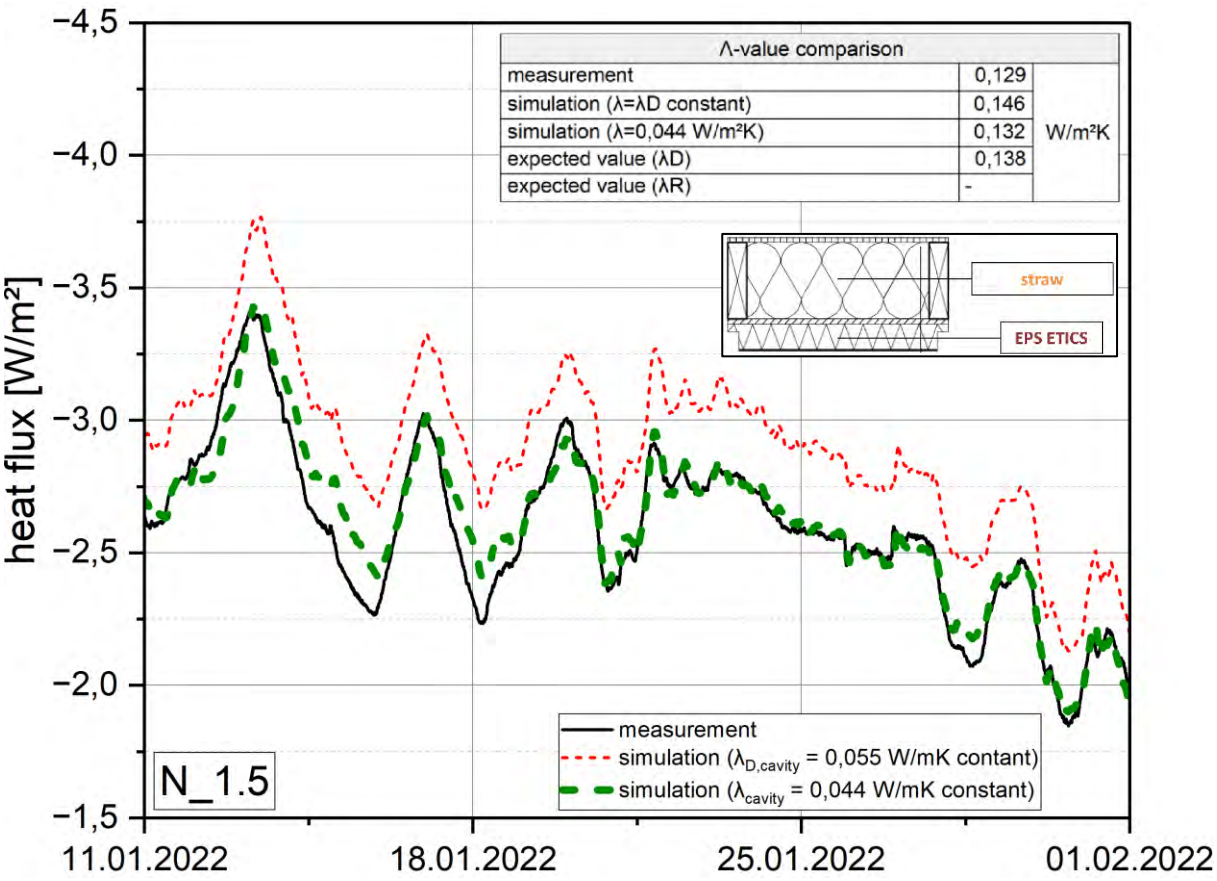

Figure 64 : Comparison between the measured and simulated heat flows (24h moving average) of the structure with straw blow-in insulation and EPS ETICS (N 1.5). Tabular listing of the average dynamic heat transfer coefficients (Λ_{dyn}) in the measured and simulated period, respectively, as well as their expected value calculated for the considered period based on the manufacturer's data on the nominal value (λ_D) of the insulation materials.

Also for the straw variant with WF ETICS (N 2.5, Figure 65), the measurement-based Λ_{dyn} is clearly below the nominal value-based thermal transmittance ($\Lambda_{dyn,\ measurement}$ = 0.136 W/m²K, $\Lambda_{dyn,\ nominal\ values}$ = 0.143 W/m²K). Assuming the 0.044 W/mK approximated above for the moisture-independent thermal conductivity of the straw insulation, for the variant with WF ETICS (N 2.5, Figure 65) the heat flows are somewhat overestimated. It can be assumed that the reason for this lies in the data set, which does not realistically describe the sorption processes in this specific straw material. As already mentioned with respect to the sheep wool variants (Figure 62, Figure 63), inaccuracies in the sorption isotherm affect the simulated latent heat effects and its energy balance. To realistically quantify the latent heat effects, a product-specific data set including the moisture-dependent thermal conductivity and sorption isotherm would be necessary.

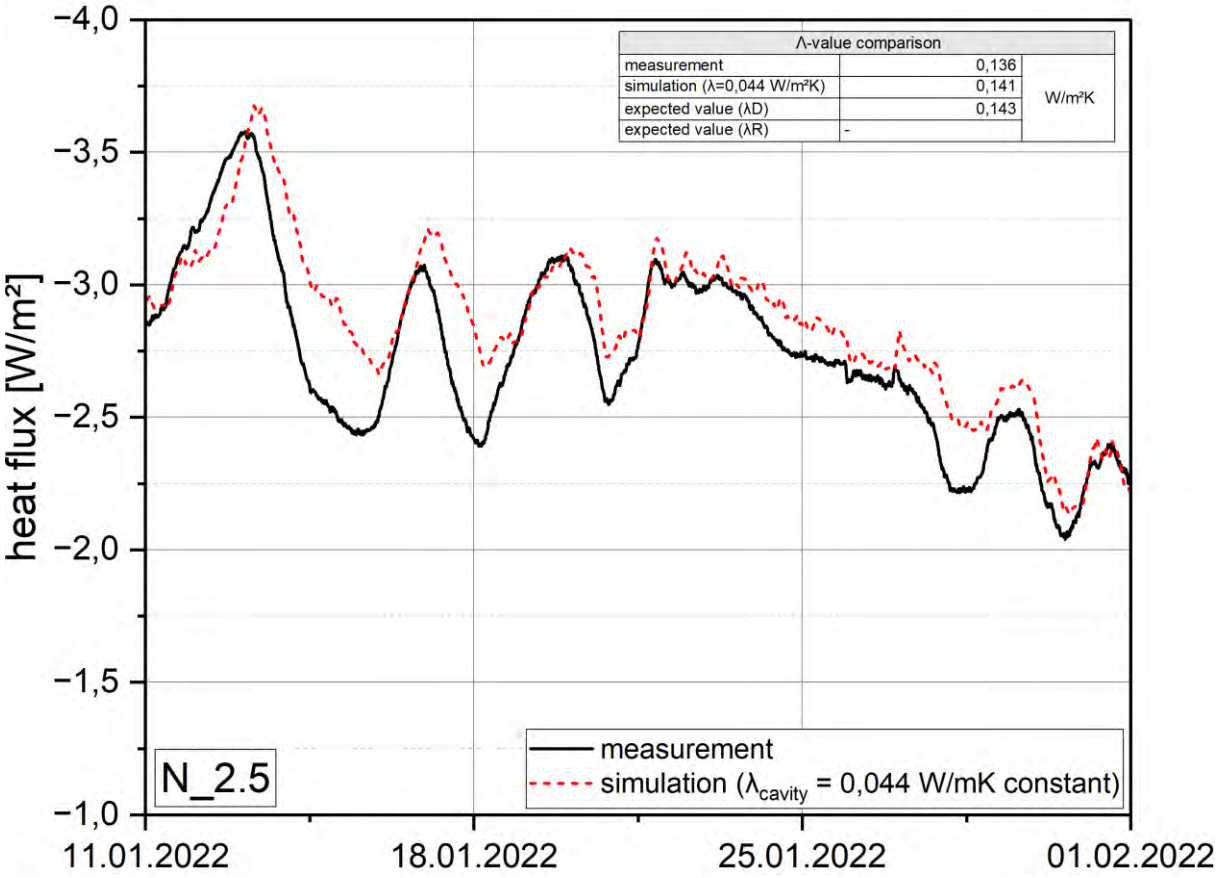

Figure 65 : Comparison between the measured and simulated heat flows (24h moving average) of the structure with straw blow-in insulation and EPS ETICS (N 1.5). Tabular listing of the average dynamic heat transfer coefficients (Λ_{dyn}) in the measured and simulated period, respectively, as well as their expected value calculated for the considered period based on the manufacturer's data on the nominal value (λ_D) of the insulation materials.

Summary of in-situ heat flow measurements

The reproduction of the measurements using hygrothermal simulation showed a good agreement with the measured heat flows for the cases where the hygrothermal data was known with sufficient accuracy. Overall, it was shown that the moisture content induced increase in thermal conductivity is only small up to about 95% RH, occurring predominantly under real life conditions. Only at higher humidity levels or dew water formation the influence becomes significantly higher, mainly due to the more dominant latent heat effects under these conditions.

For the cellulose fibre variants, significantly higher heat flows were measured than expected based on the technical specifications. A subsequent density measurement showed that the permitted compression density was clearly exceeded. In addition to eventual latent heat effects, the high increase is almost certainly caused by this fact. That highlights once more the importance of complying with the requirements for the blow-in density.

The straw blow-in insulation showed significantly lower heat flows (-5% to -7%) than the technical characteristic values provided by the manufacturer would suggest. Whether these values were declared by the manufacturer with increased certainty is not known. Despite this, the result indicates that the potential of these insulation materials has not yet been exploited.

In Table 5 the data shown in Figure 56 to Figure 65 is summarized and compared with the deviations between measurement and expected values. In most cases, with exception of the straw variants, the measured heat transmission coefficients ($\Lambda_{dyn,\ measurement}$) are higher than the heat transmission coefficients ($\Lambda_{dyn,\ nominal\ value}$) calculated based on the nominal thermal conductivity value. The relative deviations for the insulating materials are in a range between about 4% and 20%. The proportionally high deviation for the cellulose variants is mainly attributed to the blow-in density, which is clearly too high for the measured variants. Looking at the other cases, the deviations indicate that a surcharge of 5% on the nominal value for wood fibre insulation materials according to DIN 4108-4 is rather not excessive on an annual average. The available results even indicate that for purely thermal design, a slightly higher surcharge (between 5% and 10%) could possibly also be justified in some cases. On the other hand, a general moisture surcharge of 20% on natural fibre insulation materials, as applied in ÖNORM B 6015-2, is clearly too high.

Table 5 : Summarized comparison of the average heat transfer coefficients Λ of the different variants resulting from the heat flow measurements in the period between 11.01.2022 and 01.02.2022 compared with its expected values calculated based on the nominal values stored in the technical product data sheets.

Variant		Measurement Λ ($\Lambda_{dyn,\ measurement}$)	Expected value Λ ($\Lambda_{dyn,\ nominal\ value}$ - base λ_D - manufacturer's specification)	Deviation
Cavity insulation	ETICS			
Mineral wool	EPS	0,101	0,098	+ 3,0%
Mineral wool	WF	0,110	0,101	+ 8,2%
Wood fibre	EPS	0,118	0,109	+ 7,6%
Wood fibre	WF	0,123	0,112	+ 8,9%
Cellulose	EPS	0,129	0,107	+ 17,1%
Cellulose	WF	0,139	0,110	+ 20,9%
Sheep wool	EPS	0,124	0,111	+ 10,5%
Sheep wool	WF	0,119	0,114	+ 4,2%
Straw	EPS	0,129	0,138	- 7,0%
Straw	WF	0,136	0,143	- 5,2%

4.3 Laboratory measurements of moisture-dependent thermal conductivity (thermal conductivity)

4.3.1 Objective and preliminary investigations with hygrothermal simulation with WUFI®

The aim of the laboratory measurements is either to identify a test scenario that directly provides usable and realistic thermal conductivity values for practical applications or that, in combination with hygrothermal simulations, indirectly provides the measurement basis for such values. To limit the laboratory effort, some preliminary investigations are therefore carried out first to exclude less suitable procedures in advance. Condensation should be avoided as far as possible in laboratory tests, since under these conditions moisture is redistributed until the vapor pressure in the specimen has dropped to a level where no more condensation occurs on the cold side. However, in the case of insulation materials with sorption moisture and liquid transport, latent heat transport takes place even if no condensation occurs and the moisture profile is in equilibrium. This is because liquid transport starts in the fibres or pores of the materials above about 75% to 80% RH. Since liquid transport always proceeds towards the lower moisture content, it opposes vapor transport in the temperature gradient, i.e. it partially transports the water from the humid cold side back to the drier, warm side. This permanent transport of vapour from warm to cold and liquid water back from cold to warm, which occurs at a steady moisture profile, is also known as "heat pipe effect". In one direction, heat transport occurs by desorption (evaporation) and adsorption (“condensation” below the saturation vapor pressure), but in the other direction (liquid transport) this heat transport does not occur or only to a much smaller extent. Figure 66 shows on top schematically the heat and moisture flows during the redistribution phase ("Phase A" in Figure 68) and on bottom in the equilibrium state ("Phase C") during a thermal conductivity measurement.Accordingly, avoiding condensation shortens the transient phase.

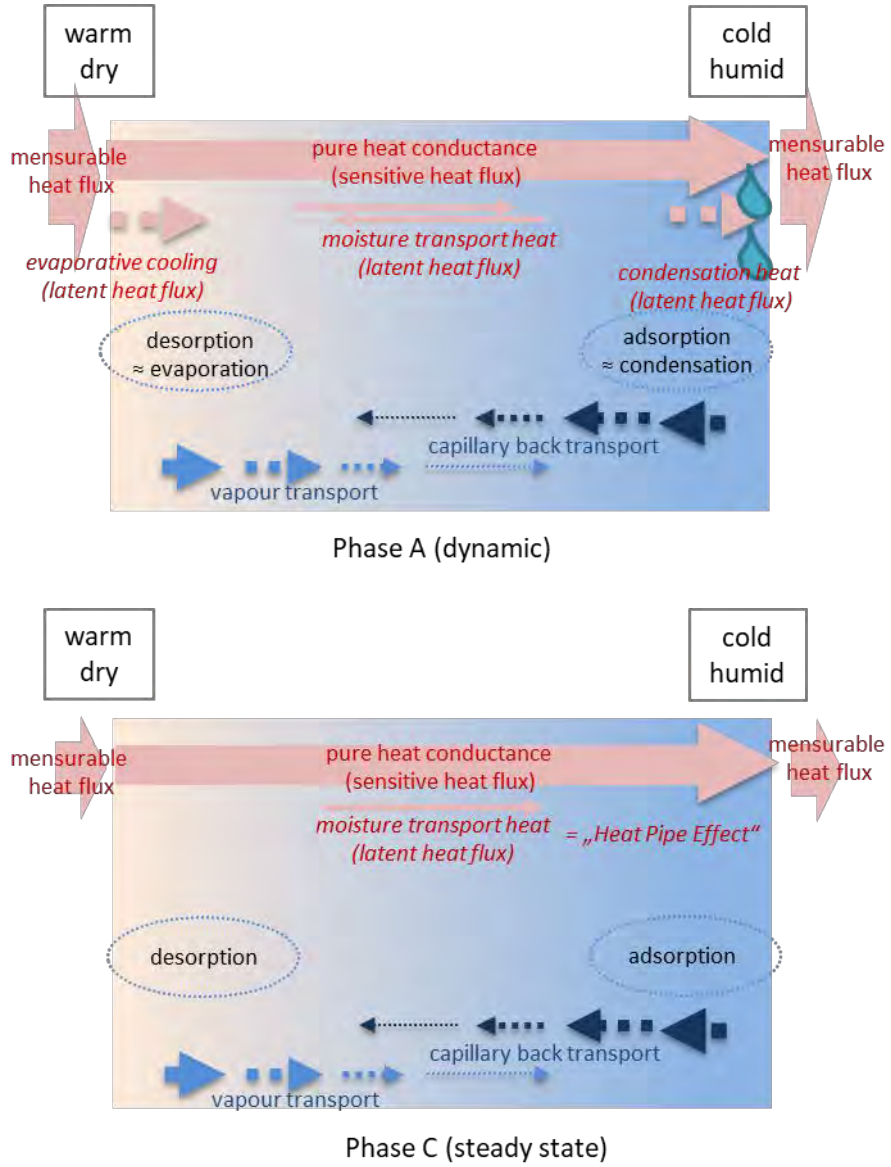

Figure 66: Schematic drawing of heat and moisture transport in the moisture redistribution phase (top, corresponds to "Phase A" according to ISO 10051) and in the final equilibrium state (bottom, "Phase C") during thermal conductivity measurement of a material.

Most of the latent heat flows can thus be avoided by preventing relative humidities close to 100% on the cold side of the specimen, while the smaller part caused by the heat pipe effect is unavoidable both in the laboratory and in real life. For the laboratory test, therefore, a small temperature gradient of 1 K per cm (here 10 K for the 10 cm thick specimen) is selected based on preliminary calculations in order to avoid condensation with preconditioning of the specimens at 80% RH and to limit the duration of the test until equilibrium is reached. The temperatures at the two surfaces are assumed to be constant at 5 °C and 15 °C. The surfaces are vapor-tight, so that no moisture exchange with the environment is possible, only a redistribution within the specimen. The initial moisture content is assumed to be homogeneously distributed in the material and amounts to 11.4 % by mass, which corresponds

to the equilibrium moisture content (EMC) at 80% RH and thus to the conditions during preconditioning. The hygrothermal parameters for the investigated wood fibre material were comprehensively measured in the IBP hygrothermal laboratory (chapter 4.5.1).

One measurement approach that has been used repeatedly in recent years involves dividing the material into individual layers that are separated from each other with vapor-tight foils. This prevents vapor transport across the interfaces between the layers, which means that the moisture cannot be transported through the whole specimen to the cold side and condense there. Since only small temperature differences occur within the individual layers, the partial pressure difference also remains small. Since the method is particularly complex, it is recalculated by the help of hygrothermal simulation and compared with the measurement of the whole panel without dividing.

To quantify the magnitude of the remaining latent heat effect, the measurement of the whole board with 10 cm thickness is simulated at first. During a normal hygrothermal simulation performed with the software WUFI® [43], the heat of evaporation of 2500 kJ/kg (related to the evaporated amount of water) is withdrawn at the respective position during evaporation or desorption and the corresponding amount of heat is added again at the position where condensation or absorption takes place. For analytical purposes, however, this latent heat transport can also be deactivated in the simulation. In that case the moisture distribution is calculated without changings in the moisture balance, but the influences on the heat balance are not taken into account.

Humidity and temperature profiles of the simulation of the whole board are shown in Figure 67 on the left. The relative humidity increases to a maximum of 92% on the cold side, so no condensation occurs. Simulation "with" latent heat results in an effective thermal conductivity of the whole board of 0.0389 W/mK in the steady state, while this value drops to 0.0387 W/mK when calculated "without" latent heat. The difference of 0.0002 W/mK would accordingly be due to the latent heat effects, or, since no condensation occurs on the cold side of the specimen, to the heat pipe effect. The thermal conductivity was initially taken from the manufacturer's specifications during the pre-calculation for the laboratory measurement. In the case of the specimens shown in Figure 67 and described here, the final solution (see chapter 4.5.3) with the moisture-dependent thermal conductivity was used and re-simulated.

Figure 67 shows on the right side the calculated temperature and humidity profiles after reaching the equilibrium state for the individual 20 mm thick layers separated by foils. While the relative humidity in the whole board increases from approx. 62% on the warm side to 92% on the cold side, the range in the vapor-tight separated layers remains significantly lower, as expected, with values of approx. 77 to 86% RH.

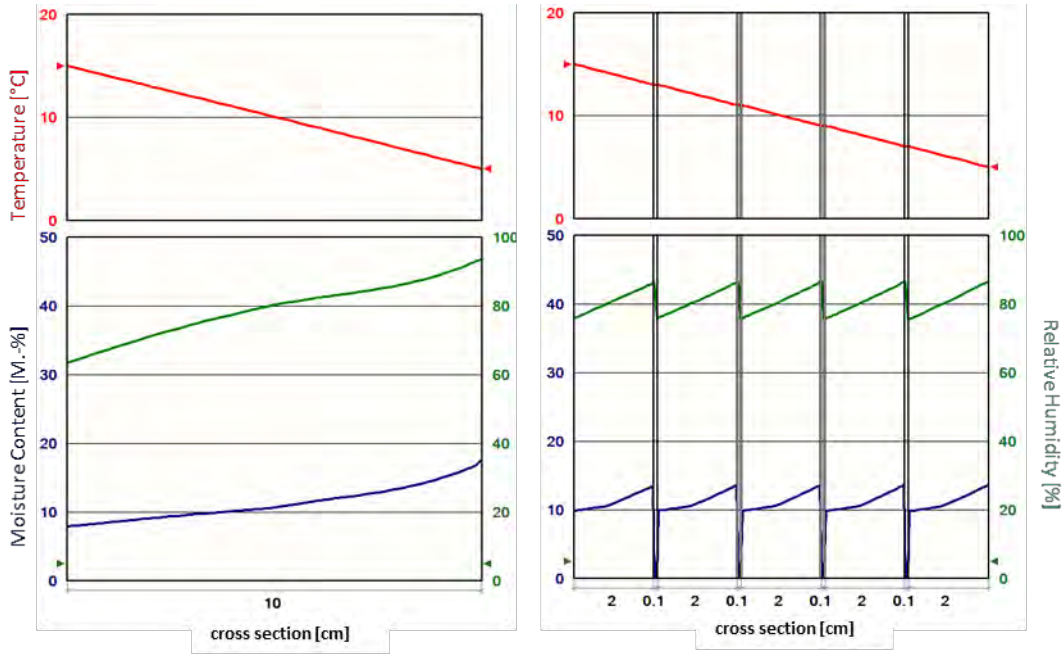

Figure 67 : Calculated profiles of temperature (red), relative humidity (green) and water content (blue) in a wood fibre insulation material in the equilibrium stateafter completed moisture redistribution under boundary conditions corresponding to the thermal conductivity test. On the left, simulation of the test on the whole board, on the right on the layered board with vapor-tight foil between the individual layers.

The evaluation of the effective thermal conductivity now results in a value of only 0.0388 W/mK for simulation with latent heat instead of 0.0389 W/mK without film separation, while the value without latent heat is 0.0387 W/mK as before. The remaining increase in heat transport due to the heat pipe effect can thus be reduced from 0.0002 to 0.0001 W/mK, but still not completely eliminated. The improvement is also limited by the fact that the moisture level on the cold side also reaches about 18 % by mass, while it rises only to a maximum of below 14 % by mass at the interfaces of the individual layers. Part of the higher effective thermal conductivity in the measurement of the whole board could therefore also be due to the non-linear increase in thermal conductivity at this higher water content.

In summary, it can be stated that with a suitable choice of preconditioning and temperature gradient in the thermal conductivity measurement, the remaining latent heat effects remain very low and, at a maximum of 0.5%, well below the measurement accuracy limit of the thermal conductivity measurement (2 - 3% as standard). The complex procedure of measuring with vapor-tight separated layers can halve the latent heat effect under optimistic assumptions, but it cannot eliminate it completely either. This measurement method is therefore not used in the following. Instead, the measurements are carried out on whole and layered boards, whereby the individual layers with temperature measurement at the layer boundaries have the advantage that different thermal conductivities can be correlated with the water content of the partial layers determined after the measurement.

4.3.2 Measurement method

The determination of thermal conductivity for thermal insulation in buildings is carried out according to DIN 4108-4 in accordance with DIN EN 12664 [44]. DIN EN 12664 includes the procedure according to ISO 10051 [45] for the measurement of moist samples. In principle, the Guarded-Hot-Plate method (GHP) measurement is a direct static measurement method in which a temperature gradient is applied between the hot and cold side. This gradient is kept constant until all heating or storage processes have been completed and a constant heat flow is established. The thermal conductivity is then calculated from the measured heat flow in equilibrium stateand the temperature difference measured during this process and is related to the thickness of the specimen. If the specimen is dry or vapor-tight, the steady-state condition is reached within 4 to 24 hours, depending on the specimen, and the measurement can be evaluated. In the case of moist specimens, however, various moisture transport processes occur in the specimen, as described above, which may significantly influence the thermal behaviour. The procedure according to ISO 10051 stipulates that the measurement is evaluated either at the beginning, before the transport processes for the moisture begin (phase A in Figure 68) or after the transport is completely finished and a stable condition is reached (phase C).

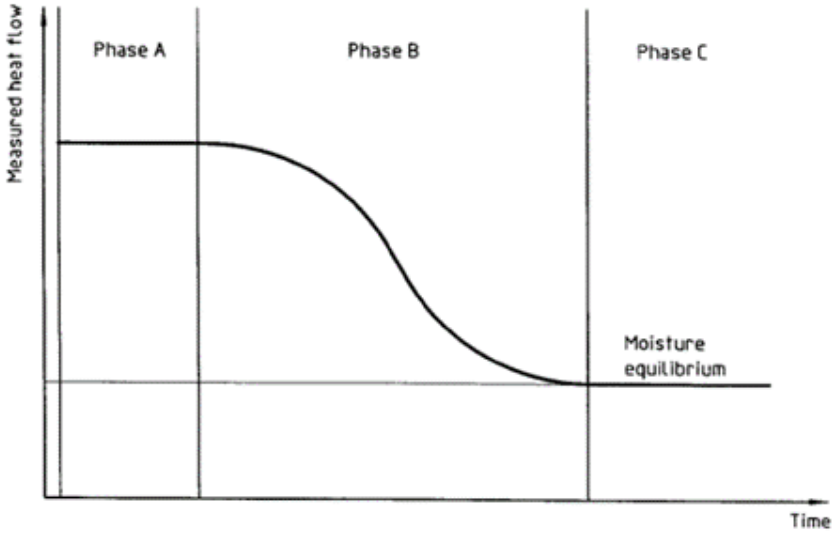

Figure 68 : Phase sequence in the determination of thermal conductivity in moist samples Source: ISO 10051.

It is already known from earlier measurements at Fraunhofer-IBP that no evaluation is possible in the phase A range for renewable raw materials such as wood fibres, which are characterized by a high equilibrium moisture content and low diffusion resistance. This confirms the theoretical considerations in the previous chapter. Moisture transport starts immediately with the application of a temperature gradient. Therefore, the evaluation of the measurement in phase C must take place when the redistribution processes are completed. It may take a long

time until the heat flow is stable, so that the usual measurement duration in the Guarded-Hot-Plate apparatus of less than 24 h must be extended to several days or even weeks. According to EN 12664 A.3.11, the measurement is considered to be "in steady state" if the value of thermal conductivity does not change by more than 1.0% within one test period. The test period must be determined based on the sample thickness, thermal conductivity and heat capacity according to the standard and is approx. 24 h for a wood fibre board with a thickness of 100 mm. Thus, the change in thermal conductivity within 24 h must not be greater than 1.0% so that the measurement can be evaluated. In addition, the thermal conductivity must not be monotonically decreasing. In the sample, a gradient of the moisture distribution will occur from the lower to the higher partial pressure. The part of the sample facing the warm side will get drier due to the higher partial pressure there, while the part of the sample on the cold side will get moister. Depending on the equilibrium moisture content of the specimen and the temperature on the cold side, condensation may also occur, and water may appear in liquid form in the specimen. To determine the moisture dependence of the thermal conductivity, ISO 10051 requires the specimens being prepared in a special way: The specimen is cut into individual slices of equal thickness prior to measurement. An additional temperature sensor is placed between each slice. The mass of the individual layers is determined before and after measurement and in the dry state. From these data, the moisture content of each individual sample slice is determined. With the additional temperature sensors, the thermal conductivity can be determined for each layer individually based on the constant heat flow. On this basis, the thermal conductivity can be determined for each layer as a function of the respective moisture content.

4.3.2.1 Measurement devices

The laboratory measurements for moisture-dependent thermal conductivity were carried out in the laboratory of Fraunhofer-IBP in Stuttgart. The measurements on the moist samples were carried out in a GHP apparatus of the type Netzsch-Taurus TLP 900 with protected heating plate and gradient protection with a measuring area of 50 cm x 50 cm and protective ring of 20 cm (heating plate 90 cm x 90 cm). The instrument can be used as a one-plate or two-plate apparatus. The sample installation is horizontal, the heat flow direction is therefore vertical. Thermocouples with 0.5 mm diameter are deposited directly onto the specimen as temperature sensors. For the measurements on the single slices, the apparatus was equipped with additional measurement technology. A multiplexer from Agilent with additional 0.2 mm diameter thermocouples was used. Instead of using the internal reference temperature in the multiplexer, the precision of the temperature measurement was optimized by using an electronic ice point. The thin thermoelements with a thickness of only 0.2 mm allow the temperature in the intermediate layers to be measured with minimal heat flow in the transverse direction and little deformation of the surfaces. For comparative measurements on the dry samples, a GHP-Titan type apparatus from the same company was used. The device has a measuring area of 15 cm x 15 cm with a heating plate of 30 cm x 30 cm.

4.3.2.2 Error consideration

The determination of the thermal conductivity according to DIN EN 12664 in the GHP apparatus with protected heating plate is a direct measuring method. According to EN 12664, the expected measurement accuracy is to be assumed to be 2% of the measured value (Annex B 1.5.3 in EN 12664). In addition to this measurement uncertainty, the method according to ISO 10051 with additional temperature sensors at the layer boundaries of the sliced specimen adds a non-negligible amount of uncertainty. For a layer thickness of 20 mm and a temperature gradient of 1 K / cm, a temperature gradient of 2 K results for each layer. The thermocouples have a accuracy of ± 0.1 K. The thickness of the samples can be adjusted and determined to an accuracy of about 0.2 mm due to the rather soft material. Combined, a measurement uncertainty of approx. 3% - 4% of the measured value must be expected.

4.3.3 Investigations and results

4.3.3.1 Tested materials and sample preparation

For the laboratory measurements, a wood fibre insulation manufactured in dry-production process with a nominal bulk density of 110 kg/m³ was used. The insulation board is to be classified as vapor permeable with the declared water vapor diffusion resistance value μ of 3.0. The boards are supplied in the dimensions of length 1000 mm x width 400 mm x thickness 100 mm. Since the panel used has a measuring area of 500 mm width, the sample body must be assembled from several parts to cover the measuring area. To minimize the number of cut surfaces in the measuring area, the specimens were assembled from 2 boards of 800 mm x 400 mm each. The free-standing part of the heating plate of 50 mm width was covered with a protective ring made of EPS of the same thickness. The influence of the specimen assembled to the measured value was controlled by measuring a smaller specimen of 300 mm x 300 mm in a small GHP apparatus. The real density of the supplied panels ranged from 85 kg/m³ to 115 kg/m³. The influence of density was considered by selecting the specimens so that specimens with possibly similar density were measured. For the measurement according to ISO 10051, a set of specimens was sliced to produce layers of 20 mm thickness. The boards were cut to 25 mm thickness using a band saw and then ground to uniform and even 20 mm thickness using a thickness grinder.

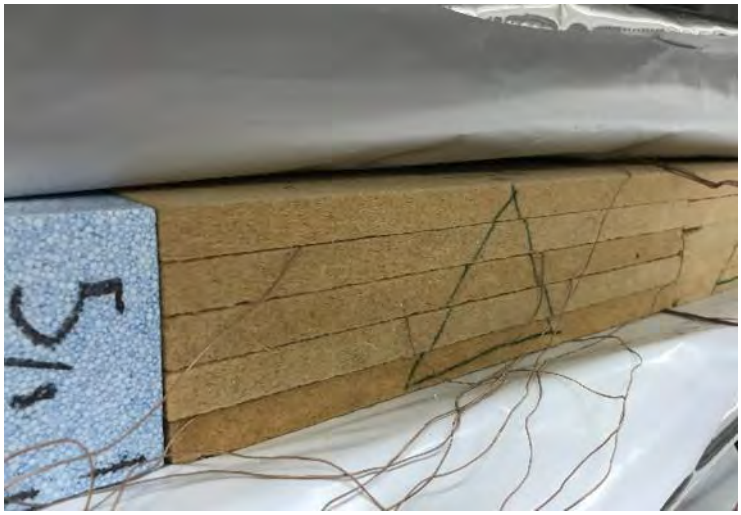

Figure 69 : Separated specimen installed in the GHP apparatus with thermocouples between the layers. The sides are insulated with EPS. The whole specimen is sealed on all sides with a vapor barrier.

For the measurements in the dry state, the specimens were dried at 70 °C. Humidification of the specimens was carried out in a climatic chamber at 23 °C and 70% or 80% relative RH. To prevent drying of the specimens during measurement in the GHP apparatus, the specimens were wrapped in an aluminium-coated vapor barrier and sealed.

4.3.3.2 Overview of the measurements performed

The following measurements were performed. The temperature difference between the cooling and heating plates was always 20 K for dry measurements and 10 K for wet measurements:

Dry measurement:

- Whole boards, thickness 100 mm, L 400 mm x W 800 mm, mean temperature 0 °C to 20 °C
- Halved panels, thickness 50 mm, L 300 mm x W 300 mm, mean temperature 10 °C
- Sliced into individual layers of 20 mm each, total thickness 100 mm, L 400 mm x W 800 mm, mean temperature 0 °C to 20 °C

Moist measurements:

- Whole boards, thickness 100 mm, L 400 mm x W 800 mm, mean temperature 10 °C, moisture content 9.1 % by mass. Measurement duration 120 h
- Whole boards, thickness 100 mm, L 400 mm x W 800 mm, mean temperature 10 °C, moisture content 11.6 % by mass. Measurement duration 250 h
- Sliced into individual layers of 20 mm each, total thickness 100 mm, L 400 mm x W 800 mm, mean temperature 10 °C, moisture content 8.7% by mass. Measurement duration 120 h
- Sliced into individual layers of 20 mm each, L 400 mm x W 800 mm, mean temperature 10 °C, moisture content 11.8 % by mass. Measurement duration 250 h

The results of the measurements are described in the following chapters.

4.3.3.3 Measurements on dry samples

The thermal conductivity after drying at 70 °C was determined for various mean temperatures between 0 °C and 20 °C. For all porous materials, the thermal conductivity increases with a rising sample mean temperature. The increase is mainly due to the higher mobility of the gas or air molecules in the pore space. Figure 70 shows the results for the specimen consisting of five layers of 20 mm each and the whole board with the thickness of 100 mm. The measured values for both specimens are close to each other. Thus, splitting the specimens has no significant effect on the measured thermal conductivity. By averaging all measured data, the thermal conductivity at 10 °C is λ_{10} = 0.0380 W/(m·K) and the temperature coefficient (increase with sample mean temperature) for the thermal conductivity is 0.089 mW/(m·K)/K. The density of the measured samples is on average 111 kg/m³ for the whole boards and 104 kg/m³ for the boards that consist of five layers.

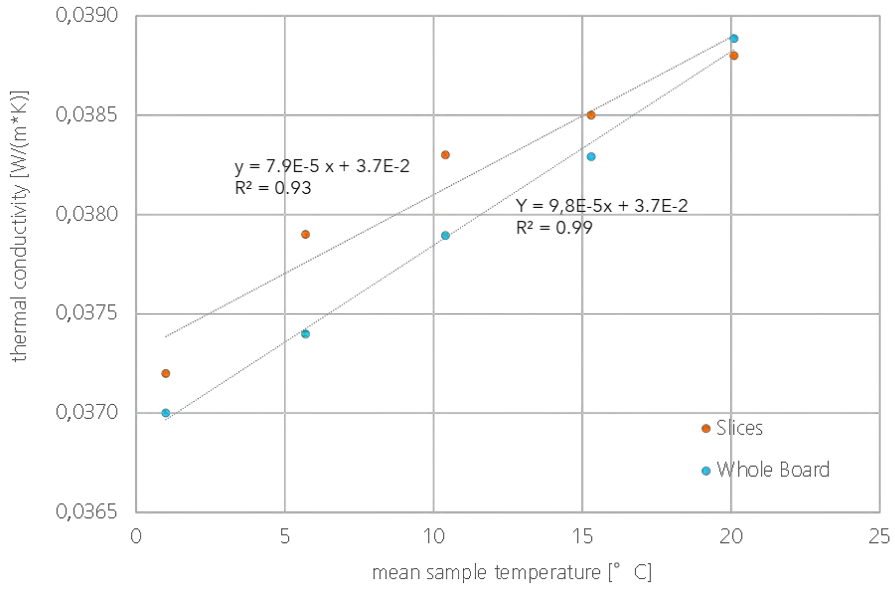

Figure 70 : Measured temperature dependence of the thermal conductivity of the dry samples as individual measuring points and linear regression degrees for the whole and the layered board, each with indication of the mathematical equation.

To make sure that the measurement of the boards composed of two parts of 400 mm each does not lead to a large influence on the thermal conductivity, another measurement was carried out on samples in a small GHP apparatus. Here a sample with 300 mm x 300 mm base area and up to 70 mm thickness can be measured. Samples with the largest and smallest densities were selected from each of the boards. The specimens were cut to 300 mm x 300 mm and halved in the middle. This resulted in two specimens, each 50 mm high. The thermal conductivity (in each case at 10 °C specimen mean temperature) was 0.0359 W/(m·K) at a bulk density of 88.8 kg/m³ and 0.0378 W/(m·K) at a bulk density of 112.4 kg/m³.

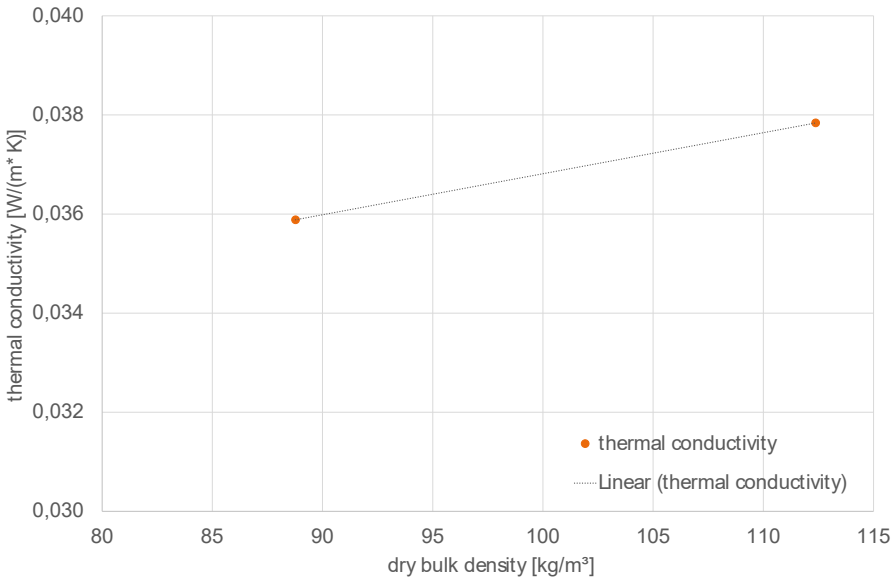

Figure 71: Thermal conductivity at 10 °C as a function of bulk density (small specimens with 50 mm thickness)

For the further evaluation, therefore, the mean value of all measured data of 0.0380 W/(m·K) is used as a reference value for the dry thermal conductivity. In Table 6 the details of the measurement of the specimen in individual layers are listed.

Table 6 : Bulk density, mean temperature and measured value of dry thermal conductivity on two specimens divided into 20 mm thick layers with the heating plate in the middle. Averaged thermal conductivity for both boards is 0.0383 W/(m·K) at 10.4 °C mean temperature.

Layer	Bulk density, dry	Mean temperature	Thermal conductivity
	kg/m³	°C	W/(m·K)
Cooling plate			
1	117	6,3	0,0374
2	100	8,4	0,0372
3	93	10,5	0,0374
4	108	12,5	0,0381
5	112	14,5	0,0386
Hot plate			
1	105	14,5	0,0400
2	102	12,6	0,0379
3	92	10,5	0,0382
4	100	8,5	0,0370
5	113	6,4	0,0376
Cooling plate			

4.3.3.4 Moist measurements

As described above, the samples were conditioned prior to measurement in a climatic chamber at 23 °C and 70% or, for the second measurement, at 80% RH. The samples were stored in the climatic chamber until constant weight. Immediately after removal from the climatic chamber, the mass was determined, the samples were wrapped in foil to be water vapor tight and then installed in the GHP apparatus. The temperature control of the GHP apparatus was started before installation so that the target temperature at the specimen surface was reached as quickly as possible.

Figure 72 shows the measured course of the surface temperature and the thermal conductivity in minute steps for the first 24 hours. The temperatures at the surfaces were stable within 5 hours. The thermal conductivity still fluctuates strongly during the heating phase. After the temperature difference is constant, the heat flow reaches a plateau and then gradually decreases.

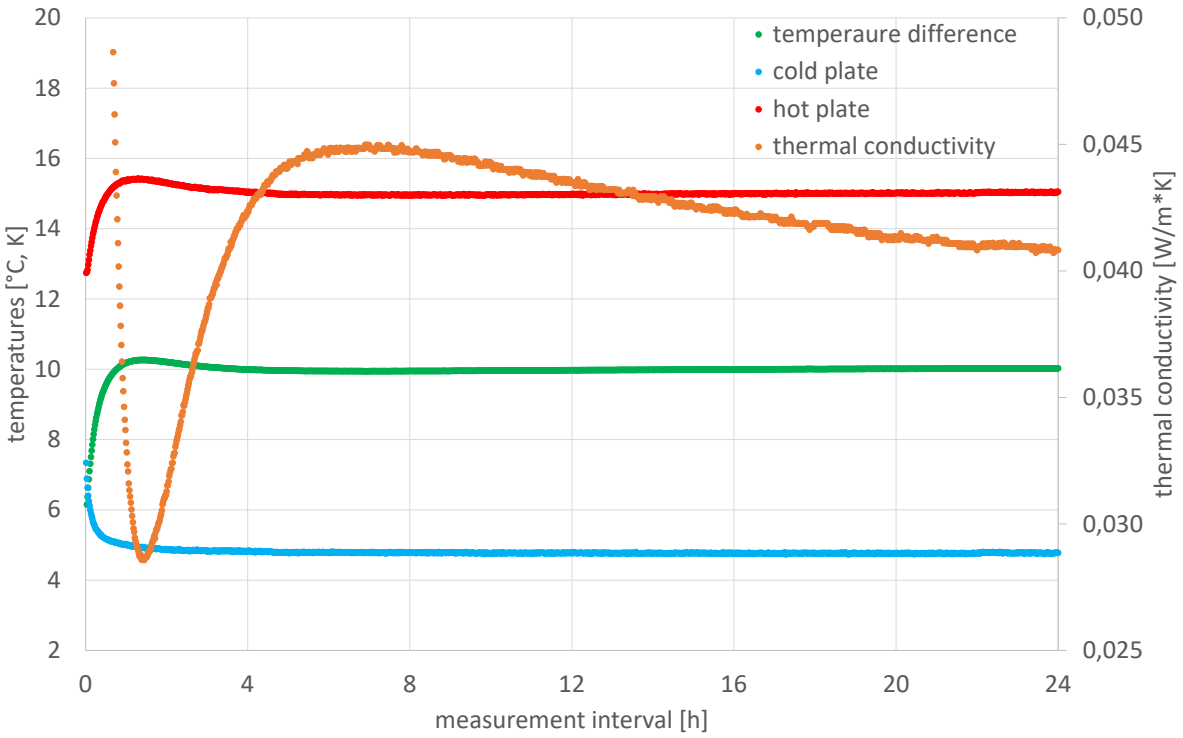

Figure 72 : Measured course of the temperatures at the specimen surface and the average thermal conductivity in the first 24 h at an average moisture content of 8.7 % by mass on the specimen divided into five layers.

Figur 73 shows the same measured values as Figure 72 but now over the whole test period of 120 hours. The temperatures remain constant from about 5 to 120 h, while the thermal

conductivity decreases from 0.045 W/(m·K) to 0.0382 W/(m·K) at the end. This is close to the dry value of 0.0380 W/(m·K).

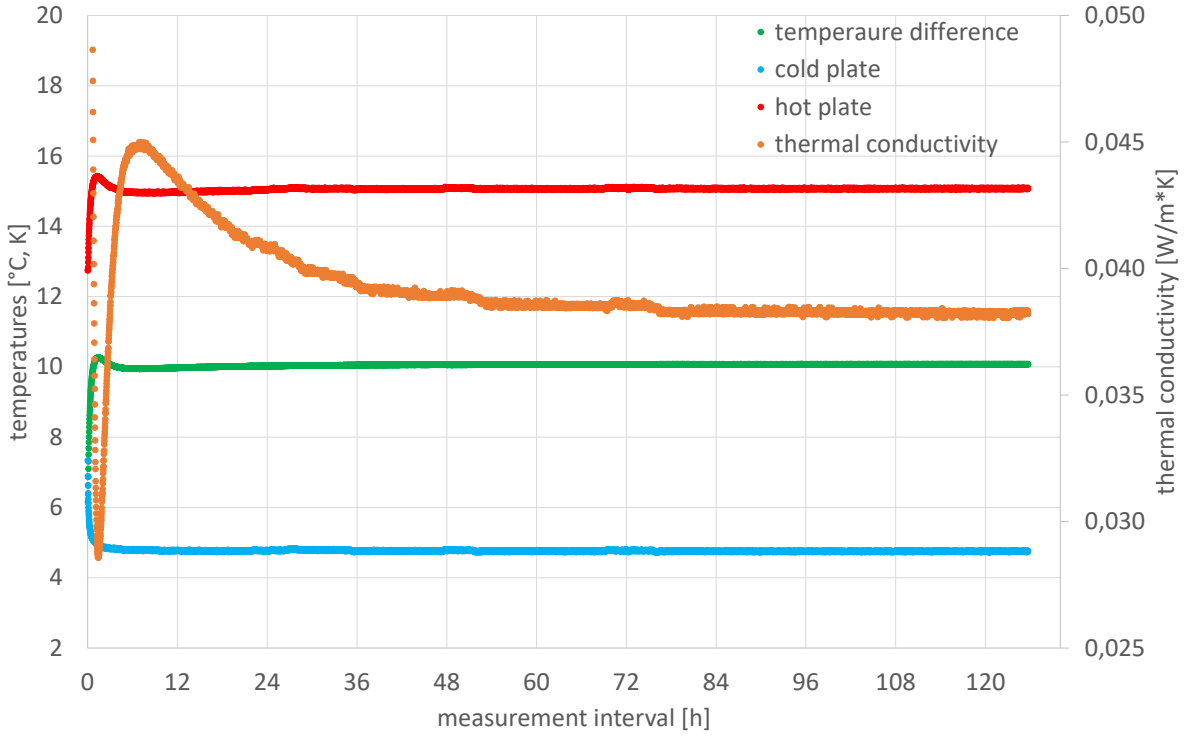

Figure 73 : Measured course of the temperatures at the specimen surface and the average thermal conductivity over the whole test period of 120 h at an average moisture content of 8.7 % by mass on the specimen divided into five layers.

According to EN 12664 (see above), the measured value must not change by more than 1% within one test period and the curve must not be monotonously decreasing. Figure 74 shows the measured thermal conductivity and the rate of change of the thermal conductivity as well as the respective 1% limit value for two different moisture contents.

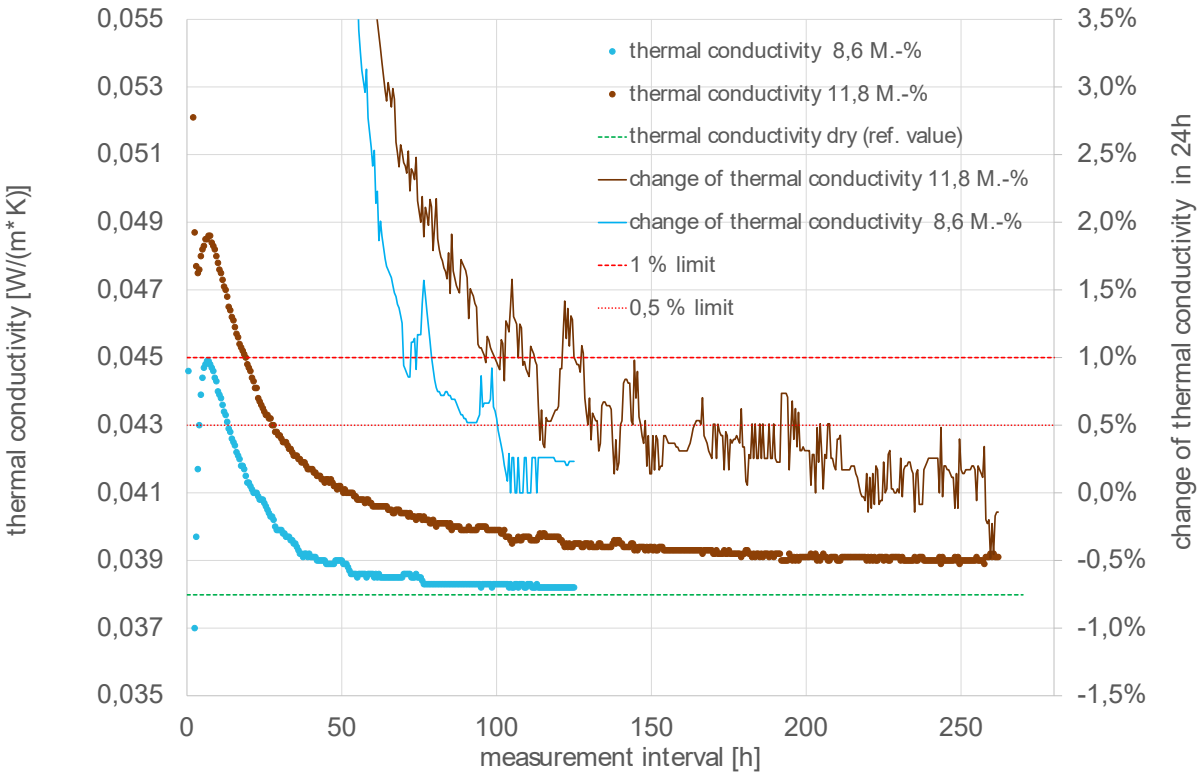

Figure 74 : Course (thick line) and rate of change (thin line) of thermal conductivity over 250 h. Measurement of thermal conductivity at 8.6 and 11.8 % by mass moisture in the specimens divided into layers.

The termination criterion of 1% change is already reached after 3 or 4 days. However, since the curve is still monotonically decreasing, the measurement must be continued for about 5 or 12 days. Stopping and evaluating the measurement earlier would give a too high value for the thermal conductivity. The final results of the four measurements carried out on moist samples are summarized in the following table:

Table 7: Results thermal conductivity moist

Sample	Arrangement	Pre-Condi-tioning	Measurement duration	Moisture content [% by mass]	Thermal conductivity in steady state [W/mK]
Whole board 100 mm	Two-plate measurement	23°C-70%rH	120 h	8,8	0,0386
	Two-plate measurement	23°C-80%rH	250 h	11,6	0,0385
Composed of 5 slices of 20 mm	Two-plate measurement	23°C-70%rH	120 h	8,6	0,0382
	Single-plate measurement	23°C-80%rH	250 h	11,8	0,0390
Reference value of dry sample λ_{10}					0,0380

The thermal conductivity increased in all cases by a maximum of 1 mW/(m·K) or 2.6% based on the dry value at low moisture contents. Contrary to expectation, the measured thermal conductivity of the whole board conditioned at 80% RH is slightly lower than the value conditioned at 70% RH. Thus, the results show that the moisture-related increase is small for moisture contents up to 80% RH. When evaluating the results, the measurement uncertainty of 2% for measurements in the GHP apparatus should be considered in accordance with EN 12664. The increase in thermal conductivity due to humidity in the specimen is so small in the material tested here that the effect between 70% and 80% RH is largely overshadowed by the general discrepancy in the measurement. The measurement in individual layers results in similar measured values as the measurement on the unseparated board.

4.3.3.5 Evaluation method according to ISO 10051 with single layers

In the previous chapter, the evaluation of the measurement was made for the whole specimen, i.e. from the heat flux and the temperature difference from cold side to hot side over the whole specimen with 100 mm thickness. According to ISO 10051, the thermal conductivity for each individual layer (see

Table 6) should be determined in relation to the respective moisture content at the end of the measurement.

According to ISO 10051, the specimens were removed directly after measuring the thermal conductivity and the moisture content of each layer was determined immediately. The thermal conductivity in each layer can be determined with known heat flow via the temperature sensors between the layers and the resulting temperature gradient. Table 8 and Table 9 summarize the results for the two measurements. As explained above, the thermal conductivity increases with the sample mean temperature. Thus, a different sample mean temperature is present in each layer. Therefore, to make the results comparable, the measured thermal conductivity must be converted to 10 °C. For the conversion, the factor 0.089 mW/(m·K) /K previously determined in the dry measurement (see chapter 4.3.3.3) was used.

Table 8: Evaluation of individual layers according to ISO 10051 - Thermal conductivity after 120 h, moisture content 8.6 % by mass.

Layer	Dry bulk density	Mean temp.	Thermal conductivity converted to 10 °C	Moisture content before measurement	Moisture content after measurement sung	Mass Modification
	kg/m³	°C	W/(m· K)	M.-%	M.-%	g
Cooling plate						
1	117	5,8	0,0376	8,6%	9,5%	7.5
2	100	7,9	0,0376	8,6%	8,9%	2.3
3	93	10,0	0,0367	8,1%	8,0%	-0.5
4	108	12,1	0,0377	8,5%	7,8%	-5.6
5	112	14,1	0,0389	8,7%	7,2%	-10.8
Hot plate						
1	105	14,1	0,0391	8,9%	7,5%	-10.0
2	102	12,1	0,0384	8,7%	8,0%	-5.2
3	92	10,0	0,0379	8,7%	8,6%	-1.0
4	100	8,0	0,0373	8,8%	9,1%	2.0
5	113	5,9	0,0378	8,5%	9,6%	8.2
Cooling plate						

Table 8 shows the results for each layer. As expected, the moisture content increases on the cold sides and decreases on the warm sides. The relative humidity in the individual layers is roughly calculated via the sorption isotherm of the investigated material to be between about 60% RH on the warm side and 80% RH on the cold side. The effective redistribution takes place mainly from the warmest to the coldest layer. However, the thermal conductivity does not show the expected result that the most humid layer (on the cold side) should have the highest thermal conductivity, while the driest layer on the warm side should have the lowest thermal conductivity. Instead, the thermal conductivity is highest on the warm side, then decreases toward the middle and increases again toward the cold side. Even the outermost and thus moistest layer does not have the highest thermal conductivity.

Table 9 : Evaluation of the individual layers according to ISO 10051 - Thermal conductivity after 250 h, moisture content 11.8 % by mass

Layer	Medium temp.	Dry bulk density		Thermal conductivity by calculates to 10 °C		Moisture content after measurement sung	
	°C	kg/m³		W/(m· K)		M.-%	
		left side	right side	left side	right side	left side	right side
Cooling plate							
1	5,9	118	117	0,0390	0,0397	13,8%	13,9%
2	7,9	103	100	0,0383	0,0371	11,7%	12,1%
3	9,9	92	93	0,0376	0,0379	11,2%	11,3%
4	11,9	110	108	0,0389	0,0390	10,2%	10,3%
5	13,9	118	112	0,0393	0,0398	9,2%	9,3%
Hot plate							

In the second measurement with increased humidity (on average 80% RH with about 67% on the hot side and 92% on the cold side), a single-plate measurement was performed on only one specimen, so that the heat flow runs only from bottom to top. The same result is obtained with this variant: the thermal conductivity does not seem to increase but to decrease with increasing humidity, is highest on the warm side, decreases towards the center and then increases again towards the cold side.

The evaluation of the individual layers to determine the influence of moisture on the thermal conductivity according to the standard, thus proves to be impossible, since a physical implausible correlation would result: the measured thermal conductivity decreases with increasing moisture content. The cause is presumably to be found in the Figure 66 described “heat-pipe-effect”. Moisture evaporates in the warm areas and extracts heat there and then condenses on the cold side and adds heat. In the coldest layer, the moisture content increases, which initially leads to higher thermal conductivity and losses. However, the effect is overcompensated by the heat gains from condensation. The two processes, heat conduction and moisture transport, cannot be recorded separately and meaningfully determined by this measurement method. Figure 75 shows the relationship between thermal conductivity and moisture content in the individual layers. The values are already converted to 10 °C to eliminate the temperature dependence of the thermal conductivity. In addition, the increase in thermal conductivity is determined for each individual layer in relation to the previously determined dry value. In relation to the dry value of the thermal conductivity of the individual layers, no proportional relationship between moisture content and thermal conductivity can be identified.

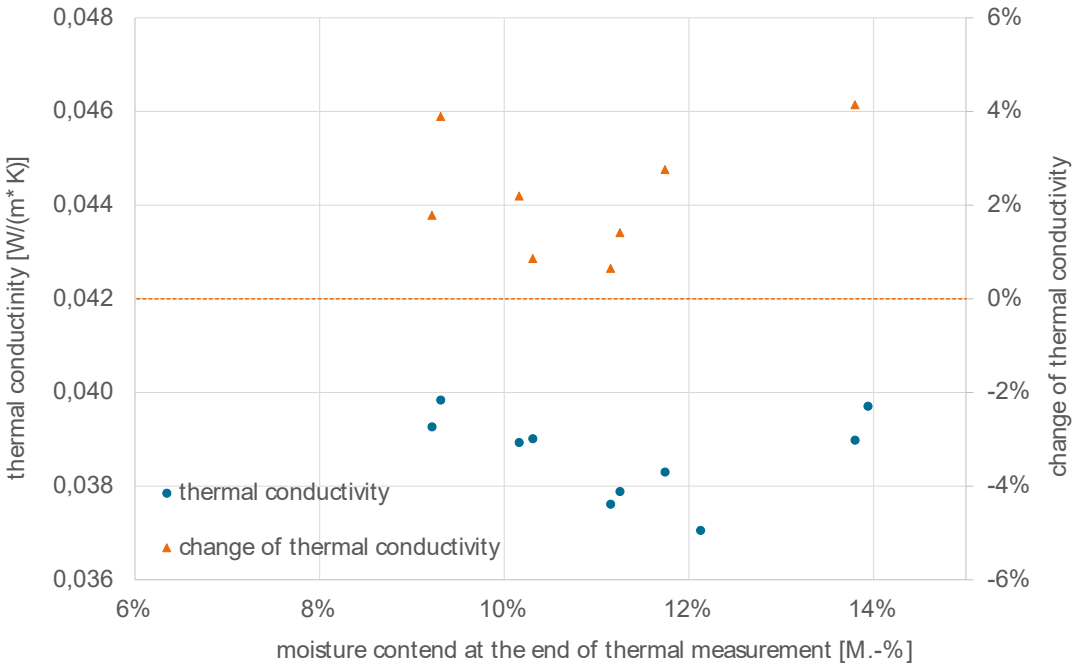

Figure 75 : Measured humid thermal conductivity (blue dots) converted to 10 °C for the individual layers in relation to the moisture content. Change in thermal conductivity (orange triangles) in relation to the previously determined dry thermal conductivity.

4.3.4 Summary Laboratory tests

The measurement of the humid thermal conductivity must be carried out over a rather long period to reach equilibrium conditions in the specimens. The test duration increases from the usual maximum of 24 h to several days or even weeks. At the beginning, the measured thermal conductivity increases significantly. At the end, however, with the material tested here and the initial average humidity corresponding to preconditioning at 70% or 80% RH, the value drops so far that it is less than 3% or 1 mW/(m·K) above the dry value. Thus, the surcharge according to DIN 4108-4 of 5%, but at least 2 mW/(m·K) added to the nominal value (see Sect. 4.1) would be appropriate for thermal calculations without condensation processes – even including some safety buffer.

If the measurement is stopped too early, this will result in an excessively high value for the thermal conductivity capability, since the still ongoing redistribution of moisture will increase the heat transfer by the latent heat. A separation in several individual layers according to ISO 10051 does not provide any additional meaningful findings for the insulation materials tested within this project. Even after 12 days, there is obviously still some moisture redistribution in the sample despite no changings in the moisture profiles. This "heat pipe effect" significantly complicates the evaluation.

Both the results for the average thermal conductivity over all individual layers and the measurement on a specimen in nominal thickness (without slicing) give almost the same

values. Due to the added value aimed for but not actually achieved, the effort of slicing the samples can be avoided and measurements can be made directly on the unseparated boards. Since the measurements rather long time which increases costs and effort for the laboratories or manufacturers, it seems worthwhile to continue research into an accelerated method. Various approaches could be used for this purpose. On the one hand, the sample thickness could be reduced - according to [46] a promising approach. The samples would then no longer be measured in nominal thickness, but only as a thin layer of 2 cm to 3 cm. In addition, with an optimized temperature difference, the measurement could come into equilibrium statemore quickly. However, it should be considered that no condensation water must occur in the samples. It is not clear from the publication whether an occurrence of condensation water was checked. In addition, it should be noted that a thinner specimen and a lower temperature difference have a negative effect on the measurement accuracy. Another possible approach would be to develop a descending function for thermal conductivity of different materials. Thus, one could predict the final value after several days from the measurement data of 1 - 2 days. The approaches would require extensive laboratory testing with different material types.

4.4 Recalculation of laboratory tests with hygrothermal simulation and evaluation

The Lab tests described in chapter 4.3.3 will be re-simulated using the well validated hygrothermal simulation model WUFI® developed at Fraunhofer-IBP [43]. The aim of these simulations is a more precise differentiation between the increase in heat transport due to the moisture-induced increase in thermal conductivity and the remaining latent heat effects. For this purpose, the test with the insulation board sliced into five layers is used, since here the temperature difference at the interfaces and the respective water content of the layer appear to be the most appropriate. This could enable a calculation-based differentiation between the various effects, which is not possible solely with measurements. Reason is, among other things, the limited measurability of the parameters required. The temperature at various positions can be measured with comparatively high accuracy - but even here the limits are reached, since the sensors and cables are thermally inert, show thermal bridge effects and can be positioned with an accuracy of only ± 1 mm in the best case. Even these small deviations can change the temperature values by several percentage points in relation to the 2 cm thick sub-layers during measurement. Concerning the measurement of RH, even with high-quality sensors and perfect positioning, the measurement accuracy itself is around ± 1%. In the high humidity range above 95% RH, the accuracy decreases further. The heat flows at the individual layer boundaries of the subdivided samples can no longer be sensibly recorded due to the size of the sensor system, and the water contents can also only be determined by weighing the individual layers following the measurement and with the rather coarse resolution of 2 cm. The effects of these inaccuracies in the measurement could be analysed, quantified and evaluated using simulations.

4.4.1 Performed simulations

The boundary conditions for the simulation are used analogously to the conditions during the measurement: The material samples are divided into five layers, each 20 mm thick. Surface conditions and preconditioning correspond to those described in chapter 4.3.2.

The hygrothermal parameters for the wood fibre material under consideration were measured in detail in the IBP hygrothermal laboratory. In addition to the sorption and liquid transport properties for normal hygroscopic building materials, also the strength of the incipient liquid transport was measured by the so-called "Kapi-Test" [47, 48]. In this test, a specimen is exposed to a temperature gradient so that the moisture content accumulates on the cold side of the specimen via vapor diffusion until liquid transport slowly begins to return to the warm side from about 75% to 80% RH and thus slows down the further moisture increase. In this test procedure, preconditioned specimens are exposed to a temperature difference of 11 K in the climatic chamber at 23 °C and 65% RH for up to two additional months and the moisture distribution within the specimens is regularly recorded by NMR measurement (with a resolution of 0.8 mm). The liquid transport coefficients already determined by suction and drying tests are then refined for the low capillary water range in such a way that the measured moisture profiles as well as their time course can be well represented in the simulation. This measurement scenario represents the most current state of the science.

First, the thermal conductivities of the individual layers are determined from thickness, heat flux density and temperature difference. Figure 76 shows the thermal conductivity and water content of the individual layers as a comparison between simulation and measurement. The thermal conductivities calculated from the simulation are shown as green dots, those from the measurement as orange dots with error bars of ±3%. For the calculation of the thermal conductivity, it is assumed that the measured heat flow is constant over the whole specimen thickness and all layers – however, just one single measured value on the cold side is available, since there is no space for additional heat flow meters between the layers. The temperature differences are based on the measured values at the layer boundaries. All layers are assumed to have the same thickness of 20 mm. Resulting differences in thermal conductivities are accordingly due to the different temperatures and moisture contents in the individual layers. The linear temperature dependence of the thermal conductivity is calculated with the coefficient of 0.0001 W/mK per 1 K determined in the laboratory test (chapter 4.3.3.3) and its moisture dependence is derived from the measured values on the dry material specimen and the material specimen moistened at 80% RH (Section 4.3.3.4). A distinction between the pure moisture-dependent heat conduction (sensitive heat flux) and the latent heat flux (caused by heat pipe effect, which still occurs even in equilibrium state) is not possible during the measurement because only the total heat flux can be measured.

4.4.2 Comparison of simulation and measurement

Three variants with slightly different initial assumptions are analysed. For variant #1 (Figure 76, left), both the local temperature difference and the local heat flow in each slice are explicitly considered to calculate the thermal conductivity of the resp. slice. As expected, the resulting thermal conductivity values show a slightly increasing tendency with increasing water content. However, the agreement with the measurement results is not particularly satisfying, both with respect to the level and the trend over the sample thickness. It should also be noted that the latent heat flux at the layer boundaries cannot be easily evaluated in the simulation either, since the vapor can simply move on to the next layer without a phase change.

In variant #2, the heat flow is assumed to be the same for all slices, as in the measurement. This variant corresponds most closely to the determination from the measurement, since the heat flow arriving at the cold side is also used with the same value for all layers, as well as the temperatures simulated at each layer`s boundaries are used for the determination of thermal conductivity for the respective slices. The heat flow arriving at the cold side contains the latent heat part both in the measurement and in the simulation, since moisture cannot escape at the vapour tight boundary. The thermal conductivities from the simulation determined on this basis show even more clearly increasing thermal conductivity values with increasing water content than variant #1 with varying heat flux in the singe slices. Unfortunately, however, the agreement of the thermal conductivity with the measured values is still worse than before - especially in the middle area of the material, where according to the measurement lower values occur, while the simulation results in higher values than on the cold side.

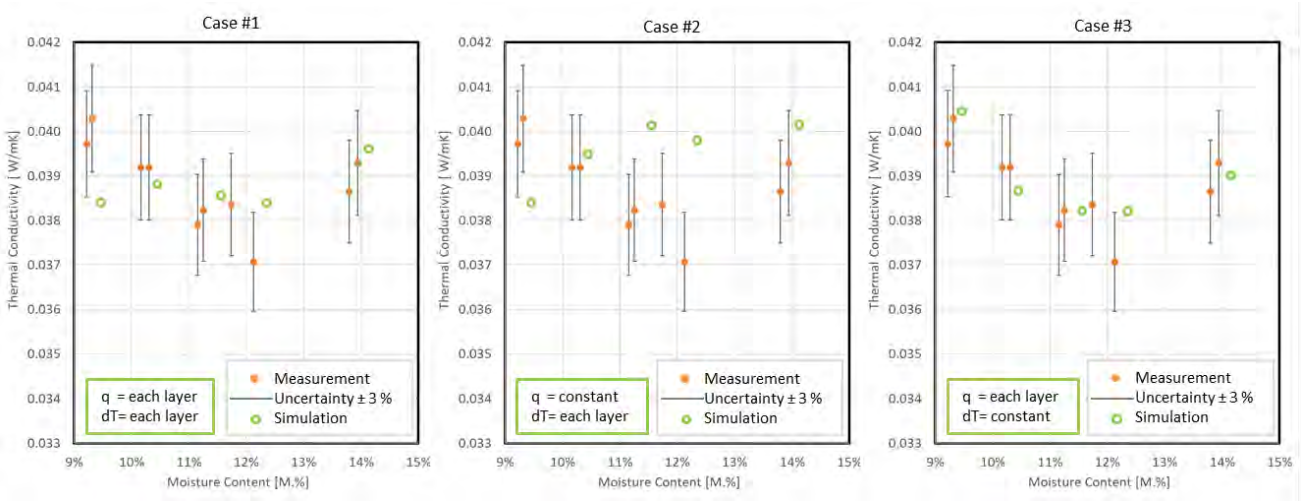

Figure 76 : Thermal conductivity determined from measurement (orange dots with error indicator - same for all three variants) and from simulation (green dots) as follows:

Left: Variant #1 with local heat flux and local temperature difference.
Middle: Variant #2 with constant heat flux and local temperature difference.
Right: Variant #3 with local heat flux and constant temperature difference of 2.0 K.

The temperature and humidity dependence of the thermal conductivity are considered as described in the previous chapter.

In variant #3, the local heat flow from the simulation together with a constant temperature difference of 2.0 K according to the simplified steady-state assumpotion are used for calculation. This variant is not very plausible, however, since the different thermal conductivities of the slices also lead to varying temperature gradients in the different slices. The thermal conductivity values determined in this way show, however, better agreement with the measurement results in terms of levels and distribution than variants #1 and #2.

Despite the already complex procedure, too many uncertainties remain for the desired differentiation. The insulation boards are divided into individual layers of 2 cm thickness. With a careful procedure, an accuracy of about ± 1 mm can be achieved here due to the inhomogeneous and soft material characteristic. The selected preconditioning results in a moisture profile in the equilibrium state at which about 95% - 97% RH is achieved on the cold side and about 60% - 70% on the warm side. Condensation does not occur under these conditions. Towards the end of the test, the effective heat flow in the equilibrium condition is therefore assumed to be the same over the whole sample - which is nevertheless not quite correct, since latent heat flow also occurs in addition to pure heat conduction. Even in the equilibrium state, this continues to transport vapor from the warm to the cold side and, in the other direction, the moisture accumulating on the cold side is transported back in the liquid phase to the warm side. This happens without changing the moisture profile. The water content, which is determined by weighing the individual layers after the measurement, ranges from 9.3% by mass on the warm side to 13.9% by mass on the cold side. The values simulated with WUFI® are usually somewhat higher than the measured values. At the edges of the samples, the difference is about 0.1 to 0.2%, while in the middle area it is up to about 0.4% by mass. These differences may be due to slightly different material properties as well as to the inhomogeneous property range across the thickness (bulk density, diffusion resistance etc.). For the recalculation of the laboratory tests, both are assumed to be homogeneous in a simplified way. The heat flows at the individual slice boundaries cannot be measured with reasonable effort and are therefore missing as a comparison parameter for the simulation. Further differentiation with respect to the moisture content by means of even thinner layers is not feasible any more.

Thus, the re-calculations of the lab tests show that an agreement of detailed and local heat flows between simulation and measurement is only possible with difficulty and would require very precise input parameters. On the measurement side, uncertainties, missing local heat flows, remaining variation in thickness and inhomogeneity of the test specimens are noticeable. On the simulation side probably the homogeneous description of the material properties of a non-homogeneous material (natural fibre with hydrophobic coating, binder and air space) as well as the effect that moisture transport and sorption are not described in an exactness required for the specific problem can cause inaccuracy. Some of the problems described for the measurement cannot be solved at all, others only with great effort. The latter also applies to simulation: although detailed material parameters up to a two-dimensional

analysis would be possible but the additional effort would be rather high and necessary for each individual material to be investigated.

4.4.3 Findings from the recalculations of the laboratory tests

The comparisons between simulation and laboratory tests show that a detailed and local differentiation of the total heat flux into sensible moisture-dependent heat conductivity and latent heat flux requires a very high accuracy of the input parameters and that even small differences lead to significantly different distributions of the heat conductivity over the individual layers.

At the same time, the results show that the process described in chap. 4.3 is well suited for determining the effective thermal conductivity over the whole layer. The reproduction of the measurement by simulation is also possible with this effective value (incl. the remaining latent heat effects) for the whole layer thickness with good accuracy - even if the distribution between sensible and latent heat flux in the individual sub-layers is obviously not reproduced quite correctly.

When simulating the thermal conductivity measurement of a wood fibre insulation material, it should still be noted that these insulation materials are rather inhomogeneous materials. They consist of the wood fibres, the air cavities between them and, occasional, an additional "coating" of the fibres by binder and water-repellent agents. While moisture can be transported through the materials comparatively quickly via diffusion, it may take considerably longer for the water molecules that have already reached the air space next to the fibre to migrate through the hydrophobic coating, for example, and be absorbed by the wood fibre itself. The μ value determined for the material describes the low resistance through the material to the coated fibre surface, but not the greater resistance through the coating into the fibre, so that the duration of humidification (absorption) and dehumidification (desorption) processes caused by vapor diffusion, may not be accurately represented in the simulation in terms of time (only in terms of moisture level). This is usually a negligible problem under normal conditions, because moisture absorption and desorption are permanently alternating. In a laboratory test with constant boundary conditions, however, this difference can be more noticeable. The level and distribution of moisture within the specimens are therefore considered more than the temporal course in the simulation of the laboratory tests.

4.5 Review of the measurement procedure

Already in chapter 4.3.1 it was mentioned that a large part of the latent heat effects can already be excluded by the choice of boundary conditions in the laboratory. The remaining latent heat part due to the "heat pipe effect" is with the ratio of 0.5% even below the measurement accuracy limit (approx. 3% by default). On this basis, it was already decided not to perform the lab test with vapor-tight separation of the sliced and sealed layer considering the low cost-

benefit ratio for the possible reduction to 0.25%. Also by the test with sliced specimen (without foil) carried out iteratively in several and steps with refining of the setup and subsequent reproduction in the simulation (Chapter 4.4) a differentiation between the moisture-induced increase in sensible and latent heat flux is not reliably possible. However, it proved to be not necessary due to the small magnitude. The measurement with the whole insulation board without slicing (chapter 4.3.2) also requires a corresponding long duration until the equilibrium state is reached. However, the effort for preparation and evaluation is significantly lower. The only minor additional findings of the sliced and sealed test setup, on the other hand, do not justify the additional effort.

For these reasons, the single-layer test is considered most appropriate as a basis for determining the moisture dependent thermal conductivity of natural fibre insulation.

4.5.1 Review with different natural fibre insulation materials

To check whether the latent heat content also remains negligibly small in other natural fibre insulation materials, further materials made from renewable raw materials are investigated by simulation. For this in part investigations from an earlier research project [34] are used, where the thermal conductivity was measured both in the dry state and after conditioning at 80% RH. Again, for each material the required hygrothermal material parameters for the simulation are available. The temperature and humidity dependence of the thermal conductivity is generally determined as described in chapter 4.3.3.3 and chapter 0. The simulations are performed by adjusting the boundary conditions of temperature and thickness of the specimens according to the measurements performed, once again with and without consideration of the latent heat effects. The resulting thermal conductivity values are listed in comparison to the measured values in Table 10. Also included are the measured values from the current project.

Table 10 : Thermal conductivity of four different natural fibre insulation materials with different bulk densities determined from measurement and simulation. For the thermal conductivity values from the respective simulation, the difference to the value from the measurement is given in brackets.

condition		thermal conductivity [W/m·K]			
		material			
		wood fibre board 96 [kg/m³]	wood fibre board 115 [kg/m³]	wood fibre board 172 [kg/m³]	hemp fibre board 148 [kg/m³]
measurement		0,0387	0,0392	0,0444	0,0429
simulation	with latent heat	0,0389 (+ 0,0002)	0,0394 (+ 0,0002)	0,0449 (+ 0,0005)	0,0431 (+ 0,0002)
	without latent heat	0,0387 (+ 0)	0,0394 (+ 0,0002)	0,0445 (+ 0,0001)	0,0430 (+ 0,0001)

	increasing by latent heat	0,0002	0	0,0004	0,0001

In these simulations also the final description of the moisture-dependent thermal conductivity is used, resulting in slightly higher values in the simulation than in the measurement for safety reasons. The evaluation shows that simulation with and without latent heat results in an average difference of only 0.000175 W/mK for all four materials. The maximum value of 0.0004 W/mK is reached for the board with a bulk density of 172 kg/m³, and no difference at all can be determined for the board with a bulk density of 115 kg/m³.

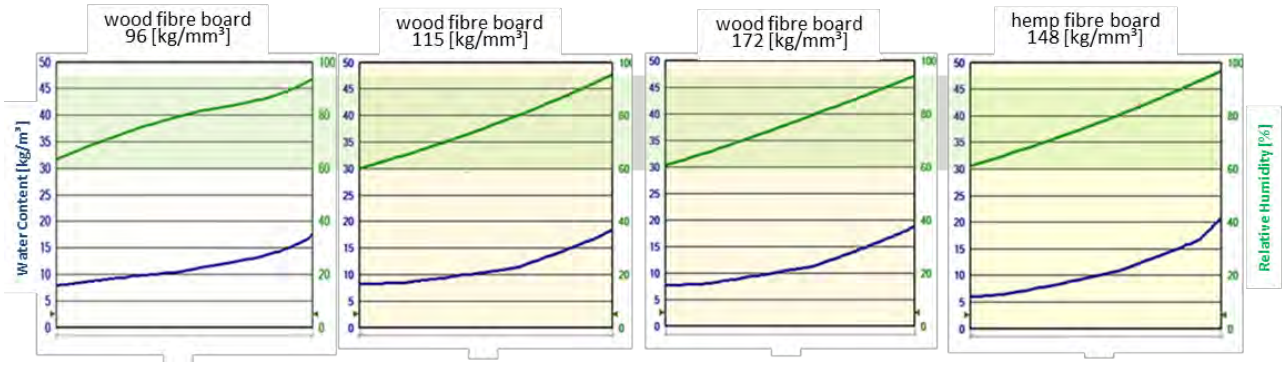

Figure 77 : Simulated moisture distribution in the four different natural fibre materials after reaching the equilibrium state at the lab test conditions (warm side left). The green curve represents the relative humidity profile and blue the water content. The green area represents the relative humidity range from 60 to 95%.

The moisture distribution in the materials after reaching equilibrium state is shown in Figure 77. The relative humidity over the sample cross-section ranges for all four natural fibre materials between about 60% RH on the warm side and approx. 95% RH on the cold side (on the right side of each figure). The selected test conditions thus do not lead to condensation on the cold side in any case, which eliminates most of the latent heat effects.

For the four materials investigated, the increase in thermal conductivity due to remaining latent heat influences ranges from 0% for the wood fibre insulation board with a bulk density of 115 kg/m³ to just below 1% for the wood fibre insulation board with 172 kg/m³. Here, a correlation with the bulk density of the materials is obvious: the more wood fibre mass is present, the more moisture can be stored, and the more liquid transport can take place in these materials - accordingly, the latent heat fraction caused by the "heat pipe effect" increases, but also remains here with an increase of just below 1% clearly lower than the measurement accuracy of 3% specified in the standard.

In summary, it can be stated that the selected test scenario with preconditioning at 80% RH and a low temperature gradient of about 1 K per 1 cm material thickness ensures that even on

the cold side the humidity remains clearly below 100% RH and thus no condensation conditions will be achieved. The latent heat component, which cannot be eliminated by moisture redistribution with a stable moisture profile due to the "heat pipe effect," remains negligibly small. The investigations in chap. 4.3.3.5 have also shown that the evaluation of the individual layers, despite considerable more effort, does not provide a clear result with regard to the differentiation between moisture-related increase in thermal conductivity and latent heat effect in the single slices. However, this and the direct measurement results also prove that in the range up to 95% RH, which is implicitly considered by the proposed measurement procedure, there is only a slight increase of the thermal conductivity. Therefore, the moisture dependent thermal conductivity can be described in a simplified linear way which well represents the predominant moisture conditions in the materials that occur in practice.

As already explained, the moisture ranges from about 60% RH on the warm side up to 95% RH on the cold side in the unsliced specimen. The mean value corresponds to the water content at 80% RH for which the test specimen was preconditioned, and which does not change during the test due to the vapor-tight sealing. Implicitly, the measurement of the humid thermal conductivity of the material contains the moisture contents from 60% up to 95% RH. Therefore, a possible over proportional increase in thermal conductivity in the moisture range up to maximum 95% is already included in the average value. In the test with the sliced specimen without foil, no reliable difference could be derived from the measurements - neither directly nor indirectly via additional hygrothermal simulations. Therefore, it can be assumed that the differences in thermal conductivity between 60 and 95% are not significant. A linear extrapolation of the thermal conductivity from the dry value via the value determined at 80% RH to the value at 95% RH therefore appears well acceptable.

From previous studies [49, 50] it is known that the thermal conductivity of insulating materials with high porosity in the high moisture range (up to the free saturation of the material at usually over 900 kg/m³), does not continue to increase linearly but rather exponentially and approaches a final value of about 0.6 W/mK. This value corresponds to the thermal conductivity of liquid water, which is plausible since the insulating material in this state consists almost only of water. Therefore, the description of the moisture-dependent thermal conductivity of natural fibre insulation materials for hygrothermal calculations is proposed as follows: until 95% RH, the thermal conductivity is assumed to increase linearly, with the slope being determined from the dry value and the measured value of the sample preconditioned at 80% RH. Above 95%, the thermal conductivity increases exponentially to 0.6 W/mK at maximum saturation. Since insulation materials have a very high porosity of about 90 to 95%, a maximum saturation of about 900 to 950 kg/m³ results when the available pore space is completely filled with water.

This approach is verified by reproducing the thermal conductivity measurements with four natural fibre insulation materials by simulation. The proposed approach of a combination of linear and exponential increase is compared with two other possible approaches in which only

the linear progression (common, but incorrect in the high moisture range) or only an exponential progression (difficult to determine in the low moisture range, therefore mostly used as a standard function based on the dry value) is used. Table 11 shows the thermal conductivity determined from measurement and simulation for the three variants. The results show that for simulation with a continuous exponential slope (according to the dry value and standard curve), the calculated thermal conductivities are up to 0.014 W/mK (3.1%) lower than the measured values. When simulating with linear slope of thermal conductivity according to the actual measurement, the deviation remains significantly lower. Here, the simulated values are at most 0.0004 W/mK (0.8%) lower than the measurement. This results from the too low thermal conductivity at higher moisture contents. With the proposed combined description of the moisture dependence of the thermal conductivity, the deviation is only minimally larger than with the linear approach and now with 0.0005 W/mK (1.1%) slightly above the measured value and thus on the safe side. Since the effort for a further and better differentiation of the increase with the water content would be quite high, as already mentioned several times, the approach which is with 1.1 % only slightly on the safe seems to be pretty reasonable.

Table 11 : Thermal conductivity from measurement and simulation of the lab test (with three variants to describe the moisture dependent thermal conductivity - linear, exponential, combined). The values in brackets are the absolute deviations from the respective measurement result.

condition		thermal conductivity [W/m·K]			
		material			
		wood fibre board 96 [kg/m³]	wood fibre board 115 [kg/m³]	wood fibre board 172 [kg/m³]	hemp fibre board 148 [kg/m³]
measurement		0,0387	0,0392	0,0444	0,0429
simulation with different approaches for the moisture-dependent thermal conductivity	linear increase	0,0388 (+0,0001)	0,0392 (± 0,000)	0,0440 (- 0,0004)	0,0427 (- 0,0002)
	exponential increase	0,0383 (- 0,0004)	0,0380 (- 0,0012)	0,0430 (- 0,0014)	0,0417 (- 0,0012)
	up to 95% RH linear then exp.	0,0388 (+ 0,0001)	0,0394 (+ 0,0002)	0,0449 (+ 0,0005)	0,0431 (+ 0,0002)

4.5.2 Characterization of moisture-dependent thermal conductivity in hygrothermal material data sets

Figure 78 shows an example of the description of the moisture-dependent thermal conductivity of a wood fibre insulation board according to the proposed approach in the WUFI® database. The table on the left lists the water contents in the first column and the corresponding thermal conductivity at the respective water content in the second column. Start value at the top is the dry value, then follows the value determined on basis of the measurement at 80% RH. The gradient coefficient of the thermal conductivity per 1 kg/m³ increase in water content can be determined in [(W/mK)/(kg/m³)] and thus the value at 95% RH can be determined. The thermal conductivity values above 95% RH up to the maximum water content (1000 kg/m³ x porosity [-]) are added with the standard exponential curve which ends at the value of water at 0.6 W/mK. Generally, an adjustment is still required for the transition of the two curve ranges. For this purpose, the value at 50 kg/m³ can be linearly interpolated as the starting point of the exponential curve between the value at 95% RH (19.55 kg/m³ in this example) and the value at 100 kg/m³.

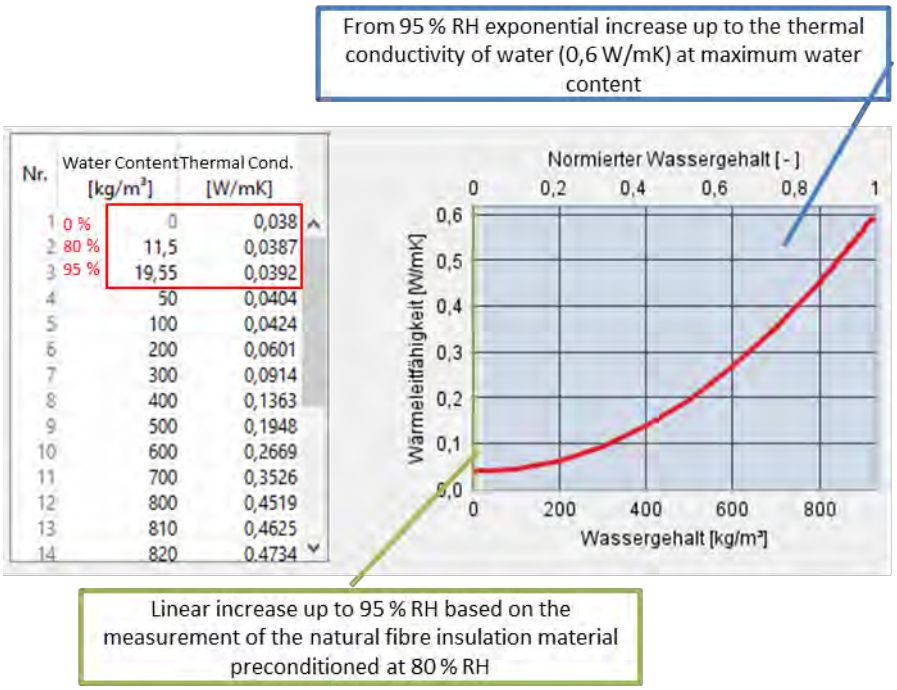

Figure 78 : Description of the moisture dependent thermal conductivity in WUFI®. On the left is the tabular input and on the right is its graphical plot

4.5.3 Summary of moisture dependency of thermal conductivity

In this chapter, the moisture-related increase in thermal conductivity of natural fibre insulation materials was investigated using simulations.

The first step was to simulate the laboratory measurement of a wood fibre insulation board composed of five thin boards, which was carried out as part of this project. The original idea, which was to determine the increase in thermal conductivity and its local distribution due to the water content by recalculating the measurements, was not feasible with the desired accuracy. This is due the measurement uncertainties, which are too large for this aim, the inhomogeneity of the material and the fact that the moisture distribution in the simulation cannot be represented accurately enough, especially in case of "heat pipe effects", which would require a much more complex determination of the moisture-related material parameters.

By reproducing the thermal conductivity measurement of the whole board by simulation, the following findings were obtained in comparison with the sliced and sealed samples: The simulation with and without latent heat showed that its influence on the thermal conductivity measurement remains negligible if the measurement is carried out according to EN 12677 without condensation on the cold side. The provided termination criterion needs to be considered accurately. The description of the moisture-dependent thermal conductivity can be derived until 95% RH directly from the proposed laboratory test. The remaining increase until maximum saturation is then considered in a simplified way via an exponential curve ending at the thermal conductivity of water (0.6 W/mK). The validation of this approach based on the analysis of four different natural fibre insulation materials shows that the results obtained by a reproduction of the measurements by hygrothermal simulation remain only slightly on the safe side in all four cases and are thus appropriate.

4.6 Validation of the laboratory data with field tests

The results from chap. 4.2 have shown that the increase in thermal conductivity at higher humidity levels of sorptive insulation materials in practical application is caused less by the moisture content of the material itself, but mainly by latent heat effects. In the laboratory method, the moisture-dependent thermal conductivity of a soft wood fibre insulation material (nominal density: 110 kg/m³) could be determined with negligible influence of latent heat effects (0.0002 W/mK). For the variants W 1.1 and W 1.2, exactly this soft wood fibre product was used in the ETICS.
In Figure 79 and Figure 80 the simulation-based reproduction of these variants using the material data set determined in the laboratory, including the moisture-dependent thermal conductivity is shown. In both cases, the moisture level in the ETICS was between 60% and 100% RH during the considered period, so that a quite large moisture range including values above 95 % RH were reached.

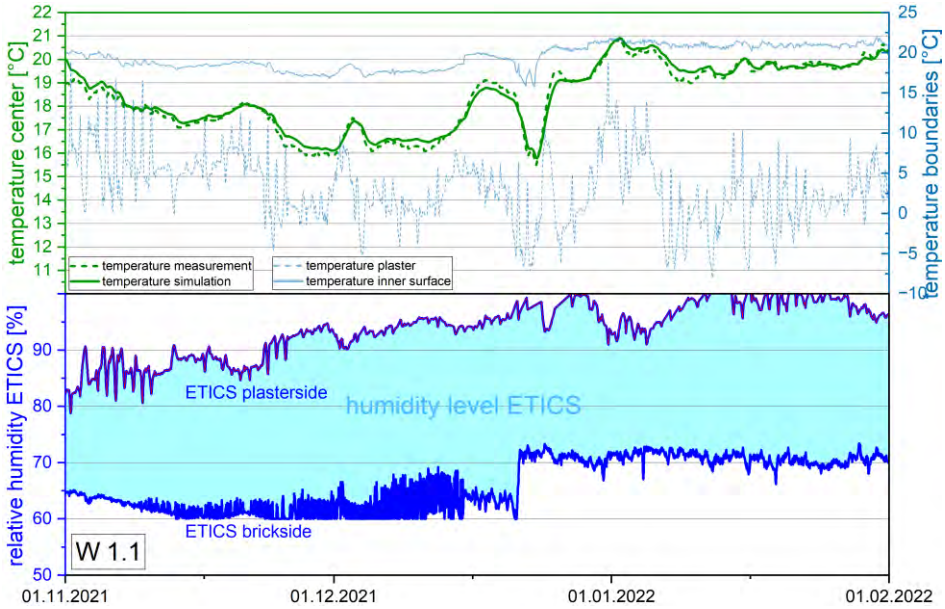

Figure 79 : Comparison of the measured and simulated temperatures at the measuring point "m" for the structure W 1.1 with 250 mm masonry and 220 mm WF ETICS (top). Moisture level in the ETICS during the observation period (bottom).

In both cases, a sufficiently accurate prediction of the temperature can be achieved by the simulation. It can therefore be concluded that the method used in the laboratory is suitable for determining the moisture-dependent thermal conductivity of sorptive insulation materials in real life. Latent heat effects are reduced to a negligible level in the measurement, so that the results from the thermal conductivity measurement can be used directly in hygrothermal simulations without having to consider latent heat effects twice.

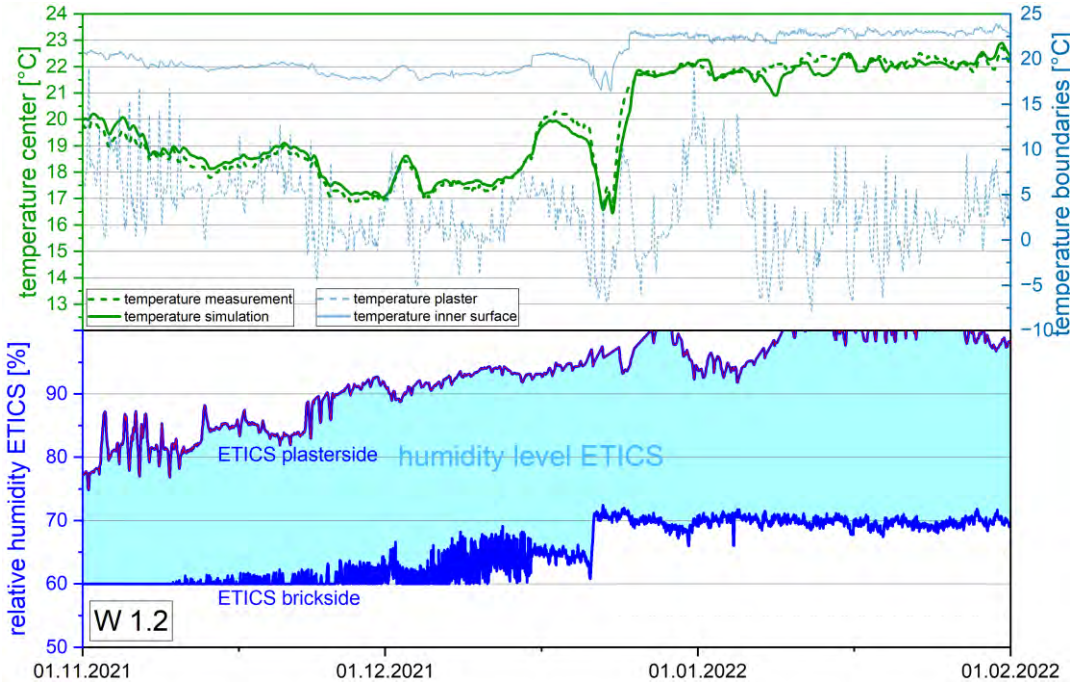

Figure 80 : Comparison of the measured and simulated temperatures at the measuring point "m" for the structure W 1.2 with 150 mm masonry and 220 mm WF ETICS (top). Moisture level in the ETICS during the observation period (bottom).

4.7 Conclusions and outlook

4.7.1 Heat flow evaluation by field tests and hygrothermal simulation

The in-situ measurements and their simulation-based reproduction allow in combination with the laboratory tests to conclude that the moisture related increase of thermal conductivity in natural fibre insulation materials remains rather low until a moisture level of approximately. 95% RH. That is the moisture range with dominates in the materials in real life. Also, the latent heat effects occurring up to that RH, the so-called "heat pipe effects", which redistribute moisture at constant moisture profiles are of little relevance concerning the thermal performance.

At moisture contents above 95% RH, the heat transport increases more strongly. At higher relative humidity the sorption moisture contents and thus also the thermal conductivity increase more strongly. But also, the latent heat flows occur to a greater extent at higher moisture levels. This applies in particular to dew water formation, which should anyway be avoided as far as possible for reasons of durability.

The variants with non-sorbent insulation materials generally showed slightly lower heat flows than the natural fibres, but also, they were increased compared to the values expected on basis of the thermal conductivity design values. The reproduction of the measurements of these variants by hygrothermal simulation suggests as well that the moisture-related increase oft the heat flows (both sensible and latent heat) in the range up to 95% RH is lower than the

one of sorption capable natural insulation materials. Nevertheless, it must be assumed that the humidity influence will not remain significantly lower than for other insulation materials at higher moisture levels or the occurrence of dew water. Since no mineral fibre ETICS was investigated, only the first aspect can be derived directly from the measured values. Another difference of sorption-capable materials results from the fact that they "store" moisture at higher relative humidity levels in the summer, which is then redistributed or released to the outside in the fall and winter including evaporation cooling effects.

In summary, it can be concluded that a surcharge of 5% on the nominal value for wood fibre insulation materials according to DIN 4108-4 is probably not excessive on an annual average. The available results even indicate that for purely thermal design calculations (e.g. for energy certificates), at least in the first few years, a somewhat higher surcharge of between 5 and 8% could be justified, but needs to be further examined on the basis of a broader material base. However, the test results do not provide a reason for reducing the 5% surcharge. On the other hand, an overall moisture surcharge of 20% on sorption-capable natural insulation materials, as specified in ÖNORM B 6015-2 for materials without monitoring during production, seems to be too far on the safe side. A reduction to the range between 10 and 15% would be clearly more realistic.

4.7.2 Additional results from the field tests

Irrespective of the moisture-related change, it was found that an increased blow-in density above the required and approved range for cellulose fibre insulation can lead to strongly increased heat flows. Therefore, an installation in accordance with the regulations is of particular importance.

The straw blow-in insulation showed on the other hand significantly lower heat flows than the technical product data would have suggested in this case. The nominal value (λ_D) provided by the manufacturer is therefore obviously set very high at 0.055 W/mK.

4.7.3 Lab test to determine the moisture-dependent thermal conductivity and verification by hygrothermal simulation.

The simulation-based preliminary study has shown that with suitable preconditioning of the sorptive insulation specimens in combination with a suitable temperature gradient, condensation processes can be avoided during the measurement. In this case, the remaining latent heat effects are reduced to a maximum of 0.5% of the measured thermal conductivity and are thus below the accuracy limit of the thermal conductivity measurement (usually 2% - 3%). The initially envisaged method with sliced samples and foil-separated layers has proven to be not suitable. Despite the unreasonable higher effort for sample preparation, only a negligible reduction of the latent heat effect during the measurement can be achieved.

From the measurements with the GHP apparatus, it can be concluded that the most efficient method to determine the moisture-dependent thermal conductivity is the one on the whole samples without slicing. A detailed analysis of the heat and moisture flows within the foil separated slices sometimes leads to physically nonsensical correlations. Cause is the limited accuracy of the measurement data and material parameters. Therefore, this procedure does not offer any relevant added value, which could only be achieved by a considerable and probably uneconomical increase in the measurement effort. For these reasons, the method according to DIN EN 12664 or ISO 10051 on the whole specimen is recommended as the most suitable for determining the moisture-related thermal conductivity. The anticipated residual uncertainties are negligibly small, since the material-related scattering of the thermal conductivity values alone has a greater range of variation.

The simulation of the laboratory tests has shown that a simulation-based differentiation between the the sensitive and latent moisture-related increase in heat flow is not reliably possible below 95% RH. But this differentiation is also not necessary, due to the low level of influence determined during the laboratory measurement. The effects in the higher humidity range, on the other hand, are probably well captured, as the mostly quite good agreement of the simulations with the measured data in the tests suggests. The simulation-based verification of the laboratory test results of wood fibreboards of different densities as well as a hemp fibreboard prove that the latent heat effects amount to maximum 1% of the total heat flow under these conditions. It is also found that the selected test scenario with 80% RH and a temperature difference of about 1 K per 1 cm of material thickness ensures that the RH on the cold side safely remains below 100% RH and thus no condensation conditions occur. The specified measurement procedure includes the influence of a humidity range beteween about 60% RH on the warm side to 95% RH on the cold side in the samples. Since there is no strong increase in thermal conductivity during the measurement, a linear relationship between the RH in the pores and the moisture-dependent thermal conductivity up to 95% can be assumed in simplified form. To describe the moisture-dependent thermal conductivity of a material based on the measurements, therefore the following procedure is specified: the measured value of the thermal conductivity is related to the average RH of 80 % RH in the pores of the material during the measurement. Linear interpolation is performed between the value of the dry thermal conductivity and the value at 80% pore RH and extrapolated until 95%. Between 95 and 100 % RH an exponential increase to 0.6 W/mK (thermal conductivity of water) is assumed.

The application of this data set for the simulation based reproduction of the field test has shown that the thermal conductivity determined in that way from the proposed lab test procedure represent the real behaviour in hygrothermal simulations with sufficient accuracy.

4.7.4 Outlook

The influence of latent heat transport processes on the thermal insulation performance of a building component with sorptive insulating materials under transient boundary conditions

emerges as quite relevant. Although these can be well reproduced with a hygrothermal simulation, the purely thermal values for the thermal conductivities provide a somewhat too optimistic picture for the investigated products. In subsequent investigations, this influence should be checked by means of further parameter variations (diffusion properties outside/inside, moisture load in the interior, roof/wall component, density variations for the same material, etc.) and, for more precise quantification, additionally in suitable laboratory tests.

Due to the fact that in real life drying tends to be particularly good in structures with curtain walls (ventilated facades), a lower moisture level in the cavity and thus a correspondingly lower influence of the latent heat can be expected in these. This is also indicated by the in-situ measurements performed on the ventilated variants [37]. On this basis suitable and even product and density specific moisture surcharges for purely thermal dimensioning (e.g. energy performance certification) could be determined. For straw-based blow-in insulation materials detailed hygrothermal properties should be determined to enable a simulation-based description of their hygrothermal performance in real life, which could be better than assumed according to the preliminary results.

The proposed test procedure for the moisture dependent thermal conductivity simulation can now be applied for different sorptive insulation materials to verify its general suitability and check for remaining weak points or improvement potential.

5 Literatur

[1] *Teibinger, M.; Bachinger, J.; Matzinger, I.:* Winddichtheit von Unterdächern. Holzforschung Austria, Wien Ausgabe 2014.

[2] *Kehrer, M.; Künzel, H.M.; Sedlbauer, K.:* Dämmstoffe aus nachwachsenden Rohstoffen - ist der Feuchtezuschlag für die Wärmeleitfähigkeit gerechtfertigt? – IBP-Mitteilung. Fraunhofer IBP, 2001, https://www.ibp.fraunhofer.de/content/dam/ibp/ibp-neu/de/dokumente/ibpmitteilungen/1-400/301-400/390_IBPmitteilung.pdf [Zugriff am: 11.05.2020].

[3] ÖNORM B 8110-2: Wärmeschutz im Hochbau - Teil 2: Wasserdampfdiffusion, -konvektion und Kondensationsschutz. Ausgabe Januar 2020.

[4] *Kehl, D.; Plagge, R.; Grunewald, J.:* Wann geht Holz kaputt? - Nachweistechnische Beur- teilung von Holz zerstörenden Pilzen. *In:* BuFAS e.V. (Hrsg.): 23. Hanseatische Sanierungstage – Feuchte - Wärme - Schimmelpilz. Fraunhofer IRB Verlag; Beuth, Heringsdorf, Usedom, 2012, S. 61-74.

[5] *Viitanen, H.:* Factors affecting the development of mould and brown rot decay in wooden material and wooden structures – Effect of humidity, temperature and exposure time. Uppsala, Swedish Univ. of Agricultural Science Dept. of Forest Products, Dissertation, 1996.

[6] *Viitanen, H.; Toratti, T.; Makkonen, L. et al.:* Towards modelling of decay risk of wooden materials. *In:* Holz als Roh- und Werkstoff 68 (2010), Heft 3, S. 303-313.

[7] WTA 6-8: Feuchtetechnische Bewertung von Holzbauteilen – Vereinfachte Nachweise und Simulation. WTA-MERKBLATT, Ausgabe 2016.

[8] *Zirkelbach, D.; Schöner, T.; Tanaka, E. et al.:* Consistent European Guidelines for Internal Insulation of Building Stock and Heri-tage Einheitlicher europäischer Leitfaden für die Innendämmung von Bestandsbauten und Baudenkmälern – Einheitlicher europäischer Leitfaden für die Innendämmung von Bestandsbauten und Baudenkmälern. Fraunhofer Institut für Bauphysik, Holzkirchen/Dresden/Limelette Ausgabe Juli 2022.

[9] ÖNORM B 6015-2: Bestimmung der Wärmeleitfähigkeit mit dem Plattengerät - Teil2: Ermittlung des Nennwertes und des Bemessungswertes der Wärmeleitfähigkeir für homogene Baustoffe. Ausgabe 2009.

[10] DIN 4108-4: Wärmeschutz und Energie-Einsparung in Gebäuden - Teil 4: Wärme- und feuchteschutztechnische Bemessungswerte. Ausgabe November 2020.

[11] *Kehrer, M.; Künzel, H.M.; Sedlbauer, K.:* Bestimmung feuchtetechnischer Kennwerte an Dämmstoffen aus nachwachsenden Rohstoffen. Fraunhofer IBP Ausgabe 2001.

[12] DIN 68800-2: Holzschutz - Teil 2: Vorbeugende bauliche Maßnahmen im Hochbau. Ausgabe Februar 2012.

[13] Ongoing research project - Zirkelbach, D*; Schöner, T.; Tanaka, E. et al.:* Energieoptimiertes Bauen: NaVe - Nachweisverfahren für Schadensmechanismen bei der hygrothermischen Simulation Ausgabe PTJ 2022 (FKZ: 03ET1649B).
[14] ÖNORM B 3802-2: Holzschutz im Bauwesen - Teil 2: Baulicher Schutz des Holzes. Ausgabe Januar 2015.
[15] *Zirkelbach, D.; Tanaka, E. (Hrsg.):* Evaluation of decay resistance of wood fibre insulation based on hygrothermal simulation and comparative laboratory tests, 2021.
[16] METEONORM – Global Meteorological Database, http://www.meteonorm.com [Zugriff am: 31.01.2020].
[17] *Viitanen, H.; Toratti, T.; Makkonen, L.:* Towards modelling of decay risk of wooden materials. *In: :* Holz als Roh- und Werkstoff, S. 303-313.
[18] *Brischke, C.; Soetbeer, A.; Meyer-Veltrup, L.:* The minimum moisture threshold for wood decay by basidiomycetes revisited. A review and modified pile experiments with Norway spruce and European beech decayed by Coniophora puteana and Trametes versicolour. *In:* Holzforschung 71 (2017), Heft 11, S. 893-903.
[19] DIN 113-1: Dauerhaftigkeit von Holz und Holzprodukten - Prüfverfahren in Bezug auf Holz zerstörende Basidiomyceten - Teil 1: Bewertung der bioziden Wirksamkeit von Holzschutzmitteln. DIN EN, Ausgabe Februar 2021.
[20] *Greenspan, L.:* Humidity fixed points of binary saturated aqueous solutions. *In:* Journal of Research of the National Bureau of Standards Section A: Physics and Chemistry 81A (1977), Heft 1, S. 89.
[21] *Suzuki, K.:* Moisture Content Levels and Decay of Hemlock Ausgabe 1986.
[22] *Suzuki, K.:* Effect of Cyclic Change of Temperature on Fungal Growth and Mass Loss. The International Research Group on Wood Preservation Ausgabe 1994.
[23] *Fukuda, K.; Okayasu, Y.; Haraguchi, T.:* Influence of Temperature on the Growth and Wood-decomposing Ability of Wood-rotting Fungi. *In:* Bulletin of the Experiment Forests (1981), Heft 17, S. 49-55.
[24] *Maeda, H.:* Analysis and Modelling of the Change of the Density and Strength distribution during the Wood Rot Processing. Tokyo, Tokyo University, 2013.
[25] *Saito, H.; Fukuda, K.; Sawachi, T.:* Integration model of hygrothermal analysis with decay process for durability assessment of building envelopes. *In:* Building Simulation 5 (2012), Heft 4, S. 315-324.
[26] IBK, IBP & BTU: Energetisches Bewertungsverfahren für Bestandsgebäude mit Holzbalkendecken. IBK, IBP & BTU Ausgabe 2016.
[27] *Sedlbauer, K.:* Vorhersage von Schimmelpilzbildung auf und in Bauteilen. Stuttgart, Universität Stuttgart, 2001.
[28] *Viitanen, H.:* Untersuchungen und dynamische Simulationen zum Schimmelpilzwachstum in Holzbauquerschnitten – Simulation and modelling critical conditions for fungi to develop in wood, Holzbauphysik Kongress,, München, 2010.

[29] BuFAS e.V. *(Hrsg.):* Wann geht Holz kaputt? - Nachweistechnische Beurteilung von Holz zerstörenden Pilzen, 23. Hanseatische Sanierungstage - Feuchte - Wärme - Schimmelpilz, Fraunhofer IRB Verlag; Beuth, Heringsdorf, Usedom, 2012.

[30] *Zirkelbach, D.; Ruisinger, U.;* et.al: Consistent European Guidelines for Internal Insulation of Building Stock and Heritage Ausgabe 2022.

[31] *Hukka, A.; Viitanen, H.:* A mathematical model of mould growth on wooden material. *In:* Wood Science and Technology 33 (1999), Heft 6, S. 475-485.

[32] *Viitanen, H.:* Factors affecting the development of mould and brown rot decay in wooden material and wooden structures – Effect of humidity, temperature and exposure time. Uppsala, Swedish Univ. of Agricultural Science, Dissertation, 1996.

[33] SN EN ISO 10456 ; SIA 279.041:2007: Baustoffe und Bauprodukte - Wärme- und feuchtetechnische Eigenschaften - Tabellierte Bemessungswerte und Verfahren zur Bestimmung der wärmeschutztechnischen Nenn- und Bemessungswerte (ISO 10456:2007). Ausgabe 2018.

[34] Fraunhofer Institut für Bauphysik*;* Forschungsinsitut für Wärmeschutz e.V. (FIW): Energieeffizienzsteigerung durch Innendämmsysteme - Anwendungsbereiche – Chancen und Grenzen. Fraunhofer Institut für Bauphysik; Forschungsinsitut für Wärmeschutz e.V. (FIW) Ausgabe 2019.

[35] Fraunhofer IBP: Energieeffizienzsteigerung durch Innendämmsysteme : Anwendungsbereiche, Chancen und Grenzen : Forschung für energieeffiziente Gebäude und Quartiere. FIW, IBP, München, Holzkirchen.

[36] ongoing diploma thesis Hinteregger, D.: working title: Hygrothermische in situ Messungen an Dämmmaterialien aus nachwachsenden Rohstoffen, TU Graz, diploma thesis, 2023.

[37] *Tieben, J.; Nusser, B.; Zirkelbach, D.:* Nachhaltig gedämmt – Ist der normative Feuchtezuschlag für Gefachdämmungen aus Schafwolle und Strohfasern gerechtfertigt? *In: :* Holzbau - die neue quadriga, Heft Heft 3. Kastner, Wolnzach (D), 2022, S. 21-25.

[38] DIN EN ISO 10456:2010-05: Baustoffe und Bauprodukte - Wärme- und feuchtetechnische Eigenschaften - Tabellierte Bemessungswerte und Verfahren zur Bestimmung der wärmeschutztechnischen Nenn- und Bemessungswerte.

[39] Fachagentur Nachwachsende Rohstoffe e. V. (FNR): Untersuchungen zur Optimierung und Standardisierung von Dämmstoffen aus nachwachsenden Rohstoffen – Gemeinsamer Abschlussbericht zum Verbundvorhaben. Fraunhofer Institut für Bauphysik; Institut für Holztechnologie Dresden gGmbH; Institut für Betriebstechnik und Bauforschung *et al.* Ausgabe Januar 2008.

[40] *Engelund Thybring, E.; Fredriksson, M.; Zelinka, S.L. et al.:* Water in Wood – A Review of Current Understanding and Knowledge Gaps. *In:* Forests 13 (2022), Heft 12, S. 2051.

[41] *Chen, M.; Coasne, B.; Guyer, R. et al.:* Role of hydrogen bonding in hysteresis observed in sorption-induced swelling of soft nanoporous polymers. *In:* Nature communications, Vol. 9 (2018), Iss. 1, p. 3507.

[42] *Lopez Hurtado, P.; Rouilly, A.; Vandenbossche, V. et al.:* A review on the properties of cellulose fibre insulation. *In:* Building and Environment 96 (2016), S. 170-177.
[43] *Künzel, H.M.:* Verfahren zur ein- und zweidimensionalen Berechnung des gekoppelten Wärme- und Feuchtetransports in Bauteilen mit einfachen Kennwerten, Stuttgart Ausgabe 1994.
[44] DIN EN 12664:2001-05, Wärmetechnisches Verhalten von Baustoffen und Bauprodukten_- Bestimmung des Wärmedurchlasswiderstandes nach dem Verfahren mit dem Plattengerät und dem Wärmestrommessplatten-Gerät_- Trockene und feuchte Produkte mit mittlerem und niedrigem Wärmedurchlasswiderstand; Deutsche Fassung EN_12664:2001. Ausgabe 2001.
[45] 10051: Determination of thermal transmissivity of a moist material. ISO, Ausgabe 1996.
[46] *EL Assaad, M.; Colinart, T.; Lecompte, T.:* Thermal conductivity assessment of moist building insulation material using a Heat Flow Meter apparatus. *In:* Building and Environment 234 (2023), Heft 3, S. 110184.
[47] *Binder, A.:* Entwicklung eines Testverfahrens zur Quantifizierung des kapillaren Rücktransports kapillaraktiver Innendämmstoffe Ausgabe 2010.
[48] *Binder, A.; Zirkelbach, D.; Künzel, H.:* Test method to quantify the wicking properties of insulation materials designed to prevent interstitial condensation, Buildings IX: thermal Performance of the Exterior Envelopes of Whole Buildings,, Atlanta, 2010.
[49] *Commerer, W.F.:* Der Feuchteeinfluss auf die Wärmeleitfähigkeit von Bau- und Wärmedämmstoffen, Band 6; S. 259-266 Ausgabe 1987.
[50] *Cammerer, J.:* Einfluß des Feuchtegehaltes auf die Wärmeleitfähigkeit von Bau- und Dämmstoffen. Forschungsinstitut für Wärmeschutz e.V., München Ausgabe 1984.

Appendix
Development of evaluation and prediction models for decay in natural fibre insulation materials

Stage	Methods, limits values, standards	Advantages, disadvantages, features
1	20 % by mass (solid wood) or 18 % by mass (wooden materials) may not be exceeded in the long term. No exceedance for solid wood for 6 months (3 months - Austria) and for wood-based materials for 3 months up to 22 and 20% by mass respectively. **State of the art**: Regulated in DIN 68800-3 ("Wood protection standard") or ÖNORM B 3802-2.	Simple assessment. Distinction between rot and load-bearing capacity not always entirely clear. Limit values for non-load-bearing wood-based materials as fibre insulation materials not authoritative - but no others known either. The effect of temperature, which is also relevant for wood biodegradation, is not considered. The limit values include a very high safety buffer regarding real decay. The assessment is therefore rather far on the safe side.
2	Relative humidity limit curve as a function of temperature (see Figure 31). No exceedance on basis of a 24-hour average. **State of the art**: Regulated in WTA 6-8	More accurate than stage 1, but still clearly on the safe side. The limit value of 20 % by mass (corresponding to approx. 86% RH) for solid wood (stage 1) now only applies at 30 °C. At lower temperatures, higher humidity is permissible up to max. 95% RH (equivalent to approx. 26 % by mass) at 0 °C. The limit moisture level still includes sufficient safety buffers and is accordingly clearly lower than the results of the lab test from this project as well as from literatures. Failure in case of short-term exceedances which remain harmless in real life. Aspect of time (transient assessment) is missing: How long must the conditions occur before

		the fungus can grow and degrade the material?
3	New limit curves for decay of wood fibre materials. Prediction of mass loss using the bio-hygrothermal model. The limit curves of wood decay fungi are fixed for solid wood and different wood fibre materials (depending on their susceptibility against decay). **New result of this project**	The duration until the beginning of the wood degradation processes are considered. To represent delay of material degradation as well as the mass losses determined in the laboratory tests with the prediction model WUFI® decay a new limit curve "ThermNat II" is introduced, which represents solid wood and equal or more resistant fibre materials. For wood fibre materials that are less resistant than solid wood, the curve "ThermNat I" is introduced.
4	Publication of a practical evaluation tool **New result of this project**	The prediction model is validated by the lab and field tests performed within the current project. Now additional practice evaluation is required. To simplify the interpretation of the results, a traffic light scheme is established (**green** if the limit curve is not exceeded or only for very short periods - **yellow** if the limit curve is exceeded but no or only marginal mass loss is predicted - **red** if significant mass loss is predicted).
5	Prediction models with material-specific limit curve **Outlook – current topic of research**	Material-specific limit curves will increase the accuracy of the prediction and can optimally consider the individual performance of a material. For this reason, a method is to be developed for determining an individual limit curve from the simplest possible laboratory investigations.
6	Further development of transient prediction model for other materials	To assess realistically also the durability of wooden construction materials (not only

	Outlook – planned future project	fibre insulation) also here the courses of temperature and relative humidity in the material should be considered. In the transient prediction models, the temporal effect - including short- or long-term interruptions of the optimal conditions for wood degradation processes - should be investigated in more detail.

Investigations on the durability of cellulose blow-in insulation materials

Addendum to final report

(ThermNat - Building components with insulation material from renewable resources: Focus on (Hygro-)Thermics)

Project no.: 877670

HFA-No.: 50900

Funded by FFG

Authors

Dr. J. Bachinger, Mag.a N. Pfabigan, DI J. Tieben (HFA),
E. Tanaka, D. Zirkelbach (IBP)

Project staff

B. Brunnhuber, L. Orlowski, M. Senoner BSc., G. Soukup, J. Reiter (HFA)

Project partners

best wood SCHNEIDER GmbH, Daniel Kehl - büro für holzbauphysik, EGS-plan GmbH, Energie- und Umweltzentrum am Deister GmbH, GUTEX Holzfaserplattenwerk GmbH & CO. KG, Hanffaser Uckermark eG, Holzbau Deutschland Institut e.V., ISOCELL GmbH & Co KG, Isolena Naturfaservliese GmbH, LOPAS GmbH, Martin Epple - Bau.Tragwerk Ingenieurbüro, SonnenKlee GmbH ,Soprema GmbH, STEICO SE, Sto GmbH, Tobias Tumfart GmbH, Verband Dämmstoffe aus nachwachsenden Rohstoffen e.V.

Vienna, 30.06.2023

1 Method of investigation

The test specimens (cellulose blow-in insulation material, with and without boron) were dried for 48 hours at (60 ± 2) °C, weighed to ± 0.01 g and then sterilized by means of ionizing irradiation. Under sterile conditions, the test specimens were placed in experimental vessels and conditioned for 4 weeks at 100% relative humidity (RH) and 15 °C, and at 97% RH and 25 °C and 30 °C, respectively. The relative humidities in the experimental containers were adjusted to 97 % with saturated potassium sulfate solution (K_2SO_4) and to 100 % with sterile water. Inoculation of the test specimens was carried out after conditioning the specimens with three fungus-covered softwood dowels each 10 mm in length and 8 mm in diameter, each covered with one of the following three experimental fungi:

- *Coniophora puteana*
- *Trametes versicolor*
- *Schizophyllum commune*

Subsequently, the specimens were incubated under the above conditions. Three specimens were used for each climate variant and time period. Specimens of pine sapwood of dimension (50 ± 0.5) mm x (50 ± 0.5) mm x (10 ± 0.5) mm were used as reference specimens.

After previously defined periods of time, the test specimens were removed from the test vessels, weighed, the dowels carefully removed without losing cellulose fibers, weighed again, dried for 48 hours at (60 ± 2) °C, and weighed again. From the difference before and after the fungal experiment, adjusted for the weight of the wire basket and dowels, any loss of mass was determined. In order to take into account any changes in mass occurring during the incubation period which were not due to fungal degradation, correction samples not inoculated with fungi were included in the test at 25 °C and 97 % RH. The mass changes occurring in these correction samples were subtracted as correction values from those of the samples inoculated with fungi.

Setting the RH at 97 % with a saturated solution of K_2SO_4 resulted in some inherent uncertainty in the experiment. Due to the temperature dependence of the process, a relative humidity of 97.3 ± 0.5 % is obtained at 25 °C and 97.0 ± 0.4 % at 30 °C.

The test at 100 % RH and 15 °C was carried out at IBP, those at 97 % RH and 25 °C and 30 °C at HFA.

2 Results

Loss of mass not due to fungal degradation occurred only in the cellulose with boron to a minor extent of 0.5%, as shown in Table 1.

Table 1: Mass loss of specimens not inoculated with fungi (correction specimens) after 7 months of incubation at 25 °C and 97 % RH.

Specimen	mass loss [wt. %]
Cellulose with boron	0.5
Cellulose without boron	0.0
pine sapwood (reference)	0.0

The mass losses of the specimens at the respective humidity and temperature conditions are listed in Table 2 to Table 4. Figure 1 and Figure 2 show the results graphically. It can be seen from the data that there are small, apparently unexplained, decreases in mass loss over time. This is attributed to large scattering in biological data. A range of up to 1.5% mass loss was therefore taken as the limit of measurement inaccuracy in the present study.

As can be seen from the tables and figures, the cellulose with boron did not show more than 1.5 % mass loss at any time under any of the temperature and moisture conditions investigated. This is within the range of measurement inaccuracy and is at or below the level of mass loss for the pine sapwood (reference).

Apart from a single outlier value (3.8% after 1.5 months), the cellulose without boron showed a maximum mass loss of 1.9% in the tests at a 97% RH. The same result was obtained after 5.25 months at 15 °C and 100 % relative humidity. After 10.5 months, on the other hand, significant mass losses of up to 5.3% were present under these conditions. It should be noted that the pine-sapwood reference showed even higher mass losses under these conditions than the cellulose without boron (Figure 2).

Table 1: Mass loss [wt. %] of test specimens; incubation at 25 °C and 97 % RH.

Specimen	time [months]					
	1	1,5	2	3	5	8
Cellulose without boron	1.7	-0.6	1.9	1.6	1.7	0.9
	1.3	1.5	1.9	1.4	1.3	0.7
	1.3	3.8	1.9	1.5	1.7	0.9
Cellulose with boron	0.7	0.7	1.2	0.8	1.1	0.4
	0.5	0.6	1.2	0.9	0.8	0.0
	0.9	1.1	1.1	0.8	0.9	0.1
pine sapwood	1.2	1.2	1.4	1.9	1.9	2.1
	1.1	0.7	1.6	1.8	1.8	2.0
	1.1	1.2	1.5	1.8	1.8	2.1

Table 2: Mass loss [wt. %] of test specimens; incubation at 30 °C and 97 % RH.

Probekörper	time [months]					
	0.75	1.25	1.75	2.5	4	6
Cellulose without boron	1.2	1.2	1.0	1.3	1.4	1.5
	0.9	1.1	1.6	1.3	1.4	1.4
	1.0	1.2	1.4	1.2	1.3	1.2
Cellulose with boron	0.8	1.0	1.2	0.8	1.3	1.4
	1.1	1.1	1.3	1.1	1.5	1.1
	1.1	0.9	1.3	1.2	1.5	1.2
pine sapwood	0.9	0.9	1.0	1.4	1.9	1.3
	0.9	1.0	0.8	1.4	2.0	1.2
	0.8	0.9	0.9	1.4	1.8	1.1

Table 3: Mass loss [wt. %] of test specimens; incubation at 15 °C and 100 % RH.

Probekörper	time [months]	
	5.25	10.5
Cellulose without boron	1.7	2.1
	1.7	5.3
	1.9	4.1
Cellulose with boron	1.1	1.0
	1.2	1.0
	1.0	1.1
pine sapwood	2.9	10.1
	2.2	5.1
	3.8	9.6

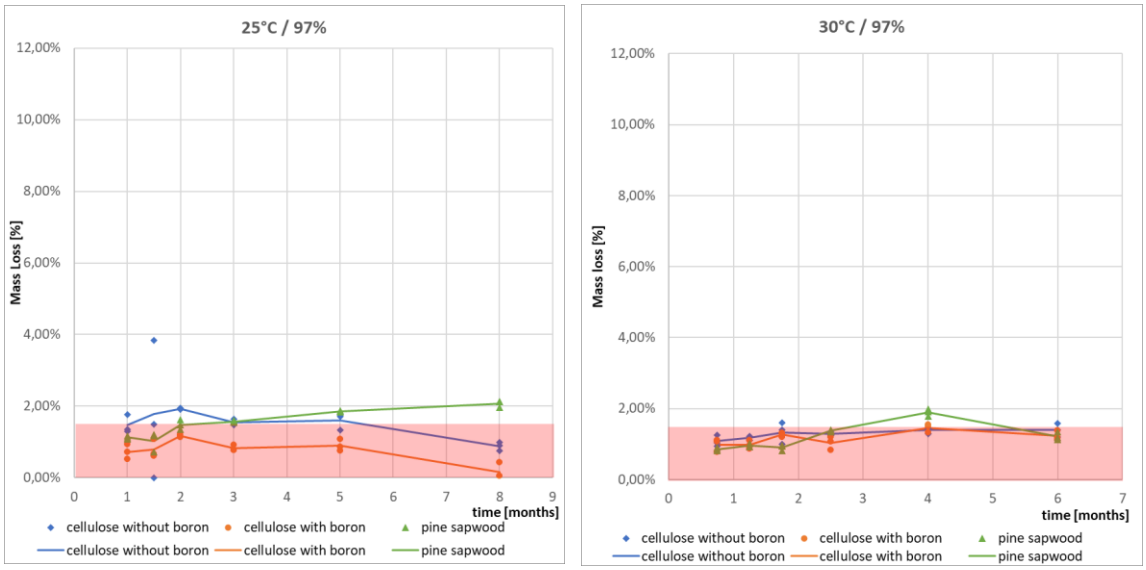

Figure 1: Mass loss of test specimens; incubation at 25 °C and 30 °C as well as 97 % RH. (transparent red marked = range of measurement inaccuracy of 1.5 wt.%).

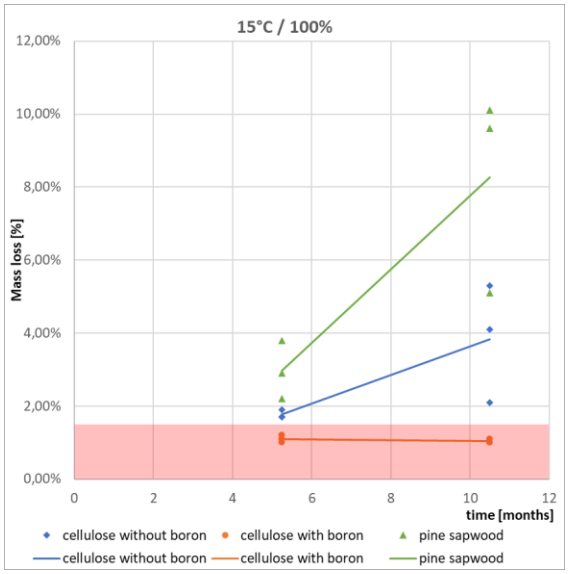

Figure 2: Mass loss of test specimens; incubation at 15 °C and 100 % RH. (marked transparent red = range of measurement inaccuracy of 1.5 wt.%)

3 Interpretation of the results

The test results show that the cellulose insulation materials tested with and without boron salt are both more resistant to wood-destroying fungi in the long term than the reference wood. The mass loss of the samples with boron remained below the measurement uncertainty limit of 1.5 wt.% at all climates investigated (25 °C and 30 °C /97 % RH, 15 °C/100 % RH). In the sample without boron, on the other hand, a loss in mass of up to 5 wt.% was observed at 15 °C / 100 % RH. after approx. 10 months, and at 25 °C / 97 % RH. a loss in mass of up to 2 wt.% and thus 0.5 % higher than for the cellulose with boron was observed. As a result, the measurement accuracy range of 1.5 % without boron was temporarily exceeded in the first two months, and the material without boron here also temporarily shows somewhat higher mass loss than the reference wood. This proves that the absence of boron salt is associated with lower resistance to wood-destroying fungi.

This statement is further supported by another observation: During the tests at 15 °C and 100% RH, mold growth had occurred on the material surfaces of the cellulose samples without boron, despite conditions that were as sterile as possible, whereas this was not the case for the samples with boron. Accordingly, it can be assumed that the resistance to microbial attack is nevertheless significantly increased by the addition of boron, and that cellulose fiber insulation without this addition is subject to different limits of use.